

143 pages



החברה הגיאולוגית הישראלית
Israel Geological Society

INIS-mf--13912 .



LAST VIEW OF GENESARETH.

INIS DOCUMENT

TRN IL 9405669 -IL940567



ANNUAL MEETING, 1994



EDITED BY:

Rivka Amit,¹ Yaacov Arkin,² Francis Hirsch²

¹Department of Physical Geography,
The Hebrew University, Jerusalem

²Geological Survey of Israel, Jerusalem

NOF GINOSAR

28 FEBRUARY – 2 MARCH

1994

Chernobyl in Israel

Butenko, V.,¹ Ne'eman, E.,¹ Brenner, S.,¹ Kronfeld, J.,² Gilat, A.³

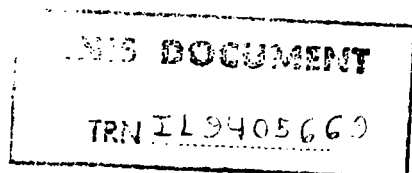
1. Environmental Research Laboratory, Ministry of the Environment, Sackler Medical Building, Tel Aviv University, 69978 Tel Aviv

2. Dept. of Geophysics and Planetary Sciences, Tel Aviv University, 69978 Tel Aviv

3. Geological Survey of Israel, 30 Malkhe Yisrael Street, 95501 Jerusalem

The radioactive plume arrived over Israel, accompanied by a patchy rainfall, approximately ten days after the nuclear accident (April 26, 1986) at the Chernobyl reactor in the Ukraine. The first study of possible soil contamination was recently carried out. Approximately sixty samples, of soils in the Galilee region and 22 samples in the Judean Hills region including a wide range of important and/or historical sites such as the Israel Geological Survey and the Valley of the Cross, the Hebrew University and the Old City among others were analyzed.

Soil samples were collected to a depth of 5 cm. The samples were analyzed by gamma-ray spectrometry using a solid Ge detector. This enabled the precise identification of gamma-ray energy peaks. In all cases the presence of the short-lived (2 year half life) radiocesium isotope, ^{134}Cs , identifies the presence of Chernobyl-related contamination. The activity of this isotope is, in many cases still after 3 1/2 half lives, greater than that of the naturally occurring ^{40}K . The 662 KeV peak of the long-lived ^{137}Cs (30 year half-life) is usually the dominant peak in all of the spectrums. The ^{137}Cs activity is found (so far) to range between 0.1K and 13K Bq/m². The average radiocesium burden of the soils today is approximately 5000-8000 Bq/m². This demonstrates that the Chernobyl contamination in Israel was not trivial as was previously assumed. Indeed, the external radioactive dose rate was undoubtedly significantly higher soon after its precipitation.



Sulfur Isotopes Evidence for Sulfate Removal Processes from Subsurface Brines, Heletz Formation (Lower Cretaceous), Israel

Gavrieli, I.,¹ Starinsky, A.,² Spiro, B.,³ Nielsen, H.,⁴ Aizenshtat, Z.⁵

1. Geological Survey of Israel, 30 Malkhe Yisrael Street, 95501 Jerusalem

2. Dept of Geology, The Hebrew University, 91904 Jerusalem

3. NERC Isotope Geosciences Laboratory Keyworth, U.K., NG12 5GG

4. Dept. of Geochemistry, Gottingen University, Germany

5. Dept. of Chemistry, The Hebrew University, 91904 Jerusalem

Subsurface brines associated with oil ("oil brines") from four oil fields, Heletz, Brur, Kokhav and Negba, in the southern coastal plain of Israel show a deficiency in SO_4 concentrations compared to brines from dry wells ("dry brines") in the same fields only a few hundred meters away. Both types of brines have SO_4/Cl ratios lower than seawater or evaporated seawater with the same salinity. Previous studies suggested that the brines have evolved from evaporated Miocene seawater, which precipitated the sulfates in the Mavqim Fm. ($\delta^{34}\text{S}=21.7\text{-}22.7\text{‰}$). The present study shows that the residual brine in the Mavqim Fm. has sulfate with $\delta^{34}\text{S}=26.4\text{‰}$. The $\delta^{34}\text{S}_{\text{SO}_4}$ of the oil brines from the oil producing Heletz Fm. is $35.4\text{-}59.0\text{‰}$ while the associated H_2S has sulfur composition of about $30\text{-}31\text{‰}$. The oil has sulfur concentrations of $2\text{-}3\%$ with relatively heavy sulfur isotopic composition of $+13$ to $+15\text{‰}$.

The following overall evolutionary path for these brines was reconstructed on the basis of their sulfate concentration, SO_4/Cl ratio and $\delta^{34}\text{S}$ in the SO_4 , H_2S and the oil.

- (1) Evaporation of a Messinian seawater which led to the precipitation of gypsum.
- (2) Precipitation of gypsum following dolomitization.
- (3) Bacterial sulfate reduction.

Stages (1) through (3) removed some 50% of the initial sulfate content of the brines, changing the sulfate isotopic composition from marine ($\delta^{34}\text{S}\approx 20\text{‰}$) to $\approx 26\text{‰}$.

- (4) Migration of the residual brines eastward into the Lower Cretaceous Heletz Fm. and mixing with oil.
- (5) Bacterial sulfate reduction in the oil reservoir resulting in further decrease in SO_4/Cl ratio and increase of $\delta^{34}\text{S}$ in the remaining sulfate.
- (6) Possible secondary enrichment of the oil with sulfur through reaction with the increasingly ^{34}S enriched H_2S and SO_4 .

INIS DOCUMENT

TRN IL 9405670

Neutron Shielding by H₂O in Clay Minerals - an Explanation for ³⁹Ar Deficit in Irradiated Clay Fractions

Kapusta, Y., Steinitz, G., Kotlarsky, P.

Geological Survey of Israel, 30 Malkhe Yisrael Street, 95501 Jerusalem

The neutron fluence and its variation as utilized in ⁴⁰Ar-³⁹Ar dating is determined by using a mineral-monitor which is irradiated in a nuclear reactor together with the sample. It is assumed that the efficiency of the ³⁹K(n,p)³⁹Ar reaction in the monitor and the sample is the same. Using standard monitors (LP-6, HD-B1, MMhb-1 etc.) for ⁴⁰Ar-³⁹Ar dating of clay minerals yields ages significantly too high. The conventional explanation assumes a ³⁹Ar deficit within the mineral, due to its "recoil" from the fine grains, as the cause for the phenomenon.

Two different aliquats (0.028, 0.351 gr) of the same clay fraction (<0.2μ) irradiated together contained different amounts of ³⁹Ar (1.3*10⁻⁷, 1.96*10⁻⁷ cc/gr). The dependence of the ³⁹Ar concentration on the mass of the sample indicates a varying neutron flux in the sample. In the irradiated samples no loss of ⁴⁰Ar_{rad} was observed nor could implanted ³⁹Ar be detected in the aluminum foil used for packing the samples.

The measured ³⁹Ar content in different clay fractions irradiated together shows a linear correlation between the calculated ³⁹Ar deficit (using their K-Ar age) and their H₂O content (determined by DTA). This implies that the water in the clay minerals moderates and/or absorbs the neutrons and thus is the source of the ³⁹Ar deficit relative to the monitors which are devoid of water.

It is suggested to use clay fractions with calibrated K-Ar ages and known water contents as additional neutron flux monitors for ⁴⁰Ar-³⁹Ar dating of fine clay minerals. A first test using this approach yielded ⁴⁰Ar-³⁹Ar ages of H₂O bearing clay fractions close to their K-Ar ages. The deviations may be due to difference in size and geometry between the clay monitors and the samples. The results open the possibility of extending the approach to step-wise heating experiments.

INIS DOCUMENT

TRN IL940567A

Isotopic Differences Between Bones of Different Periods: Climatic or Diagenetic Changes?

Shahack-Gross, R.,^{1,2} Tchernov, E.,² Kolodny, Y.,¹ Luz, B.¹

1. Institute of Earth Sciences, The Hebrew University of Jerusalem, 91904 Jerusalem
2. Dept. of Evolution, Systematics and Ecology, Institute of Life Sciences, The Hebrew University of Jerusalem, 91904 Jerusalem

The isotopic composition of oxygen in bone phosphate (δ_p) in mammals is related to the isotopic composition of the carbon in bone carbonate ($\delta^{13}C$) in herbivorous mammals yields information about the kind of vegetation in the mammal's diet. Both δ_p and $\delta^{13}C$ depend on the climate in the mammal's habitat.

δ_p and $\delta^{13}C$ were measured in two mammal species from Israel: vole (a rodent) and gazelle. The analyses were carried out on recent populations from different areas of the country and on fossil populations from Ha'yonim cave (western Galilee). The cave material we selected derives from two prehistoric periods: the Kebaran (19–14500 years B.P.) and the Natufian (12500–10300 years B.P.).

In order to make sure that the isotopic results reflect the original δ_p we measured the state of preservation of the material (bones and teeth) by X-ray diffraction, IR spectroscopy and the isotopic composition of oxygen in bone carbonate (δ_c). In the first two methods crystallinity indices were calculated.

The spectral methods show change in the crystallinity indices between recent and fossil material, due to diagenesis, but among fossil samples there are no clear criteria to distinguish samples with original δ_p from samples with diagenetic δ_p . According to the IR data, the fossil vole bones and the fossil tooth enamel of the gazelles did not change their mineralogical structure. Thus we assume that they preserve their original isotopic signature. δ_c results do not show any clear connection to diagenesis.

δ_p results of the recent vole populations show good correlation with the relative humidity of the collection sites. The results of the fossil voles are qualitative. It shows that relative to present levels, humidity in the Ha'yonim cave area was lower during the Kebaran and slightly higher during the Natufian. The gazelle populations shows the same pattern. These results agree with palaeontological and palynological studies on the same periods.

$\delta^{13}C$ results shows similarity in the diet of Natufian and recent gazelles, which implies no severe change of temperature. These results do not agree with palaeontological and palynological studies.

Sr Isotopes in a Red Sea Core — Inferences for the Red Sea History During the Last 400 kyr.

Stein, M.,¹ Almogi-Labin, A.,² Goldstein, S.L.,³ Hemleben, C.,⁴ Starinsky, A.¹

1. Institute of Earth Sciences, The Hebrew University of Jerusalem, 91904 Jerusalem

2. Geological Survey of Israel, 30 Malkhe Yisrael Street, 95501 Jerusalem

3. Max-Planck Institute für Chemie, Postfach 3060, Mainz

4. Tübingen University, Tübingen

We report on $^{87}\text{Sr}/^{86}\text{Sr}$ ratios in seventeen carbonate samples (foraminifers, pteropods and secondary carbonate) from the Red Sea core KL11 (located at $18^\circ 46.3' \text{N} / 39^\circ 19.9' \text{E}$). The core, 20.93 m in length covers the last 400 kyr. Strontium isotopes were measured in dynamic mode on a Finnigan MAT261 at MPI-Mainz. Twenty five measurements of NBS-987 standard yielded $^{87}\text{Sr}/^{86}\text{Sr} = 0.710259 \pm 9$ (2s). The samples were measured in duplicates. The foraminifers are mainly *Globigerinoides sacculifer* made of low magnesium calcite, and the pteropods are made of aragonite. The average $^{87}\text{Sr}/^{86}\text{Sr}$ ratios of samples from glacial and interglacial periods are 0.70917 ± 1 (1s) and 0.70921 ± 4 (1s) respectively. In comparison, a core from the Arabian Sea (Clemens et al. 1993) which represents open ocean conditions shows similar, but less amplified patterns of $^{87}\text{Sr}/^{86}\text{Sr}$ ratios. While most samples from glacial periods yielded the same $^{87}\text{Sr}/^{86}\text{Sr}$ ratios in both localities, two samples from maximum glacial conditions in the Red Sea have slightly lower ratios than contemporaneous episodes in the Arabian Sea. On the other hand, samples from several episodes of high sea-level stand in the Red Sea show higher $^{87}\text{Sr}/^{86}\text{Sr}$ ratios than those from the Arabian Sea with differences up to 0.0001. These observations suggest that: (1) at maximum glacial conditions the Red Sea became an almost closed basin, circulation with the open ocean was limited and the composition of strontium in the water was affected by magmatic-hydrothermal input; (2) during interglacial high sea level stands the Red Sea surface water was affected by local input of more radiogenic strontium which was derived from the surrounding shield.

INIS DOCUMENT

TRN IL 9405673

The Radon Flux Along the Western Rift Fault at Enot Zuqim – Evidence for Geophysical Control

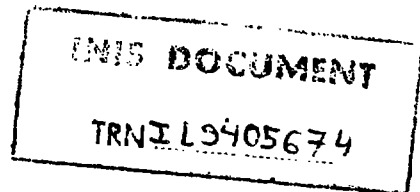
Steinitz, G.,¹ Vulkan, U.,² Assael, Y.,² Yaffe, Y.²

1. Geological Survey of Israel, 30 Malkhe Yisrael Street, 95501 Jerusalem
2. Soreq Nuclear Research Center, Yavne

Monitoring of the radon flux along the western boundary fault of the Rift is being carried out at Enot Zuqim, northwestern corner of the Dead Sea, over a 3 km long sector along the Rift main fault. Three monitoring sites are located on Rift alluvium adjacent to the fault scarp. Two additional sites are located within the Rift, 100 and 500 m east of the main fault. The measurements are integral over 3-4 days.

Data collected for 1992 (and partially 1993) show that the high radon flux is controlled by relatively deep features and events in the subsurface. Thus the temporal variation of the radon flux is considered to be a geophysical phenomenon. Among the indicative features are:

1. Large (order of magnitude) temporal variations in the radon flux are recorded within site and between sites.
2. The three on-fault sites show a similar long term variation (circa 1 year cycle).
3. The two off-fault sites also show a concordant long term variation, which differs from that of the on-fault sites (circa 1/2 year cycle).
4. Statistical analysis indicates a significant correlation of the (temporal) flux between the three on-fault sites.
5. Short term fluctuations (7-20 days) are superimposed in all sites on the long term variation. These fluctuations are radon flux "events". Out of the 18 events defined in the time interval of days 80-366 in 1992, 5 were recorded at all five sites, 2 at four sites and 3 events at three sites.



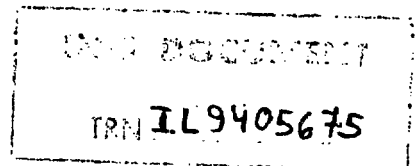
Tracing the Sources of Contaminated Groundwater by Boron Isotope Composition

Vengosh, A.,¹ Heumann, K.G.,² Juráske, S.,² Barth, S.³

1. The Hydrological Service, P.O.B. 6381, 91063 Jerusalem
2. Institute of Inorganic Chemistry, University of Regensburg, Universitätsstrabe 31, Regensburg D-93053, Germany
3. Centre de Recherches Petrographiques et Geochimiques (CRPG-ENSG), 15 rue Norte Dame des Pauvres, BP 20, F-54501 Vandoeuvre-les Nancy Cedex, France

The boron isotope variations were examined in both sewage effluents and contaminated groundwater (by municipal treated sewage) in order to evaluate the potential of boron isotope composition as a tracer for sources of groundwater contamination. We show that the boron isotope composition of raw and treated sewage effluents from the Dan Region Project, Israel ($\delta^{11}\text{B}=5\text{‰}$ to 14‰ ; $\delta^{11}\text{B}$ is defined as $[\frac{^{11}\text{B}/^{10}\text{B}}{\text{sample}} / \frac{^{11}\text{B}/^{10}\text{B}}{\text{NBS 951}} - 1] \times 1000$) overlap with those of natural borate minerals (-0.9‰ to 10.2‰), slightly higher than sodium perborate which is added to detergents (3 ± 1 ; a single sample), and is significantly different from those of regional, uncontaminated groundwater in Israel ($\delta^{11}\text{B}\sim 30\text{‰}$) and sea water ($\delta^{11}\text{B}=39\text{‰}$). The application of sodium perborate as a bleaching agent in detergents and some household cleaners and its discharged to the environment during production and end use lead to a significant enrichment of boron in sewage effluents (0.5 to 1 mg/l in Dan Region Project) relative to natural groundwater ($\text{B}=0.05$ mg/l).

The combination of high boron content coupled with a distinguished isotopic signature is reflected by the compositions of contaminated groundwater associated with artificial recharge of treated sewage effluents ($\delta^{11}\text{B} = 7\text{‰}$ to 25‰). The elemental B and $\delta^{11}\text{B}$ variations reflect both mixing with regional groundwater and boron adsorption onto clay minerals. Nevertheless, the distinctive isotopic signature of anthropogenic boron can still be recognized in most of samples and is different from those of other (natural) sources of salinization in the Coastal Plain Aquifer of Israel, such as marine-derived saline groundwater ($\delta^{11}\text{B}=35\text{‰}$ to 60‰). This enables using the boron isotope composition of groundwater as a tracer for elucidating the sources of contamination of groundwater, particularly for distribution of detergents compounds in aquatic systems.



³⁶Cl and ¹⁴C Measurements of Brines and Fresh Water in the Dead Sea Area, Israel

Yecheieli, Y.,^{1,2} Ronen, D.,¹ Kaufman, A.,¹ Carmi, I.¹

1. Dept. of Environmental Sciences, Weizmann Institute of Science, 76000 Rehovot

2. Geological Survey of Israel, 30 Malkhe Yisrael Street, 95501 Jerusalem

The radioactive isotope concentration in salt and water samples of the Dead Sea area were measured in order to determine their age and source. The brines were found to have low ¹⁴C concentration (3.8 to 26 PMC) compared to the concentration found in the Dead Sea water (about 80 PMC) and thus a relatively old age (>10,000 years). On the other hand, fresh water was found to be younger, with ¹⁴C concentrations being between 55 to 58 PMC.

The ³⁶Cl/Cl ratio in salt of the Sedom Formation ($1.3 \pm 1.3 \cdot 10^{-15}$; found in Amiaz borehole) and in En Ashlag ($6.2 \pm 1.8 \cdot 10^{-15}$) suggest that the source of the brine chloride is not the salt of the Sedom Formation from which the spring emanates. Moreover, the relatively high ³⁶Cl/Cl ratio of En Ashlag demonstrates that this brine was not the parent solution from which the salt of Sedom Formation precipitated.

The radioactive isotope content of the studied water samples suggests that the source of the fresh groundwater is relatively recent recharge in the mountain area, while the brines are remnants of very saline water bodies which existed in the area after the deposition of the Sedom Formation (in the last 500,000 years) and probably before the formation of the present Dead Sea (hence, Lake Lisan, Lake Samra or even an older lake).

IL9405676



ANNUAL MEETING, 1994



EDITED BY:

Rivka Amit,¹ Yaacov Arkin,² Francis Hirsch²

¹Department of Physical Geography,
The Hebrew University, Jerusalem

²Geological Survey of Israel, Jerusalem

NOF GINOSAR

28 FEBRUARY – 2 MARCH

1994

Contents

	Page
AGNON, A., MARCO, S. Fault Controlled Slumping in Lake Lisan Sediments - Massada Plain	1
ALMOGI-LABIN, A. , SIMAN-TOV, R., ROSENFELD, A., DEBARD, E. Diatoms, Foraminifers, and Ostracods in the Ubeidiya Formation (Jordan Valley) and their Paleological Implications	2
AMIT, R., HARRISON, J.B.J., ENZEL, Y., PORAT, N. Use of Soils and Colluvial Deposits in Analyzing Tectonic Events — the Southern Arava Rift, Israel	3
AVNI, Y. Plio-Pleistocene Tectonic Deformation - A Key to Dividing the Continental Dead Sea Group in the Negev and the Arava Valley	4
AVNI, Y., FRIESLANDER, U., BARTOV, Y., GINAT, H., GARFUNKEL, Z. The Baraq - Zihor - Zenifim Fault: A Plio-Pleistocene Fault Line across the Southern and Central Negev	5
BAER, G., HEIMANN, A., WEINBERGER, R., MUSSETT, A., SHERWOOD, G. Late Triassic - Early Jurassic Magmatism in Southeastern Makhtesh Ramon, Israel	6
BAER, G., MIMRAN, Y. Block Rotation in the Fari'a Anticline, Eastern Shomeron	7
BAER, G., PALMER, H.C., HEIMANN, A., AHARON, L. Determination of Flow Directions in Israeli Basalts by Anisotropy of Magnetic Susceptibility: Preliminary Results	8
BAR-MATTHEWS, M., AYALON, A., SASS, E., HALICZ, L. Geochemical Evolution of Water in Karstic Terrains — Soreq Cave	9
BECK, A., RONEN, A. Infrastructure Surveys, Mapping, and Identification Using Ground Penetrating Radar (GPR)	10
BEN-GAI, Y. , GILAD, D. On the Discrepancy between Base Kurkar Group and Base Coastal Aquifer in the Southern Sharon — Results from Seismic Profiles	11
BENJAMINI, C. An Event-Stratigraphy Approach to Eocene Lithostratigraphy in Israel	12
BERGELSON, G., NATIV, R., BEIN, A. Assessment of Hydraulic Parameters in the Kinneret Basin	13

BEYTH, M., HENKEL, J., GEERKEN, R. Applying Image Processing Techniques for Analysing TM Data from the Timna and Feinan Areas and Multispectral GER-II Data from Makhtesh Ramon	14
BLUM-LAUB, R, STARINSKY, A., AYALON, A. Diagenetic Dolomite-Ankerite in Zohar Formation in the Northern Negev	15
BUTENKO, V., NE'EMAN, E., BRENNER, S., KRONFELD, J., GILAT, A. Chernobyl in Israel	16
CARMI, G., DODY, A. Runoff Simulation in a Desert Watershed and Sensitivity Analysis of a Rainfall-Runoff Model	17
CARMI, G., KARNIELI, A. Geographic Information System Use for Runoff Forecasting	18
COHEN, B., MATTHEWS, A., BAR-MATTHEWS, M., AYALON, A. Fluid-Rock Interactions During the Formation of Metamorphic Dike- Schists, Elat Metamorphic Complex	19
CONWAY, B.H. Organic Petrology: Preliminary Investigations on the Melekh Sdom 1 Borehole, Southern Dead Sea Basin	20
DRUCKMAN, Y., GELBERMANN, E., FLEISCHER, L., WOLFF, O., GILL, D. Late Cretaceous Inversion of Early Mesozoic Structures: Examples from the Negev, Southern Israel	21
ENZEL, Y., AMIT, R., HARRISON, J.B.J, PORAT, N. Morphologic Dating of Fault Scarps in the Southern Arava, Israel and Comparison to other Dating Techniques	22
EPPELBAUM, L., PILCHIN, A. New Map of Moho Discontinuity of Israel	23
EYAL, M., VOZNESENSKY, V., BENTOR, Y. The Geological Map of the Precambrian of South-Western Sinai, Scale 1:50,000	24
EYAL, Y. Stress Field Fluctuations Adjacent to the Dead Sea Rift Since the Middle Miocene	25
FRIESLANDER, U., BARTOV, J., GARFUNKEL, Z., ROTSTIEN, Y., RYBAKOV, M. The Structure of the Arava — Initial Results from Geophysical Survey	26
GANOR, E., FONER, H.A., PELED, Y., BRENNER, S., KOPELIOVICH, I. Input of Atmospheric Aerosols into Lake Kinneret — Preliminary Results	27

GANOR, J., MOGOLLON, J.L., SOLER, J.M., LASAGA, A.C. What Can Column Experiments Tell Us About Global Chemical Weathering?	28
GAVRIELI, I., STARINSKY, A., SPIRO, B., NIELSEN, H., AIZENSHTAT, Z. Sulfur Isotopes Evidence for Sulfate Removal Processes from Subsurface Brines, Heletz Formation (Lower Cretaceous), Israel	29
GEV, I., GOLDMAN, M., RABINOVICH, B., RABINOVICH, M. TDEM and NMR Geophysical Methods for a Hydrological Purpose	30
GINAT, H. Reversal of Stream Flow Direction Along the Margins of the Southern Arava Valley Resulting from Tectonic Tilting	31
GINZBURG, D. Biq'at Ginnosar in Jewish Traditional Literature	32
GITTERMAN, Y., ZASLAVSKY, Y., SHAPIRA, A. Response Spectra of Earthquakes in the Gulf of Elat Recorded by the Israel Seismic Network	33
GOLAN, G., SHOVAL, S., PITT, C.W. Scanning Acoustic Microscopy for Petrographic Imaging	34
GOLDSHMIDT, V., RYBAKOV, M., SEGEV, A., ITAMAR, A. Subsurface Structure and Composition of the Ramon Region	35
GOLTS, S., KOLTON, Y. The Influences of Tectonics in Salinization in the Coastal Aquifer	36
GONEN, O., GVIRTZMAN, H. Laboratory Simulation of Aquifer Remediation: In-situ Vapor Stripping	37
GREENBAUM, N., SCHICK, A.P. Paleofloods in Nahal Zin	38
HATZOR, Y., MIMRAN, Y. Mechanical Behavior of some Dolomites from the Judea Group: Preliminary Results	39
HIRSCH, F., FLEXER, A., ROSENFELD, A., YELLIN-DROR, A. Tectonic Setting and Crustal Structure of the Eastern Mediterranean	40
HOEK, R., ESHET, Y., ALMOGI-LABIN, A. A New Palyno-Zonation Scheme for Campanian-Maastrichtian Organic-Rich Carbonate Sequences in Israel	41
HONIGSTEIN, A., HIRSCH, F., ROSENFELD, A., FLEXER, A. Methusaleh — or Lazarus — Effect in the Ostracod Species <i>Cythereis</i> Mesa	42

HOVERS, E., GOREN, Y., RABINOVICH, R., RAK, Y. The Neanderthal Site of Amud Cave, Israel	43
INBAR, M., SHRODER, J. Late Holocene Palaeogeography of the Bethsaida Area	44
ISAAC, Y. Fluorescence Photography of Minerals	45
ITAMAR, A., SEGEV, A., PELTZ, S. Volcanic Phenomena in Quartz-Syenite Bodies in Gavnunim and Shen Ramon	46
ITKIS, S., SELIGMAN, J. , ISRAELI, S. Micromagnetic Study of Archaeological Sites in the North of Israel	47
KANEL, E. Fractal Analysis of the Earthquake Catalog of Israel	48
KAPULSKY, M. Oil and Gas Bearing Prospects of the Continental Shelf of Israel	49
KAPUSTA, Y., STEINITZ, G., KOTLARSKY, P. Neutron Shielding by H ₂ O in Clay Minerals - an Explanation for ³⁹ Ar Deficit in Irradiated Clay Fractions	50
KARCZ, Y., PERATH, I. Criteria for Archeoseismic Events: Evidence from Negev Sites	51
KATSAV, E., GVIRTZMAN, G. The Origin of the Kurkar Ridges in the Sharon (Central Coastal Plain, Israel)	52
KATSAV, E., GVIRTZMAN, G. Stratigraphy of the Quaternary Sequence of the Coastal Cliff of the Sharon (Central Israel)	53
KHESIN, B. Proposed Method for Revealing Hidden Concentric Structures in Complex Geophysical Fields	54
KLEIN, M., KOREN, N., NISHARI, A. Sedimentation Rates and Particle Dynamics in the Northern and Central Parts of Lake Kinneret	55
KNUBOVETS, R., SHOVAL, S., GAFT, M., NATHAN, Y., RABINOWITZ, J., PREGERZON, B. Infrared Study of the Carbonate Ions in Apatites from the Negev Phosphorites	56

KOFMAN, L., CNAAN, D., GADOT, I., KLAR, I. Detection of Underground Caves and Voids Using Georadar	57
KRASILSHIKOV, L., CARMI, G. Peak-Flow Prediction of Perennial and Ephemeral Streams	58
LANG, B., KILINC, A., STEINITZ, G. Petrology and $^{40}\text{Ar}/^{39}\text{Ar}$ Dating of the Qarney Ramon Basalt — Makhtesh Ramon	59
LEVITTE, D. Groundwater Pollution at the Hadera Waste Disposal Site, in the Coastal Sandstone Aquifer (Pleshet Formation)	60
LIVSHITS, Y. The Platform Structure of Israel and Sinai (Main Elements)	61
LOEWENTHAL, D., KAGANSKY, A., BUCHEN, P. Zero Moveout (ZMO) Stacking	62
LYAKHOVSKY, V., BEN-AVRAHAM, Z., ACHMON, M. The Origin of the Dead Sea Rift: Results of Computer Simulations	63
MALITSKY, A., SHAPIRA, A. Latest Results of the Experimental Seismic Antenna on Mt. Tur'an, Israel	64
MALITSKY, A., SHAPIRA, A. Software Package "Seismological Bulletin of Israel"	65
MATMON, D., GVIRTZMAN, H. The Flow Field Between the Mediterranean Sea and the Jordan Rift Valley	66
MAVASHEV, B. Analysis and Estimate of Interrelation between Ecologic and Geodynamic Processes	67
MAY, P. R. Horizontal Drilling	68
MAZOR, E. Groundwater Composition in Lithostratigraphic Units, Israel - Scientific and Management Implications	69
MELLOUL, A., GOLDENBERG, L.C. The Influence of a Year Abundant in Precipitation on the Groundwater Quality: The Case of the Israeli Coastal Aquifer in 1991/92	70
MODELEVSKY, M. Thermal and Formation Pressures Study: Implication for the Further Development of Nearly Depleted Petroleum Areas	71

MUKHIN, P., GARFUNKEL, Z. Geodynamic evolution of Andros island (Greece) Based on Structural Analysis	72
NADEL, D., NIR, Y. Water Levels of Lake Kinneret: New Archaeological Evidence	73
NATHAN, Y., SOUDRY, D., DORFMAN, E., LEVY, Y., SHITRIT, D. The Geochemistry of Cadmium in the Negev Phosphorites	74
NETSER, M., GVIRTZMAN, G. Geological Map of the Quaternary of Gush Dan (Central Coastal Plain, Israel)	75
NIEMI, T. M., BEN-AVRAHAM, Z. Lake Lisan and Dead Sea levels from Seismic Reflection Profiles in the North Dead Sea Basin	76
ORION, N. Geological Sites in Danger of Destruction	77
PARPAROVA, R. Sedimentation of Iron in Lake Kinneret	78
PATYK-KARA, N., PLAKHT, J. Red Valley and Other Concentric Morphostructures in the Eastern Makhtesh Ramon	79
PINSKY, V. Effective Noise Suppression for the Detection and Discrimination of Seismic Array Signals	80
PLAKHT, J. Pedimentation as the Leading Geomorphic Process in the Evolution of Makhtesh Ramon	81
PLAKHT, J., ZASLAVSKY, N. Features of the Late Pleistocene Development of Western Makhtesh Ramon	82
POLISHOOK, B., FLEXER, A. Stress Measurement on Eocene Chalk Rock Mass by the Hydrofracture Test	83
PORAT, N., AMIT, R., WINTLE, A.G. IRSL Dating of Fault-Related Sediments at the Nahal Shehoret Alluvial Fan, Southern Arava, Israel	84
PORAT, N., WINTLE, A.G. IRSL Dating of Kurkar and Hamra from the Givat Olga Member in the Sharon Coastal Cliff, Israel	85

RABINOWITZ, N. Is it Possible to Reach a Consensus in Seismic Hazard Evaluation in Israel?	86
RAZ, I., ADAR, E., ISSAR, A. Tracing of Water Movement in Unsaturated Sandy Dunes Using Stable Isotopes of Hydrogen and Oxygen	87
REZNIKOV, M., BEN-AVRAHAM, Z. Structure of Lake Kinneret Region from Gravity Analyses	88
ROTSTEIN, Y., SHALIV, G. Initial Results of a Seismic Reflection Survey in the Yizreel Valley	89
SALAMON, A., RON, H., GARFUNKEL, Z., HOFSTETTER, A. The Complex Deformation North of the Carmel-Fari'a Line and its Structural Significance	90
SAMOYLOV, V., BEKKER, A., EYAL, M. Early Cretaceous Basanitic Volcanic Lake	91
SANDLER, A., DOLEV, M. KNO ₃ Stalactites in a Cave at Har Nitai	92
SANDLER, A., HAMBRIGHT, K.D., BRENNER, I., HALICZ, L. Chemical Seasonal Variations in the Water Column of Lake Kinneret	93
SCHOLOMOVICH, N., BAR-MATTHEWS, M., SEGEV, A., MATTHEWS, A. Copper Sulfides in the Cambrian Timna Formation	94
SHAHACK-GROSS, R., TCHERNOV, E., KOLODNY, Y., LUZ, B. Isotopic Differences Between Bones of Different Periods: Climatic or Diagenetic Changes?	95
SHAHAR, J. The Case for Early Miocene Deposition of the Hatseva Formation in the Dead Sea Rift	96
SHAMIR, G., EYAL, Y. Reconstruction of Fault Patterns Underlying Folds — Mechanical Constraints	97
SHAMIR, G., SHAPIRA, A. Spatial and Temporal Distribution of Earthquake Sequences in the Gulf of Elat	98
SHAPIRA, A. Automatic Identification of the Time of Increased Probability for a Felt Earthquake	99

SHAPIRA, A. The Seismicity of the Dead Sea Transform with Application to the Estimation of Tectonic Movement	100
SHAPIRA, A., GITTERMAN, Y., ZASLAVSKY, Y. Semi-Empirical Attenuation Functions for Seismic Ground Motions in Israel	101
SHIRMAN, B Electrotelluric Field Anomalies Associated with Earthquakes	102
SHOVAL, S. A Regional Lower Cretaceous Hydrothermal Circulation in Makhtesh Ramon Area	103
SHOVAL, S., KNUBOVETS, R., GAFT, M., NATHAN, Y., RABINOWITZ, J., PREGERZON, B. Crystallochemical Heterogeneity of Apatites in the Negev Phosphorites	104
SHTAINMAN, B., PARPAROV, A. The Potential of Resuspension in Lake Kinneret Estimated from Current Velocity Measurements	105
SIVAN, D., GVIRTZMAN, G., KAUFMAN, A., SASS, E. The Yasaf Member: A Strombus Bearing Unit on the Coast of Galilee Representing Tyrrhenian Event in the Mediterranean	106
SNEH, A., BARTOV, Y., ROSENSAFT, M. Geological Map of Israel 1:200000 Scale, North Sheet	107
STEIN, M., AGNON, A., STARINSKY, A., RAAB, M., KATZ, A., ZAK, I. What is the "Age" of the Sedom Formation?	108
STEIN, M., ALMOGI-LABIN, A., GOLDSTEIN, S.L., HEMLEBEN, C., STARINSKY, A. Sr isotopes in a Red Sea core - inferences for the Red Sea history during the last 400 kyr.	109
STEINITZ, G., KAPUSTA, Y., SANDLER, A., KOTLARSKY, P. ⁴⁰ Ar- ³⁹ Ar Age of Authigenic Feldspar from the Cenomanian Hazera Formation	110
STEINITZ, G., VULKAN, U., ASSAEL, Y., YAFFE, Y. The Radon Flux Along the Western Rift Fault at Enot Zuqim - Evidence for Geophysical Control	111
VAPNIK, Y., FRID, V. Fluid Inclusion and Fracture Study of the Elat Granite	112

VENGOSH, A., HEUMANN, K.G., JURASKE, S., BARTH, S. Tracing the Sources of Contaminated Groundwater by Boron Isotope Composition	113
VILEN, M., EPPELBAUM, L. Multi-Criterion Estimation of Geological Prospecting Effectiveness	114
WDOWINSKI, S., ZILBERMAN, E. Large-Scale Asymmetries Across the Dead Sea Rift: a Half Graben Model for the Formation of the Arava Valley and Dead Sea Basin	115
WEINBERGER, R., RECHES, Z., SCOTT, T. E., EIDELMAN, A. A New Approach to Determine Tensile Strength of Rocks Under Confining Pressure	116
WEINSTEIN, A. Application of the Spectral Time Analysis Technique (STAN) in the Central Coastal Plain Area	117
WHYBROW, P.J., SAVAGE, J.R.G., ROTHMAN, S., ELDERFIELD, H., GOLDSMITH, N.F. SR Isotopic Calibration of N. African-Arabian Neogen Vertebrates	118
WOLFSON, N. Some New Views on the Structure of Central Israel, Based on a Synthesis of Geological and Geophysical Data	119
YECHIELI, Y., RONEN, D., KAUFMAN, A., CARMI, I. ³⁶ Cl and ¹⁴ C Measurements of Brines and Fresh Water in the Dead Sea Area, Israel	120
ZASLAVSKY, N., AVNI, Y. Freshwater Fauna in a Clastic Lens within the Ghareb Formation: Implications for a "Ramon Island"	121
ZASLAVSKY, Y., SHAPIRA, A. Spectral Analysis of Vibrations of Steel Constructions and its Applications for Estimating Dynamic Characteristics	122
ZILBERBRAND, M. Salt Precipitation in Root Zone as Affecting Groundwater Chemical Composition	123
ZILBERMAN, E., BAER, G., AVNI, Y., FEIGIN, D., GOLDMAN, M., EYAL, A. Post Arava Conglomerate Tectonic Activity Along the Arif-Batur Fault	124

Fault Controlled Slumping in Lake Lisan Sediments - Massada Plain

Agnon, A.,¹ Marco, S.^{1,2}

1. Institute of Earth Sciences, The Hebrew University of Jerusalem, 91904 Jerusalem

2. The Institute for Petroleum Research and Geophysics, P.O.B. 2286, 58122 Holon

Intraformational slumps in Lake Lisan deposits have previously been associated with seismotectonic activity, though lack of direct evidence has impeded inference of paleoseismicity. We report field evidence for faulting that controlled sedimentary slumps at the bottom of Lake Lisan. The disturbed section is close to the base of the Lisan Formation in Massada Plain, and consists mostly of laminated chalk and clay. Faults that displace the base of the exposed section by 0.5-2 m are unconformably overlain by continuous beds. The down-thrown block shows intraformational folds, the axes of which parallel the adjacent fault planes. These folds have amplitudes and wavelengths of up to 1m. Axial planes dip towards the fault plane, suggesting transport in the opposite direction. The folding is more intense close to the fault planes, with disharmonities and overturned beds.

The folded layer is overlain and, in places, truncated by a "mixture" layer up to 0.2 m thick. This "mixture" seems to consist of the detrital and authigenic components of the chalk, otherwise differentiated to varves. Fragment of the white varves (chemically precipitated aragonite), up to 1 cm long, are observed in places in the "mixture" layers. Each of the faults can be traced to at least one "mixture" layer on top of the folded sequence in the downthrown block.

The faults are normal to vertical, and display a wavy surface in a vertical section in places. The faults strike dominantly 340-350°. We traced four parallel fault planes, spaced at about 15 m, along over 100 m in the field. The largest displacement is on the westernmost fault (2 m), that throws the eastern block down. The eastern faults throw 0.5-1 m antithetically (western block down), hence forming a graben. A single fault plane which strikes 050° throws down the southern block about 1 m.

We interpret these observations as follows: faulting has repeatedly generated morphological steps at the bottom of Lake Lisan. The sediments behaved according to their degree of lithification and the distance from the interface: sufficiently compacted beds simply faulted; soft but cohesive beds from the lifted block slumped to the lowered block while folding; the least compacted (during the faulting event), uppermost beds, lost cohesion and their constituents returned to suspension during faulting. The overall picture suggests that slumping was triggered by tectonic faulting and further research on these outcrops may contribute to a quantitative history of faulting in the Lisan basin. If slumping is triggered by prominent earthquakes then the "mixture" layers, being at the water-sediment interface, should correlate over large distances. This can be tested by current dating methods.

Diatoms, Foraminifers, and Ostracods in the Ubeidiya Formation (Jordan Valley) and their Paleological Implications

Almogi-Labin, A.,¹ Siman-Tov, R.,¹ Rosenfeld, A.,¹ Debard, E.²

1. Geological Survey of Israel, 30 Malkhe Yisrael Street, 95501 Jerusalem

2. Centre des Sciences de la Terre, Universite Claude Bernard LYON1, F-69622 Villeurbanne Cedex, France

Microfossils of the Ubeidiya site in the Jordan Valley, a Pliocene lake-edge deposit which has yielded a rich vertebrate fauna and an early Acheulian lithic industry, were studied in two selected sections. Of the foraminifera, only *Ammonia beccarii tepida* and *Ammonia beccarii cf. parkinsoniana* were found at the base of the Lower Limnic Cycle (Li). Diatoms were found in the lower and upper parts of Li. Ostracods were found throughout the section. In each of the groups, diatoms and ostracods, two distinct salinity assemblages were identified. Assemblage 1 represents freshwater (to oligohaline?) salinity (<5 ‰) and assemblage 2 represents a mesohaline range (5–30 ‰). *Ammonia spp.* were found only within the mesohaline range. According to the microfossil sequence the Li cycle of the Ubeidiya Formation was deposited in a freshwater lake with mesohaline phases during its early and late stages. Reworked Paleogene foraminifera are abundant in the intermediate (freshwater to mesohaline) stage pointing to strong fluvial activity, possibly associated with turbidity which reduced diatom productivity.

Use of Soils and Colluvial Deposits in Analyzing Tectonic Events — the Southern Arava Rift, Israel

Amit, R.,¹ Harrison, J.B.J.,² Enzel, Y.,¹ Porat, N.³

1. Institute of Earth Sciences, The Hebrew University of Jerusalem, 91904 Jerusalem

2. Dept. of Geosciences, New Mexico Institute of Mining and Technology, Socorro, NM 87801, USA

3. Geological Survey of Israel, 30 Malkhe Yisrael Street, 95501 Jerusalem

An essential part of determining the seismic hazard of an area is to identify the paleoseismicity of existing faults. In non-consolidated sedimentary material, under extremely arid climatic conditions and where there is no suitable material for radiometric dating methods, two methods were developed to identify different faulting events: 1. Analyzing colluvial units along fault scarps and terrace risers; 2. Using soils as a relative dating tool.

Soils and colluvial stratigraphy along fault scarps differ clearly from those on terrace risers in the Nahal Shehoret alluvial fan, southern Arava. Several colluvial units were found on the fault scarp whereas only two were found on the terrace risers. The colluvial units on the fault scarp are triangular in shape, and those on the terrace riser are bowl shaped. Cumulic soils indicating continuous deposition were found on the terrace riser whereas episodic deposition producing buried soils characterized the fault scarp colluvium. The soils and the sedimentary composition of the colluviation processes resulting from several tectonic events, whereas those on the terrace scarp suggest low erosion rates.

A reasonable similarity was found between the age of surfaces by OSL, scarp degradation modelling and soil development. Thus, soils can be used to give an estimated age of a faulted surface, a maximum estimate of the age of scarp age, and the recurrence intervals of faulting events. Only by exposing the colluvium however can the complete record of scarp activity be obtained.

Plio-Pleistocene Tectonic Deformation - A Key to Dividing the Continental Dead Sea Group in the Negev and the Arava Valley

Avni, Y.

**Institute of Earth Sciences, The Hebrew University of Jerusalem, 91904 Jerusalem
Geological Survey of Israel, 30 Malkhe Yisrael Street, 95501 Jerusalem**

Morphotectonic and morphostratigraphic research was carried out during the last years in the Paran and the Neqarot drainage basins and the margin of the Arava Valley. Consequently, several morphostratigraphic units that developed in the region during the Pliocene and the Pleistocene have been differentiated. The key unit among these is the Arava Conglomerate, that differs from the others in its morphostratigraphic position and sedimentological characteristics. Intensive study, focusing on the reasons for the degeneration of this drainage system, demonstrates the role played by the Plio-Pleistocene tectonic deformation. The tectonic system of the region has two main components:

1. A fault system of sub-parallel fault lines, striking N 35-40°E, that vertically displace the fluvial-lacustrine units of Arava Conglomerate by more than 100 m. The faults create tilted blocks, grabens and horst structures, widespread in the central and southern Negev.
2. A regional eastward tilt that affected more than 4000 km² tilted the central and southern Negev 1-2°. The total tilting exceeds several hundred meters. The tilting is a result of the young subsidence of the Arava basin, and the contemporaneous uplift of the central Negev mountains relative to the Arava and the Wadi El-Arish basins, on both sides of the uplifted area.

The tectonic activity changed the inclination regime in the whole area and led to the generation of the Arava Conglomerate drainage system.

The wide area that was affected by the tectonic deformation enables differentiating the continental section of the Dead Sea Group in the region into two principal units:

1. Pre-tectonic. It is proposed that this unit be referred to as the Arava Formation.
2. Post tectonic units.

The Baraq - Zihor - Zenifim Fault: A Plio-Pleistocene Fault Line across the Southern and Central Negev

Avni, Y.,^{1,2} Frieslander, U.,³ Bartov, Y.,² Ginat, H.,¹ Garfunkel, Z.¹

1. Institute of Earth Sciences, The Hebrew University of Jerusalem, 91904 Jerusalem

2. Geological Survey of Israel, 30 Malkhe Yisrael Street, 95501 Jerusalem

3. The Institute for Petroleum Research and Geophysics, P.O.B. 2286, 58122 Holon

A prominent fault line, about 70 km long, is clearly recognized within the Plio-Pleistocene N 30-40 E fault system crossing the Central and Southern Negev. The fault line was divided into several segments:

The Baraq fault: From Zofar to the Paran "bottle neck". The Fault line is vertical to normal, alternating with steep flexures. In Ramat Baraq and Ramat Zofar, a few parallel faults created several horst and graben structures. In most cases, the eastern block is downfaulted 150-100 m. Only at the northern segment of Ramat Omer the western block is downfaulted. A displaced Arava Conglomerate valley indicate that the faulting took place after the deposition of the Arava Conglomerate in the Late Pliocene - Early Pleistocene. The Baraq fault is clearly identified as a wide tectonic deformation zone in the seismic reflection lines in the Arava Valley near Zofar.

Near the junction between the Baraq and the Paran faults, a number of minor parallel fault planes appear. A cluster of epicenters which had been recorded within the last ten years, as well as open fractures and collapse of massive boulders indicate a recent activity, associated with left-lateral motion.

Zihor fault: located south of the Baraq fault, between the Nahal Zihor and Ramat Ovil. The vertical displacement along the Fault is about 100 m. In the upper part of Nahal Zihor, faulting of young Pleistocene terraces has been discovered. Another segment, the Mitzpe-Paran - Zuki-Zihor is located some 3-4 km to the east of the main fault. A narrow graben developed between these faults, is a part of the graben system of the Southern Negev (Ovda and Sayarim Grabens).

Zenifim fault: A 10 km reverse fault is located on the eastern flank of the Zenifim anticlinal structure. The Arava Conglomerate was deposited within valleys incised on both sides of the anticlinal structure. A tectonic eastward tilt, postdate the deposition of the Arava Conglomerate, tilt the Zenifim anticlinal structure and emphasize its asymmetric structure. The anticlinal axis and the fault line continue to the Gebel Sueiqa structure in Eastern Sinai.

Late Triassic - Early Jurassic Magmatism in Southeastern Makhtesh Ramon, Israel

Baer G.,¹ Heimann, A.,¹ Weinberger R.,^{1,2} Mussett A.,³ Sherwood G.⁴

1. Geological Survey of Israel, 30 Malkhe Yisrael Street, 95501 Jerusalem

2. Institute of Earth Sciences, The Hebrew University of Jerusalem, 91904 Jerusalem

3. Department of Earth Sciences, University of Liverpool, Liverpool, UK

4. School of Biological and Earth Sciences, Liverpool John Moores University, Liverpool, UK

Intrusive and extrusive igneous rocks are exposed in Makhtesh Ramon, southern Israel. Radiometric dating of these rocks in the past enabled identification of several magmatic events, all during the Early Cretaceous. New basaltic outcrops, more massive and less altered than the Cretaceous basalts, have been recently identified near 'En Saharonim (coords. 1441/0022). Several noncontinuous outcrops are scattered in an area of about 400x400 m, within the gypsum layers of the Upper Triassic Mohila Formation. No baking effect has been found in the overlying layers, and it is therefore suggested that the rocks are not intrusive but have been formed as flows. The rocks average 46.8% SiO₂, 14% Al₂O₃, 9.3% CaO, 10.2% MgO, 2.7% Na₂O, and 0.7% K₂O, which according to the classification of Le Bas et al. (1986) fall in the basalt field. They show porphyritic textures with 10% to 20% olivine phenocrysts 0.2 to 1 mm large.

Two samples from one outcrop were dated by the ⁴⁰Ar/³⁹Ar method, one in the geochronological laboratory of the University of Liverpool and the other in the Geological Survey of Israel. Two samples from two additional outcrops were dated by K-Ar method in the Geological Survey of Israel. The ages obtained are 207±4 Ma (at the Geological Survey) and 215±5 Ma (Liverpool), i.e., Late Triassic or Early Jurassic. The difference between the results of the two laboratories is partly due to different calibration of international standards. Recalculation of the age obtained by the British laboratory, with the standards used in the Geological Survey yields an age of 212±5 Ma.

Paleomagnetic measurements were carried out on 12 samples from two sites. Since the number of measured sites is too small to average the secular variations, a paleomagnetic pole was not calculated. However, the directions infer that the area was located close to the equator during that period.

As basalts in general occupy areas larger than a few hundred meters, we expect that more occurrences of this basalt may be found in Makhtesh Ramon or its vicinity. Such volcanism has been unknown in southern Israel until now. The chemical and age similarities with the Asher Volcanics of northern Israel suggest that they are part of the same volcanic phase.

Block Rotation in the Fari'a Anticline, Eastern Shomeron

Baer, G., Mimran, Y.

Geological Survey of Israel, 30 Malkhe Yisrael Street, 95501 Jerusalem

A sequence of sedimentary and volcanic rocks of Jurassic to Recent age is exposed at the core and along the flanks of the Fari'a anticline in northeastern Shomeron. The NE-trending anticline is crossed by several major NW and NNW-trending faults which form a series of horsts and grabens. Most of these faults are restricted to the Fari'a anticline and do not continue northwestward or southeastward into the adjacent Shekhem and Sartaba synclines. The NNW-trending faults have been found to be younger (Shaliv et al., 1991). Paleomagnetic and structural studies have indicated that block rotation about vertical, as well as about inclined axes, played a major role in the deformation of the margins of the Dead Sea rift in northern Israel (Ron et al., 1984, 1990; Heimann, 1990).

A preliminary paleomagnetic analysis of the northeastern Fari'a anticline was carried out to test the possibility of block rotation in that area as well. The mean declination of Early Cretaceous basalts from the anticline core deviates counterclockwise by $22.6^{\circ} \pm 9.4^{\circ}$ with respect to the expected Early Cretaceous direction; the mean inclination is similar to the expected direction. The sense of deviation is similar to that of the Tiberias, Korazim and Mt. Hermon provinces, whereas the amount of deviation differs from one province to another. The Late Miocene basalts from the eastern anticline flank show directions which are essentially similar to those expected for the Late Miocene.

These results may be interpreted in two ways: (1) block rotation in northeastern Shomeron terminated before the Late Miocene; (2) block rotation may have occurred after the Late Miocene but is limited to the domain of NW trending faults at the core of the Fari'a anticline and does not occur at the anticline flanks. This interpretation is supported by the observation that the NW trending faults are also limited to the anticline and do not extend northwestward or southeastward.

Both interpretations require right lateral displacements along the NW-trending faults. No direct evidence supporting such displacements have been found so far. Counterclockwise rotation in the Fari'a anticline should be accompanied by elongation in the NW direction and shortening in the NE direction. It is speculated here that the NE shortening is expressed by the formation of a triangular "gap" in the form of the Bet She'an Valley, whereas elongation in the NW direction is expressed by narrowing of the Jordan Valley southeast of the Fari'a anticline and by the development of the steep flexures on both flanks of the anticline. The assumed boundaries of the domain under discussion are the belts of Mt. Scopus Group chalk on the anticline flanks.

Determination of Flow Directions in Israeli Basalts by Anisotropy of Magnetic Susceptibility: Preliminary Results

Baer, G.,¹ Palmer, H.C.,² Heimann, A.,¹ Aharon, L.^{1,3}

1. Geological Survey of Israel, 30 Malkhe Yisrael Street, 95501 Jerusalem

2. Department of Geophysics, University of Western Ontario, London, Ontario, Canada

3. Institute of Earth Sciences, The Hebrew University of Jerusalem, 91904 Jerusalem

Magnetic susceptibility [K] is defined by $M = [K] \times H$, where M is the induced magnetism of the rock, and H is the inducing magnetic field. Magnetic susceptibility is generally anisotropic and is expressed by a second order symmetric tensor (ellipsoid). In a single magnetic mineral, the maximum susceptibility usually coincides with its long axis. The anisotropy of the magnetic susceptibility (AMS) in the rock is caused by preferred orientation of anisotropic magnetic minerals. It may thus be utilized for inferring preferred orientations in the rock, which may be caused by flow or by weak tectonic deformation. Elongated minerals tend to align parallel to flow direction, and thus, the long axis of the susceptibility ellipsoid may indicate this lineation.

To evaluate the use of AMS measurements for the determination of flow directions in Israeli basalts, we chose examples of lavas where flow directions were clear from morphologic considerations and dikes in which the flow directions were inferred independently. AMS measurements were carried out at the University of Western Ontario, Canada, and at the Geological Survey of Israel. The AMS results were compared with the field evidence.

'En Zivan basalt, which flowed along an azimuth 281° trending riverbed from the Golan Heights to the Hula Valley, showed a maximum susceptibility direction of $0.4^\circ / 315^\circ$, a deviation of 35° from the riverbed direction. 'En Zivan basalt that flowed from Har Odem in a direction of 140° , showed a maximum susceptibility direction of $32.5^\circ / 154^\circ$, deviating by 14° from the expected direction. A horizontally propagating 300° -trending dike in Mt. Khtesh Ramon showed a maximum susceptibility direction of $6.8^\circ / 308^\circ$, and a 90° -trending dike in Tel Agol (near Giv'at Hamore') showed a maximum susceptibility direction of $53^\circ / 087^\circ$. The flow direction in that dike may be estimated from the AMS results to be oblique.

These preliminary results show a reasonable agreement between field and AMS directions, and indicate that AMS measurements could be utilized for inferring flow directions and locations of eruptive centers where the field evidence is not so clear.

Geochemical Evolution of Water in Karstic Terrains — Soreq Cave

Bar-Matthews, M.,¹ Ayalon, A.,¹ Sass, E.,² Halicz, L.¹

1. Geological Survey of Israel, 30 Malkhe Yisrael Street, 95501 Jerusalem

2. Institute of Earth Sciences, The Hebrew University of Jerusalem, 91904 Jerusalem

Ground waters percolating downward through the vadose zone the Soreq Cave via two main mechanisms: water dripping down stalactites slowly and constantly throughout the year, and fast-dripping water entering the cave only during the winter rainfall seasons.

Both water types are saturated with respect to calcite, and contain dissolved inorganic carbon (DIC) with concentrations of 5-11 mM, and Ca 0.75 - 1.75 mM. $\delta^{13}\text{C}$ of the dissolved carbon ranges from -14.5 to -12‰ PDB. The isotopic composition and the CO_2 content indicate that the water absorbed CO_2 from the soil, and dissolved the country rock during their downward migration. Mg/Ca and Sr/Ca molar ratios are in the range 0.5 to 2.0 and 0.5 to $2.0 \cdot 10^{-3}$ respectively. These ranges are consistent with petrographic evidences showing calcite deposits in voids, causing the solutions to be depleted in Ca and the ratios to increase. At the beginning of the rainy season, HCO_3^- and Ca^{2+} contents in the fast-drip water reach the highest values observed in the cave, 7.4 and 2.5 mM respectively. This water contain also the highest contents of dissolved salts, suggesting that the first rains flush downward material which had accumulated in soils and fissures during the summer.

During the winter, the oxygen isotopic composition of the two water types reflects the average composition of the rain, and are similar to the springs in the area ($\delta^{18}\text{O} = -6\%$ SMOW). During the dry seasons the $\delta^{18}\text{O}$ values of the stalactite-dripping water are higher (up to -3.5‰) due to evaporation processes in the vadose zone.

The chemical composition of the water accumulating in pools within the cave is a function of the composition of the two water types, and their modification by dissolution-precipitation processes of carbonate minerals. Pools receiving their waters mainly from fast dripping sources show significant seasonal variations, whereas pools getting their water from a stalactite-dripping source are chemically uniform. Pools that are fed by water flowing from higher parts of the cave reflect both the source water types and modifications by precipitation of carbonate minerals. In pools where deposition of calcite is not taking place, Mg/Ca and Sr/Ca ratios are similar to those of their source water. In contrast, in pools where recent deposition of calcite occur, these ratios can reach values as high as 4.5 and $4.5 \cdot 10^{-3}$ respectively, and they are linearly and positively correlated with each other. In the deepest part of the cave, recent deposition of various carbonate minerals - aragonite, high Mg-calcite and protodolomite cause these ratios to deviate from the described linearity.

$\delta^{18}\text{O}$ values in the pools are seasonally dependent. The lowest $\delta^{18}\text{O}$ values are obtained during the peak of the rainy season and they rise gradually towards the autumn. Variations in the average annual composition between rainy and dry years are also observed. Consequently rainy years are reflected in lower $\delta^{18}\text{O}$ values. These differences are recorded in the carbonate minerals deposited from these pools and thus can serve as a paleoclimatic tool.

Infrastructure Surveys, Mapping, and Identification Using Ground Penetrating Radar (GPR)

Beck, A., Ronen, A.

The Institute for Petroleum Research and Geophysics, P.O.B. 2286, 58122 Holon

During the past year the Institute for Petroleum Research and Geophysics has carried out several ground penetrating radar surveys throughout Israel. The aim of most of these surveys was to identify and map cavities and karsts at building sites by way of hazard prevention and to assist in planning the building foundations. Other surveys were designed to map the subsurface of roads and runways in the framework of a comprehensive renewal project including observation drillholes, core drillholes and so on.

The surveys were carried out using the SIR-10 radar system, manufactured by GSSI, USA, which provides interpretations of the subsurface at high resolution and at various depths depending on the type of antenna used and on the electrical properties of the surveyed area. The above surveys were carried out using the 1 GHz antenna which facilitated surveys of a section up to 1 meter in depth and identification of layers up to 10 cm thick. Changes in the subsurface can be identified as well as various thicknesses and lateral alterations which are shown by changes in the electromagnetic signals.

Correlations between radar survey sections and borehole findings enable construction engineers to design renewal programs suitable for particular stress loads.

Surveys for identification and mapping of karst cavities were carried out using the 100 and 500 MHz antenna, providing interpretation of sections to a depth of 3-4 meters and 10-15 meters, respectively. Changes in rock type along the length of the section were found in areas characterized by massive or compacted rocks as compared to areas of worn (eroded) rocks. Karst feedlines full of clay, karst spaces developing into cavities as well as faults and cracks were found. Early identification and mapping for structures such as tunnels, roads or public buildings are most important, particularly in hilly regions where karst cavities endangering the stability of structures can develop.

Radar surveys are inexpensive, fast and efficient as compared to other geophysical methods and are an important tool in safe modern structure design.

On the Discrepancy between Base Kurkar Group and Base Coastal Aquifer in the Southern Sharon — Results from Seismic Profiles

Ben-Gai, Y. , Gilad, D.

**The Institute for Petroleum Research and Geophysics, P.O.B. 2286, 58122 Holon
The Hydrological Service, P.O.B. 6381, 91063 Jerusalem**

The coastal aquifer, composed of Quaternary deposits in the coastal plain of Israel, holds about one quarter of the annual water consumption in the country. Many wells have penetrated the aquifer to various depths, but only a few reached its base. Information from these wells shows that the aquifer comprises several depositional cycles which can be linked to quaternary glacial and interglacial periods. At a time of glaciation and lower sea level, continental clay layers were deposited on the exposed coastal plain, while at the time of melting and rising sea levels, marine calcareous sandstones were deposited.

Systematic divisions of the Pleistocene section into groups and formations have been suggested by various researchers since the 1930s. On the other hand, a functional division of the coastal aquifer into subaquifers is used by hydrologists. The difference between these approaches results in a misfit between the stratigraphic definition of the Kurkar Group and the hydrographic definition of the base of the aquifer. The "Dan" Member, comprising the lower unit of the Kurkar Group, is regarded by hydrologists as part of the Saqiye due to its facial resemblance.

High resolution seismic profiles collected recently in the southwestern Sharon indicate that the base of the "Dan" Member is a prominent and continuous reflector, even more so than the base of the Dsub-unit, the lower calcareous sandstone. This may suggest that the "Dan" Member followed a major global drop in sea level in the Lower Pleistocene. Differences in compaction are probably sufficient to cause a strong reflector between the "Dan" Member and the underlain Saqiye Group.

An Event-Stratigraphy Approach to Eocene Lithostratigraphy in Israel

Benjamini, C.

Department of Geology and Mineralogy, Ben-Gurion University of the Negev, 84105 Beer Sheva

Standard stratigraphic procedure is to apply formal lithostratigraphic nomenclature to rock units of consistent lithology which, prior to erosional or structural discontinuity, were originally physically continuous. Eocene limestones and chalk sections in Israel have presented formidable obstacles to formal subdivision, as repetitive lithologies and rapid interfingering are common. Differences between limestone subunits are subtle, and chinks, even more so. Rarely can integrative units be distinguished from one another on the basis of lithologic criteria alone.

Recent advances in sequence stratigraphy suggest additional tools. Depositional sequences and their boundaries are viewed as the response of the sedimentary environment to eustatic, epeirogenic, local tectonic, or thermal stimulus. The individual depositional cycle is distinguished vertically from others by recognition of the nature and position of the bounding event. The iterative lithologies of the depositional sequence may then be considered a natural extension of deposition governed by oscillations of relative sea level.

The Eocene of Israel may be viewed as a vertical series of depositional units along a paleocontinental shelf. The depositional environment and thickness of subunits is governed by paleotopography, relative sea level change, tectonic stress, and the complexities of subsidence history. A more genetic approach to lithostratigraphic subdivision of Eocene rocks of Israel can be based on an event history of the depositional basin. However the correct assignment of rock units becomes dependent on precision of time-correlation.

Biostratigraphy has been used to reconstruct physical continuity of rock units in the Negev and Jordan Valley, although strictly speaking, the time of deposition is not part of their definition. Additionally, rock bodies at Gilboa and Shechem may be placed within the context of a regional geologic event stratigraphy. Ultimately, a unified lithostratigraphic scheme can be extended to wherever both the lithology and the event history persist.

Assessment of Hydraulic Parameters in the Kinneret Basin

Bergelson, G., Nativ, R.,¹ Bein, A.²

1. The Seagram Center for Soil and Water Sciences, The Hebrew University of Jerusalem, 76100 Rehovot

2. Geological Survey of Israel, 30 Malkhe Yisrael Street, 95501 Jerusalem

A simulation of groundwater flow and solute transport to Lake Kinneret requires data on the hydraulic parameters (i.e. permeability, storativity, porosity) of the surrounding aquifers. However, pumping tests that were carried out close to the lake, do not provide data suitable for a reliable evaluation of these parameters. Drawdown in observation wells was measured in only six pumping tests and was too rapid and too small for a calculation of these parameters. Pumping tests which were carried out upstream, in the same aquifers in the Hazon, Kalanit, and Hukuk wells may also not be suitable for extrapolation to the lake area because faults in the rift area may have affected porosity and permeability. Consequently, other methods need to be recruited to determine the hydraulic parameters.

Depletion curves of discharge (in springs and artesian wells) and water levels (in observation wells) were analyzed. Transmissivity and storativity could be estimated from the processed curves using the following equation (Jacob, 1940):

$$1/t_0 = \Pi^2 T / (4SL)^2$$

where t_0 characterizes the depletion, S = storativity, L = distance from the recharge area, and T = transmissivity.

Specific storage and porosity were evaluated using continuous groundwater pressure measurements and tidal and barometric efficiency equations (Jacob, 1940):

$$T.E. = dP / (\gamma_w dH) = (\rho_w g \beta_p) / S_s$$

$$B.E. = (\gamma_{wa} dH) / dP_A = (\rho_w g N \beta_w) / S_s$$

where T.E.= tidal efficiency, B.E.= barometric efficiency, P = pressure in the aquifer, P_A = atmospheric pressure, H = height of the tide, γ_w and γ_{wa} = specific weights and density of the aquifer fluid, respectively, S_s = specific storage, β_p = bulk compressibility, β_w = fluid compressibility, N = porosity and g = gravity. Pressure data from pressure transducers installed in four wells were used for this purpose. Tritium and carbon-14 were used to evaluate hydraulic conductivity using the following equation:

$$K = LN / JT$$

where L = distance from the recharge area, N = porosity, J = hydraulic gradient, T = residence time.

Applying Image Processing Techniques for Analysing TM Data from the Timna and Feinan Areas and Multispectral GER-II Data from Makhtesh Ramon

Beyth, M.,¹ Henkel, J.,² Geerken, R.³

1. Geological Survey of Israel, 30 Malkhe Yisrael Street, 95501 Jerusalem

**2. Institut für Allgemeine und Angewandte Geologie, Ludwig Maximilians Universit.,
Arbeitsgruppe Fernerkundung, Luisenstr. 37, 8000 Munchen, Germany**

**3. Institut für Photogrammetrie und Fernerkundung, Universität Karlsruhe, Englerstr.
7, 500 Karlsruhe, Germany**

TM data taken on July 4, 1984, were analysed for the Beer Ora-Timna Valley and Feinan areas in southern Israel and Jordan as part of a study for later assessment of MOMS-02 data. Image processing techniques such as IHS transformation and relative image combined with laboratory spectra measurements of major sedimentary rock types and detailed field work, makes it possible to present distinct images. Careful structural analysis of these key areas, located between the Dead Sea rift in east and west and the Themed and Feinan dextral faults to the south, using these images, may contribute to a general structural model for these areas. Future potential use of MOMS-02 combined with TM data as a geological mapping tool in similar environments is briefly discussed.

The Principle Component statistical analysis was used to condense the data and to improve the signal to noise ratio (SNR) of the multispectral GER-II data (64 bands) of the Makhtesh Ramon area. This, combined with a thorough visual quality control of the individual bands, makes it possible to define the rock units, the minerals and the major structural features in an arid area such as Makhtesh Ramon, even without spectral calibration.

Diagenetic Dolomite-Ankerite in Zohar Formation in the Northern Negev

Blum-Laub, R.,^{1,2} Starinsky, A.,² Ayalon, A.¹

1. Geological Survey of Israel, 30 Malkhe Yisrael Street, 95501 Jerusalem

2. Institute of Earth Sciences, The Hebrew University of Jerusalem, 91904 Jerusalem

The Middle Jurassic Zohar Formation is found in the northern Negev mainly in the subsurface; outcrops are found only in HaMakhtesh HaQatan and HaMakhtesh HaGadol. The present study concentrates on the two upper members: Tsiyah and Halamish. The purpose of this study is to reconstruct the different diagenetic processes that affected the Zohar Formation and to try to relate them to the hydrocarbon (gas and oil) accumulation in the formation. The research is based on petrographic, mineralogic, geochemical and stable isotope (oxygen and carbon) studies. Fifty-five samples were taken from surface exposures from HaMakhtesh HaQatan and the HaMakhtesh HaGadol, and from the following boreholes: Halamish 1, Zohar 5, Zohar 6, Kidod 1, Rekhme 1A, Hazerim 1 and Haluza 2. Hydrocarbons (gas and oil) were present in Zohar 5, Zohar 6 and Kidod 1.

The main minerals, which are present in different amounts in the rocks are calcite, dolomite and quartz. Most of the dolomites are iron-rich (ankerite). Three rock types were identified: (1) carbonates (calcite and/or dolomite-ankerite) that comprise at least 95% of the rock. (2) sandy carbonates that contain 10-50% quartz and (3) carbonate sandstones that contain more than 50% quartz. Minor minerals present in the rocks are feldspar, gypsum, halite, kaolinite, hematite, goethite and pyrite. The two outcrops show different patterns: ankerite is most common in the HaMakhtesh HaQatan outcrops, whereas in the HaMakhtesh HaGadol outcrops, the rocks are entirely limestone. Ankerite is also common in the Halamish Member in the Zohar 5 and Zohar 6 boreholes.

In several samples, two types of ankerite were identified. These could have crystallized from different solutions during the diagenetic history. $\delta^{13}\text{C}_{\text{PDB}}$ values of calcites and ankerites are $0 \pm 4\text{‰}$, representing marine derived CO_2 . $\delta^{18}\text{O}_{\text{SMOW}}$ values of calcites range between +13 and +31‰. Lowest $\delta^{18}\text{O}$ values were measured for calcites from the Zohar 5 and Zohar 6 boreholes, and highest $\delta^{18}\text{O}$ values were measured for calcites from the southern area (HaMakhtesh HaQatan, HaMakhtesh HaGadol and Rekhme 1A). $\delta^{18}\text{O}$ values of ankerites range between +21 to +38‰. Similar to the calcites, lowest $\delta^{18}\text{O}$ values were found for ankerite from the Zohar 5 and Zohar 6 boreholes, and highest $\delta^{18}\text{O}$ values were found for ankerites from the HaMakhtesh HaQatan outcrops. The high $\delta^{18}\text{O}$ values measured for the HaMakhtesh HaQatan carbonates may indicate formation at relatively low temperatures and from ^{18}O -enriched pore water. The low $\delta^{18}\text{O}$ values measured for the Zohar 5 and Zohar 6 boreholes may reflect higher temperatures (deeper burial depth) and ^{18}O -depleted pore water.

Chernobyl in Israel

Butenko, V.,¹ Ne'eman, E.,¹ Brenner, S.,¹ Kronfeld, J.,² Gilat, A.³

1. Environmental Research Laboratory, Ministry of the Environment, Sackler Medical Building, Tel Aviv University, 69978 Tel Aviv

2. Dept. of Geophysics and Planetary Sciences, Tel Aviv University, 69978 Tel Aviv

3. Geological Survey of Israel, 30 Malkhe Yisrael Street, 95501 Jerusalem

The radioactive plume arrived over Israel, accompanied by a patchy rainfall, approximately ten days after the nuclear accident (April 26, 1986) at the Chernobyl reactor in the Ukraine. The first study of possible soil contamination was recently carried out. Approximately sixty samples, of soils in the Galilee region and 22 samples in the Judean Hills region including a wide range of important and/or historical sites such as the Israel Geological Survey and the Valley of the Cross, the Hebrew University and the Old City among others were analyzed.

Soil samples were collected to a depth of 5 cm. The samples were analyzed by gamma-ray spectrometry using a solid Ge detector. This enabled the precise identification of gamma-ray energy peaks. In all cases the presence of the short-lived (2 year half life) radiocesium isotope, ^{134}Cs , identifies the presence of Chernobyl-related contamination. The activity of this isotope is, in many cases still after 3 1/2 half lives, greater than that of the naturally occurring ^{40}K . The 662 KeV peak of the long-lived ^{137}Cs (30 year half-life) is usually the dominant peak in all of the spectrums. The ^{137}Cs activity is found (so far) to range between 0.1K and 13K Bq/m². The average radiocesium burden of the soils today is approximately 5000-8000 Bq/m². This demonstrates that the Chernobyl contamination in Israel was not trivial as was previously assumed. Indeed, the external radioactive dose rate was undoubtedly significantly higher soon after its precipitation.

Runoff Simulation in a Desert Watershed and Sensitivity Analysis of a Rainfall-Runoff Model

Carmi, G.,¹ Dody, A.^{1,2}

- 1. Water Resources Research Center, Jacob Blaustein Institute for Desert Research, Ben-Gurion University of the Negev,, 84993 Sede Boker Campus**
- 2. Department of Geology and Mineralogy, Ben-Gurion University of the Negev, 84105 Beer Sheva**

For runoff simulation at the desert watershed located inside the Sede-Boker experimental site a distributed physically based rainfall-runoff model KINEMAT proposed by Woolhiser et al. (1990) was used.

In conditions of parameter uncertainty it was significant to estimate the optimal parameter sets. It is known (Harlin, 1991) that no single parameter optimum exist. From manual calibration, five initial parameter sets were obtained. Several storms were used for this calibration. For five initial parameter sets the model performance over complete data periods was expressed by the efficiency criterion (R^2) and the volume error (VE) in percent.

For each parameter, 500 values were randomly generated from a uniform distribution within the ranges of acceptable values. Parameter sets were formed by randomly combining the generated parameter values.

The computer program in FORTRAN codes was compiled for governing the placing of parameter sets in input files of the rainfall-runoff model, the running of the rainfall-runoff model, and comparing the output computed files with observed records and calculating R^2 and VE. Each simulation run was then classified as producing either acceptable or unacceptable results, according to whether the simulation produced at least as high an R^2 value and as low VE as the poorest of the initial parameter sets. The key idea was to compare the distribution of individual parameter values between acceptable and unacceptable results. If two distribution were significantly different, the output was sensitive to the parameter being studied. The Kolmogorov-Smirnov two-sample statistics was used to compare the cumulative distribution of the parameters which gave acceptable and unacceptable results. As a results of the sensitivity analysis parameters were found to which model output is most sensitive.

Geographic Information System Use for Runoff Forecasting

Carmi, G., Karnieli, A.

Water Resources Research Center, Jacob Blaustein Institute for Desert Research, Ben-Gurion University of the Negev,, 84993 Sede Boker Campus

In hydrological studies, physically based distributed models are often used. Our distributed model for the desert watershed suggests that the watershed surface and channel network are represented by a cascade of plane and channels. Each plane and channel are described by its unique parameters, initial conditions, and precipitation inputs. A set of planes and channels is expected to preserve the most significant spatial variations of topography, soils, cover, and rainfall, i.e. factors affecting runoff. Since there is no objective method for such selecting, it was decided to use the Geographic Information System (GIS) for studying watershed parameters and initial conditions spatial variations. The system is both a database system with specific capabilities for spatially-referenced data, as well as a set of operations for working with the data.

To create raster structural GIS for the experimental watershed the photogrammetric map, as well as air photographs in blue, green, red and infrared bands, were used. A digital map file was obtained by means of digitizing, and digital photographs by means of scanning. A Sun microcomputer and ERDAS software were utilized for data processing. Digital maps of the watershed slopes and aspects were created, color watershed images were obtained by overlaying the scanned photographs of different bands on each other.

Results of sensitivity analysis of the distributed rainfall-runoff model were used to estimate the criteria of the watershed subdivision. The following criteria were taken into consideration: aspects, i.e. slope or channel exposition, slope, types of deposits, micro topography and density of vegetation.

Fluid-Rock Interactions During the Formation of Metamorphic Dike-Schists, Elat Metamorphic Complex

Cohen, B.,^{1,2} Matthews, A.,² Bar-Matthews, M.,¹ Ayalon, A.¹

1. Geological Survey of Israel, 30 Malkhe Yisrael Street, 95501 Jerusalem

2. Institute of Earth Sciences, The Hebrew University of Jerusalem, 91904 Jerusalem

This research seeks to determine the nature of the fluid-rock interactions between metamorphic dike schists and country rocks in the Precambrian igneous and metamorphic complex of Elat. The study presents the results of petrological, geochemical, and oxygen isotope profiles across a 4m wide dike schist and the adjacent granite gneiss country rock.

Marked petrological and geochemical differences occur between the margins of the dike schist (~ 50 cm from dike wall) and its center. The central parts consist of zoned labradorite/andesine to oligoclase porphyroclasts, 20% quartz, 5-10% biotite, and several percent actinolite, whereas the margins consist of recrystallised oligoclase, 5-10% quartz and over 20% amphibole. Texturally, the margins of dike exhibit a strongly lineated mylonitized character. In concordance with the views of previous studies the mineralogical changes are considered to have developed during metamorphism and ductile shearing. Major element geochemical trends between the center and margins of the dike (e.g., increase in calcium, sodium and iron; decrease in silica) are considered to represent variations in the chemistry of the original mafic igneous rocks prior to metamorphism. The oxygen isotope compositions of quartz separates are remarkably homogenous across the dikes, averaging at $13.5 \pm 0.2\%$. These uniformly high $\delta^{18}\text{O}$ values (also shown by whole rocks) indicate that the dikes were infiltrated by an aqueous ^{18}O -enriched fluid.

The granite gneiss sampled away from the contact with the dike contains albite porphyroblasts, perthitic feldspars, massive and idiomorphic biotite, and large (2mm) k-feldspar and quartz grains. Less than 50 cm from the contact the quartz and the albite are recrystallised, perthite disappears, the amount of k-feldspar decreases, and the biotite grains become smaller and exhibit a strong preferred orientation. These textural and mineralogical changes are the counterparts in the granite gneiss of ductile shearing observed in the dike schists. The $\delta^{18}\text{O}$ values of the quartz in the granite gneiss away from the contact are 12.2‰ on one side of the dike and 12.8‰ on the other. These $\delta^{18}\text{O}$ values increase gradually in the contact zones to 13.5‰ at the contact with the dike. Correspondingly, sodium, potassium and silica concentrations in the granite change near the dike.

The uniform $\delta^{18}\text{O}$ values of quartz separates in the dike schists indicates that the infiltrating fluids penetrated along the dikes parallel to dike walls. The isotopic changes observed in the granite gneiss in the contact zone represent an advective - diffusive component of fluids which penetrated from the dike to the granite. Preliminary modelling of this fluid movement using one-dimensional transport equations indicates that the advection front penetrated 70 ± 30 cm into the granite gneiss at a permeability of $\sim 10^{-21}$ m². The correspondance of the advective-diffusive transport of fluids with the petrological, textural, and geochemical changes in the granite gneiss suggests that the deformation and fluid advection occurred during the same event. The isotopic data therefore suggest that fluid infiltration during the metamorphism of mafic dykes had a component normal to the direction of flow that penetrated the granite gneiss and probably contributed to hydrolytical weakening necessary for ductile shearing.

Organic Petrology: Preliminary Investigations on the Melekh Sdom 1 Borehole, Southern Dead Sea Basin

Conway, B.H.

Geological Survey of Israel, 30 Malkhe Yisrael Street, 95501 Jerusalem

The Melekh Sdom 1 borehole section (drilled to a depth of 3483 m.) lies in the tectonically active Dead Sea rift basin, which underwent rapid Neogene subsidence and resulted in the accumulation of a very thick fill.

Analysis of (a) Thermal Alteration Indices (to determine maturity level) and (b) Palynofacies Analysis (to recognize source beds), from a limited selection of samples, yielded the following results:

1. There is a recognizable coalification increase with depth, identified from liptinite at 881 m. depth. The section lies within the *oil-window* at 3243 m. depth (probably at even shallower depths).
2. In certain parts of the section, the Particulate Organic Matter (POM) is dominated by autochthonous aggregates of colloidal amorphogen (*oil-prone* / Type I kerogen), together with alginite (the freshwater alga *Botryococcus* is frequently encountered) and liptinite (chiefly of the water lily / *Nymphaea*).

The Neogene fill has been previously assumed to be impoverished of source beds and incapable of generating oil. This investigation proves that presumably "Plio-Pleistocene" strata (Amora Fm. and younger fill sediments) contain: (a) high quality biomacromolecules that readily thermodynamically dissociate. (b) despite their youthfulness certain strata are *mature*.

It is concluded that *mature* amorphogen rich beds generated oil in response to thermal stress, which accounts for some of the heavy oil shows of local drilling activities. These observations signal that the Dead Sea basin is a potentially attractive play.

Future investigations will be intensified, it is intended to map spacial and temporal variations of *mature* amorphogenic facies, in order to ascertain the oil-generating potential of the basin fill, integrated with evaluations of organic richness.

Late Cretaceous Inversion of Early Mesozoic Structures: Examples from the Negev, Southern Israel

Druckman, Y.,¹ Gelbermann, E.,² Fleischer, L.,² Wolff, O.,² Gill, D.¹

1. Geological Survey of Israel, 30 Malkhe Yisrael Street, 95501 Jerusalem

2. The Institute for Petroleum Research and Geophysics, P.O.B. 2286, 58122 Holon

Late Triassic and Early Jurassic tilted blocks were observed in the Negev, southern Israel. This structural pattern was inferred on the basis of abrupt thickness changes (Early Jurassic) and both thickness and facies changes (Late Triassic) in subsurface borehole sections. A later regional folding phase has affected the area in late Cretaceous to Eocene times (the "Syrian Arc" chain of structures). The resulting asymmetric anticlines have reverse faults in their deeper parts. It has been suggested that this reverse faulting resulted from an inversion of the direction of the displacement along the previous Early Mesozoic normal faults.

Detailed comparison of isopach maps of the deformed Triassic and Jurassic stratigraphic intervals with the Late Cretaceous structural contour map, derived from surface geology, borehole and seismic information, reveals that inversion may have taken place along some of the reverse faults. However, not all the reverse faults have acted previously as normal faults. It is suggested that the Early Mesozoic and Late Cretaceous deformation phases have resulted in structures of different wave lengths. The interference of these deformations resulted in "in phase" and "out of phase" summation of the two movements.

Thus, in some cases (e.g. the Qeren anticlinal trend) Mesozoic "lows" match Late Cretaceous "highs", whereas in others the opposite (e.g. the Zavoa-Sherif anticline), or some intermediate situations, can be observed. Therefore, the employment of the inversion model for exploration as a universal key for the identification of ancient "highs" may be misleading.

Morphologic Dating of Fault Scarps in the Southern Arava, Israel and Comparison to other Dating Techniques

Enzel, Y.,¹ Amit, R.,¹ Harrison, J.B.J.,² Porat, N.³

1. Institute of Earth Sciences, The Hebrew University of Jerusalem, 91904 Jerusalem

2. Dept. of Geosciences, New Mexico Institute of Mining and Technology, Socorro, NM 87801, USA

3. Geological Survey of Israel, 30 Malkhe Yisrael Street, 95501 Jerusalem

Fault scarps and terrace risers in the southern Arava, Israel were analyzed to determine the applicability of morphologic dating through a diffusion modelling approach a) as an estimator of age, and b) as a relative age dating tool. The relative importance of estimating both the initial scarp angle and the regional diffusion coefficient on the modelling results was also evaluated. Using diffusion modelling we were able to differentiate between slopes that varied in age by only a few thousands of years based on soil-geomorphic studies.

The modelling results indicate that the specifically studied fault scarp is between 50,000 and 13,000 years old. The large range of the estimated age is depending on the exact diffusion coefficient used. The model also predicted an early and middle Holocene ages for two terrace risers, respectively, which are younger than the fault scarp according to field stratigraphic relationships. The morphologic age determined by the modelling agrees well with the correlative age from earlier soil-chronosequences and geomorphologic studies and with recently acquired optically stimulated luminescence (OSL) dates. Combining the OSL dates with the morphologic ages from the modelling allowed us to calculate a diffusion coefficient of 0.0002 to 0.0003 for these scarps.

The agreement between the ages, which were independently estimated from the three methods, makes it possible to estimate a) the recurrence interval of faulting along this segment of the fault with some confidence and b) the time since faulting and intensity of the seismic activity in the region as seen from the long-term perspective. An estimation of the earthquake magnitudes associated with the studied fault indicates that all must have been smaller than 7.5 and appear to change from a possible maximum of 7 during the latest Pleistocene, to lower magnitudes of about 6 during the early Holocene. Scarp diffusion modelling provides acceptable estimates of ages of faulting events in a region where other age dating methods (numeric or correlative) are either non existence, rare, time consuming or very expensive. In addition, the ability of the modelling to distinguish between scarps of different ages provide us with a tool to group the numerous fault scarps in the southern Arava into groups and to help in any tectonic analysis of that region.

New Map of Moho Discontinuity of Israel

Eppelbaum, L.,¹ Pilchin, A.²

1. Dept. of Geophysics and Planetary Sciences, Tel Aviv University, 69978 Tel Aviv
2. Toronto, Canada

It is well-known that disposition of Moho discontinuity is very important for modeling of potential geophysical fields. For the constructing of the map of Moho discontinuity the following procedure was used. The principal papers describing the deep structure of Israel (including Moho discontinuity) were selected. In these papers the depth of Moho discontinuity was obtained, mainly, by seismic and gravity data. The depths of Moho discontinuity were correlated with values of gravity field in Bouguer reduction. Using the least-square method the correlation coefficient r and regression coefficients α and β were obtained. Correlation coefficient $r = 0.794$ and equation of the approximated line follows $y = -0.24x + 23.3$. Also the polynomial and exponential equations were obtained, but the linear approximation is more precise in these conditions.

On the new gravity map of Israel (Ginzburg et al., 1993) were selected about 600 points were selected. Then, using the obtained equation on the selected grid 600 points, the 2-D and 3-D map of Moho discontinuity was constructed. These calculations were conducted using various approximation methods which are compared and show a good agreement.

The Geological Map of the Precambrian of South-Western Sinai, Scale 1:50,000

Eyal, M.,¹ Voznesensky, V.,¹ Bendor, Y.²

1. Department of Geology and Mineralogy, Ben-Gurion University of the Negev, 84105 Beer Sheva

2. Scripps Institute of Oceanography, Geological Research Division, La Jolla, CA, USA

The geological map of the Precambrian rocks of South-Western Sinai includes the area situated east of the el-Qa'a Plain, and the blocks of Abu-Durba and Jebel Araba along the Gulf of Suez. The mapped area comprises rocks formed during the main Precambrian events in Sinai.

The Island Arc Stage (≈ 820 – 620 Ma) is represented by the Metamorphic Series, found in the Sulaf area, which is part of the Firan Group, the Wadi Shidiq and lower Wadi Isla areas, and in the Jebel Araba block. The metamorphic rocks include meta-sediments of mica and chlorite schists, calcsilicates and conglomerates, and ortho-gneisses of granitic and dioritic composition which represent the remnants of four plutons.

The Cratonization Stage (≈ 620 – 580 Ma) is represented by the widespread Calc-alkaline Magmatic Series and related sediments. The Rutig Formation of the Firani Group is exposed between the Katharina Ring-Dike and the Katharina Pluton. It comprises intermediate to acid lava flows and pyroclastics, alternating with conglomerates and arkose. The plutonic rocks range in composition from gabbro to granite, and they belong to 13 different plutons. A special case of this group is the Miar-Hibran complex which is a mixture of older dioritic rocks and younger granitic rocks that cover an area of more than 200 sq. km.

The Intra-cratonic Stage (≈ 580 – 540 Ma) is represented by the Alkaline Magmatic Series. The main representative of this group is the Katharina Ring Complex which comprises the alkali rhyolites of the Jurjunia Formation-Katharina Group, the quartz monzonites and quartz syenites of the Katharina Ring Dike, and the biotite leucogranite of the Katharina Pluton. Also belonging to this series are the volcanic rocks of Jebe Abu-Durba, and the alkali granite Sahara and Serbal plutons.

The detailed scale of the geological map enables showing of the placement and morphological peculiarities of more than 200 dikes. Two mapping units are distinguished: 1) acid dikes, 2) intermediate and basic dikes. The acid dikes trend NE and form the following dike swarms: Abu Durba and Wirka (NE 70 – 80°), Miar (NE 40 – 50°) and Thimman (NE 60 – 65°). The most typical Miar dike swarm is about 6 km wide, it comprises 35–40 dikes, and the length of individual dikes is up to 7 km. The Miar dike swarm cross the rocks of Calc-alkaline Magmatic Series, the biotite leucogranite of Abule Tabil Pluton, and the Katharina Ring-Dike. It is crossed by the Katharina Pluton.

The intermediate and basic dikes are distributed in the area more uniformly. In some places they join the acid dike swarms, but more often they form isolated groups of dikes. The intermediate and basic dikes generally cross the acid dikes. Their general trend is N, NNE and NE, and the length of individual dikes is up to 10–12 km.

Stress Field Fluctuations Adjacent to the Dead Sea Rift Since the Middle Miocene

Eyal, Y.

Department of Geology and Mineralogy, Ben-Gurion University of the Negev, 84105 Beer Sheva

The Dead Sea transform (DST) region is the sutural zone between the African and the Arabian plates which subduct northwards under the Eurasian plate. The motion of these plates is the source for their internal deformation especially in the vicinity of the DST. Geological observations indicate two distinct strain regimes adjacent to the Dead Sea rift: (1) Moderate, Turonian to M. Miocene, WNW shortening and NNE extension associated with the development of Syrian Arc fold belt, is attributed to the Syrian Arc stress field (SAS); and (2) NNW shortening and ENE extension associated with the M. Miocene to Recent formation of the DST resulted from the opening movements of the Red Sea and attributed to the Dead Sea stress field (DSS).

In spite of this distinction, trend analysis of many structures shows that formation of SAS compatible structures continued after the M. Miocene up to the Recent (e.g. the Ein Yahav dike, faults in the Gilboa region, and most E-W faults in the Galilee). In some locations structures compatible with both stress fields cross cut each other.

Schulman (1981) explains such observations, in the Golan Heights, by alternation of the stress fields on a regional scale which was "induced by differential flow of the asthenosphere." Hatzor & Reches (1990) explain similar observations in the Gilboa by modification of DSS within the DST area, into WNW trending shortening perpendicular to the DST and parallel with that of the SAS, possibly due to the weakness of the DST.

In this study it is suggested that the movements resulting in the development of the Syrian Arc and other SAS compatible structures continue to the Recent and DSS movements are superimposed on them. The mixture of SAS and DSS structures adjacent to the DST, results from local and temporal fluctuations in the combined stress field. The mechanism for such variations could be the superposition of stress drops, induced by large DST earthquakes, on a steady background remote field (plate scale) stress regime. Thus, DSS-compatible structures form in pre-seismic periods while DST related elastic strain is high. On the other hand, the SAS compatible structures from during post seismic times, subsequent to large local stress release along the DST, are dominated by the remote "Syrian Arc" stress regime.

The Structure of the Arava—Initial Results from Geophysical Surveys

Frieslander, U.,^{1,2} Bartov, J.,³ Garfunkel, Z.,² Rotstein, Y.,¹ Rybakov, M.¹

- 1. The Institute for Petroleum Research and Geophysics, P.O.B. 2286, 58122 Holon**
- 2. Institute of Earth Sciences, The Hebrew University of Jerusalem, 91904 Jerusalem**
- 3. Geological Survey of Israel, 30 Malkhe Yisrael Street, 95501 Jerusalem**

The margins of the southern and central Arava Valley, part of the Dead Sea rift, have previously been investigated in detail only through surface geological mapping. During the last year, a large seismic reflection survey was carried out in this area accompanied by gravity and magnetic surveys on the seismic lines. Partial results of an initial interpretation of these new data suggest the following:

1. A flexural structure is apparent along the western margin of the Arava, dipping gently towards the center of the rift valley.
2. A regional dip towards the center characterizes the Arava in the segment between Paran and Idan.
3. In the central Arava, south of Wadi Paran, the rift appears to be east of the survey area and is bounded to the west by the Ya'alón fault which extends from Jabel Horaj toward Timna.
4. In the vicinity of the Evrona dry lake, a fault was identified which is, possibly, an extension of the rift's western main fault in the Elat area and the Ya'alón fault. East of this fault we observe a deep basin filled with young sediments.
5. A large listric fault with a throw of several thousand meters, bounds the north Arava basin to the south and west and is the southern boundary of the Dead Sea basin.
6. North of Wadi Paran and east of Wadi Arava, we observe in the subsurface a trace of the Zofar fault which is associated with surface deformations and a stratigraphic displacement of 2000 m. The seismic records, which show obvious differences in the dip and continuity of the beds on both sides of the fault, suggest that it is part of the post Hazeva transform system which, in this area, is over 2000 m.
7. In the central Arava, coordinates 970–990, shallow magnetic bodies were identified in areas where the subsurface reflections are not continuous. We suggest that these shallow intrusions are of Early Miocene age and are equivalent to the Nahal Ashosh intrusion.

Input of Atmospheric Aerosols into Lake Kinneret — Preliminary Results

Ganor, E.,¹ Foner, H.A.,² Peled, Y.,² Brenner, S.,¹ Kopeliovich, I.²

1. Institute for Environmental Research, Ministry of the Environment, Tel Aviv University, 67978 Tel Aviv

2. Geological Survey of Israel, 30 Malkhe Yisrael Street, 95501 Jerusalem

The input of sediments from the Jordan river into Lake Kinneret has been estimated as about 70,000 tonnes/year. Measurements of dustfall carried out in the 1970s indicated that the input into the lake from this source was also significant. The present work reports the first results from a network of some 16 dustfall collectors which was set up around the lake in order to confirm this finding.

Settling particles were trapped in dustfall collectors which were constructed after the general pattern of the ASTM. In essence they consist of plastic buckets placed 2 m above the ground surface. The collectors are kept filled with distilled water to prevent outward saltation of the trapped aerosol particles. The collectors are fitted with "crowns" to prevent birds from fouling the contents. Collectors are emptied every month and the contents are analyzed chemically and mineralogically.

Total fluxes of the various fractions into the lake are shown in Table 1 below. These results relate to only the months July-November 1992; results for the whole year will be presented at the conference. As the months considered here are not the ones with the most dustfall, the values shown are presumably an underestimate. However, even on this basis, total dustfall input into the lake is about 13% of the measured riparian input. The composition of the dustfall itself is interesting: some 46% of it is inorganic water insoluble material.

Table 1. Calculated annual fluxes and inputs into Lake Kinneret

Fraction	Annual Flux (tonnes/km ²)	Input into lake (tonnes)	Percent of total input
Total insoluble	32	5480	54
Inorganic water insoluble	24	4156	39
Inorganic water soluble	23	3817	46
Organic	8	1323	16
Total inorganic	47	7973	85

Total input (OR + IN) = 9296 tonnes

What Can Column Experiments Tell Us About Global Chemical Weathering?

Ganor, J.,^{1,2} Mogollon, J.L.,³ Soler, J.M.,² Lasaga, A.C.²

1. Department of Geology and Mineralogy, Ben-Gurion University of the Negev, 84105 Beer Sheva
2. Dept. of Geology and Geophysics, Yale University, P. O. Box 6666, New Haven, CT 06511, USA
3. Inst. de Ciencias de la Tierra. Univ. Central de Venezuela. Aptdo 3895, Caracas 1010-A, Venezuela

The coupled transport-dissolution of a gibbsitic bauxite material was simulated in the laboratory, at 25°C, using a column reactor, with input pHs ranging from 3.2 to 4.5 and fluid velocities ranging from 140 to 1050 m/y. Three different responses of the column output Al concentration to the length/flow velocity (L/v) ratio and to the pH were observed: (1) For input pH in the range from 3.2 to 3.5, the output Al concentration varies as an inverse function of the flow rate. This inverse relation reflects a constant dissolution rate under far-from-equilibrium solution conditions. (2) A departure from linearity is observed at L/v values higher than 1.5×10^{-4} m/yr for input pH=3.5 experiments and at L/v values higher than 3.25×10^{-4} m/yr for input pH=3.2 experiments. This departure from linearity indicates that the dissolution rate is varying in a non-trivial manner with the solution composition. Obviously, the saturation state of the solution in part of the column is much closer to equilibrium in these cases. (3) For inputs in the pH range from 4.0 to 4.5, the output Al pH values are **independent** of L/v . These observations suggest that sufficient gibbsite was dissolved in order to enable the solutions to reach equilibrium with the solid.

One dimensional reaction-transport numerical calculations were used to reproduce the experimental output Al and pH. For these calculations we used the non-linear DG_r dependence for gibbsite dissolution rate at 80°C and pH=3.0, the measured far-from-equilibrium dissolution rate, the measured dependence of the rate on a_{H^+} and the measured solubility product, K_{sp} . Comparison of the calculated and observed output Al concentrations in the column experiments shows remarkable agreement (over the whole DG_r range) i.e., differences are less than 20%. These results verify the non-linear rate laws discovered by our group.

An important data set that is relevant to any treatment of global change, is the variation of river composition worldwide as a function of runoff. In particular, the amount of silicon should reflect the breakdown of silicates in the earth, which is the major net sink of CO_2 in geological time scales. If we describe the chemical weathering as dissolution inside a column with average length L , the mean distance traveled through a global regolith, and the river as its output, we can use our column experiments, previous water-mineral kinetic data, and our reaction-transport numerical calculations, to predict the river concentration as function of flow rate, and we infer, as a function of runoff. A comparison of calculations with observed silica concentration versus runoff for most major rivers around the world suggests that the composition of river water, especially the silica composition, is not an equilibrium feature but is governed by the kinetics of water-rock interactions, which depend strongly on the degree of saturation of the solution.

Sulfur Isotopes Evidence for Sulfate Removal Processes from Subsurface Brines, Heletz Formation (Lower Cretaceous), Israel

Gavrieli, I.,¹ Starinsky, A.,² Spiro, B.,³ Nielsen, H.,⁴ Aizenshtat, Z.⁵

1. Geological Survey of Israel, 30 Malkhe Yisrael Street, 95501 Jerusalem

2. Dept of Geology, The Hebrew University, 91904 Jerusalem

3. NERC Isotope Geosciences Laboratory Keyworth, U.K., NG12 5GG

4. Dept. of Geochemistry, Gottingen University, Germany

5. Dept. of Chemistry, The Hebrew University, 91904 Jerusalem

Subsurface brines associated with oil ("oil brines") from four oil fields, Heletz, Brur, Kokhav and Negba, in the southern coastal plain of Israel show a deficiency in SO_4 concentrations compared to brines from dry wells ("dry brines") in the same fields only a few hundred meters away. Both types of brines have SO_4/Cl ratios lower than seawater or evaporated seawater with the same salinity. Previous studies suggested that the brines have evolved from evaporated Miocene seawater, which precipitated the sulfates in the Mavqim Fm. ($\delta^{34}\text{S}=21.7\text{-}22.7\text{‰}$). The present study shows that the residual brine in the Mavqim Fm. has sulfate with $\delta^{34}\text{S}=26.4\text{‰}$. The $\delta^{34}\text{S}_{\text{SO}_4}$ of the oil brines from the oil producing Heletz Fm. is 35.4-59.0‰ while the associated H_2S has sulfur composition of about 30-31‰. The oil has sulfur concentrations of 2-3% with relatively heavy sulfur isotopic composition of +13 to +15‰.

The following overall evolutionary path for these brines was reconstructed on the basis of their sulfate concentration, SO_4/Cl ratio and $\delta^{34}\text{S}$ in the SO_4 , H_2S and the oil.

- (1) Evaporation of a Messinian seawater which led to the precipitation of gypsum.
- (2) Precipitation of gypsum following dolomitization.
- (3) Bacterial sulfate reduction.

Stages (1) through (3) removed some 50% of the initial sulfate content of the brines, changing the sulfate isotopic composition from marine ($\delta^{34}\text{S}\approx 20\text{‰}$) to $\approx 26\text{‰}$.

- (4) Migration of the residual brines eastward into the Lower Cretaceous Heletz Fm. and mixing with oil.
- (5) Bacterial sulfate reduction in the oil reservoir resulting in further decrease in SO_4/Cl ratio and increase of $\delta^{34}\text{S}$ in the remaining sulfate.
- (6) Possible secondary enrichment of the oil with sulfur through reaction with the increasingly ^{34}S enriched H_2S and SO_4 .

TDEM and NMR Geophysical Methods for a Hydrological Purpose

Gev, I.,¹ Goldman, M.,² Rabinovich, B.,² Rabinovich, M.²

1. Water Resources Research Center, Jacob Blaustein Institute for Desert Research, Ben-Gurion University of the Negev, 84993 Sede Boker Campus

2. The Institute for Petroleum Research and Geophysics, P.O.B. 2286, 58122 Holon

A correlation of geophysical data collected by the Nuclear Magnetic Resonance (NMR) and Time Domain Electromagnetic (TDEM) methods, with hydrogeological data from observation wells have been recently carried out in the Negev Desert, Israel. To date the NMR technology is widely used in many applications ranging from chemical analysis to medical tomography. For a hydrological purpose, the NMR survey was first conducted in Russia in 1982. Since then, some experiments have taken place at different sites throughout the world. In Israel this method was first used during this experiment. The TDEM method has become routine technique in mapping sea water intrusion into the coastal aquifers.

The experiment in the Negev took place near Kibbutz Revivim in the Besor drainage system. The aim of this experiment was to encounter ground water layers in the Quaternary cover filling and Eocene fractured layers to a depth of 100 m. The experiment was carried out by using the two methods in parallel, in four locations. In another two locations only the TDEM measurement were carried out. Verification of the geophysical results was done by measurements of the water level in the observation well nearest to the geophysical measurement site. In two locations the verification was carried out six month later when observation wells were drilled.

The results showed a good correlation between the water level in the observation wells, and the depth of the upper water layer that was evaluated by the NMR and TDEM methods. The advantages of the NMR method are the possibilities to define the saturated layers, the width and the average volume of the water in each layer.

In saturated fractured layers it is possible that no water will appear during the drilling. This is due to the confined flow through the fractures and as long as the drill does not cross the fractures the water will not penetrate into the borehole. In two observation wells this mechanism of late penetration was confirmed, and the steady state of the water level was delayed. In this experiment we found that the results of the NMR and TDEM methods have an advantage of averaging the depth to water layer along the area having diameter of 100 m instead of just 40 cm as in the case of observation well. This was proven by measuring the water levels in those two observation wells after they reached a steady state.

The conclusion of this experiment confirms that combining results of two different geophysical methods with hydrological data was successful, and the cooperation between geophysical and hydrogeological teams in this type of field research is therefore important.

Reversal of Stream Flow Direction Along the Margins of the Southern Arava Valley Resulting from Tectonic Tilting

Ginat, H.

Geological Survey of Israel, 30 Malkhe Yisrael Street, 95501 Jerusalem

The watershed between the Nahal Hiyyon drainage basin which flows to the Dead Sea, and those of the streams that flow to the southern Arava Valley is situated along the fault escarpment between Har Berakh and Ma'ale Shahroot. Further north, in the area between Ma'ale Shahroot and Nahal Shita, the watershed recedes far from the fault escarpment. Streams situated west of the fault escarpment drain eastward to the Arava Valley.

The lithological composition of the pebbles in the conglomerates exposed along the margins of the streams and flow structures indicate that the Shahroot, Gerofit and Qetura streams once drained westward. The Ya'alón and Shita streams to the north also flowed west toward Nahal Paran and drained areas on the eastern side of the Arava Valley. Magmatic pebbles which derive from exposures in the east and a wide strike valley with a deep canyon (30 m) in Nahal Shita are evidence for this flow. Nahal Hiyyon, which drained all these smaller streams also flowed west to Nahal Paran. Thus, wide areas which in the past drained to the west, today drain eastward to the southern Arava. The "captured" area expanded northward from Nahal Shahroot, to Nahal Gerofit, the Qetura Valley, Nahal Ya'alón, Nahal Shita and Nahal Hiyyon.

The changes of the drainage direction were caused by a slight tectonic tilt to the east, in the area between Ma'ale Shahroot and Rehes Menuha. Because of this tilt Nahal Hiyyon changed its direction by about 90° and its tributaries reversed their flow direction.

During the tilting stage, red paleosoils accumulated in the streams. This process took place while the gradient of the streams was zero. Various exposures in the Ramat Gerofit area enable detailed characterization of the different stages of the faulting which caused these reversals in the stream-flow direction.

Biq'at Ginnosar in Jewish Traditional Literature

Ginzburg, D.

Geological Survey of Israel, 30 Malkhe Yisrael Street, 95501 Jerusalem

Biq'at Ginnosar is located on the north-west side of the Sea of Galilee. The "Biq" is formed by the Arbel (Hamam), Zalmon and Amud rivers which join to develop a delta at the shore of the sea. It is a very fertile valley having a number of water sources and rich soils. The soils are mostly dark brown alluvial clay soils, weathered from surrounding basalt flows.

In traditional literature the Sea of Galilee has been referred to as "The Sea of Ginnosar" (Onkelos to Numbers: 34:11; Targum Jonathan to Joshua: 13:27). In the Midrash Rabbah Genesis (48:22): "Rabbi Berekiah said: The whole shore of the Lake of Tiberias is called Cinnereth; Now why is it called Gennesareth? The Rabbis said: The gardens of Princes (it was an extremely beautiful place). These beautiful gardens are due to the "blessings of our forefather Jacob. (Genesis, 49:21)"Naphtali is a free running deer, he delivers words of beauty". In Midrash Tanhoma (Viah, 13): Biq'at Ginnosar is described as a valley giving the first fruits as fast as a running deer". Rashi writes "This (alludes to) the Valley of Ginnosar which quickly matures its fruit. Just like a hind which is swift in running".

In Babylonian Talmud Berakhot (44,a): "Replied Rashi: This rule applies to one who eats the fruit of Genessareth". Rashi interprets this as "The fruit of the land of the Sea of Chinnereth are more important than bread". In the Mishna, Maaserot (3:7) "A Genessareth hut". Rabbi Ovadia from Bartenora explained, "The Sea of Ginnosar is a place in the Land of Galilee, whose fruits are plenty and good and the inhabitants build huts and living there during the fruit season".

Josephus in his Book on the Jewish Wars (3:10:8) described Biq'at Ginnosar as: "The land is very fertile growing all varieties of plants". Fig trees and vines produce fruits nine months of the year. Other fruits ripen one after the other throughout the year. Evidence of the fineness of the fruits of Ginnosar is found in the fact that these fruits were not brought to Jerusalem because they would devalue the "Mitzva" of the pilgrimage to Jerusalem. The Babylonian Talmud Pesachim (8, b) quotes: "R. Abin son of R. Adda said in R. Issai's name: Why are there no fruits of Gennesareth in Jerusalem? So that the Festival pilgrims would not say: "Had we merely ascended in order to eat the fruits of Gennareth (its fruit was particularly delicious) in Jerusalem it would have sufficed us, with the result that the pilgrimage would not be for its own sake".

The reference to the fruits of Ginnosar in the traditional Jewish literature describes the fruits as being large, delicious and quickly ripening. These facts point to the area of Ginnosar being of rich soils, abundant water sources and a temperate climate.

Response Spectra of Earthquakes in the Gulf of Elat Recorded by the Israel Seismic Network

Gitterman, Y., Zaslavsky, Y., Shapira, A.

The Institute for Petroleum Research and Geophysics, P.O.B. 2286, 58122 Holon

Updated building codes, particularly those for structures with high safety requirements, require the performance of a dynamic analysis of the loads on the structure during ground shaking. Essential input for such an analysis and, thus, for the design of a structure which will withstand earthquakes, is the response spectrum (RS). This spectrum differs from one earthquake to another depending on distance, characteristics of the propagation path, magnitude and source mechanism. In common practice a normalized standard response spectrum (DRS) is used; this is obtained from empirical RS functions normalized to 1g. In a specific case of loads analysis, the DRS should be scaled by an appropriate PGA calculated from the attenuation relationship.

To date, only a few (16) accelerograms from local earthquakes are available and these sparse measured acceleration data do not cover a sufficient magnitude and distance range to form a data base for a regional response spectrum. Consequently, we have used seismograms, i.e. ground velocity measurements, from which accelerations and response spectra have been calculated. The data were obtained from recent earthquake sequences in the Gulf of Eilat. Over 70 events within a magnitude range of 4.0 to 5.8 were used in the analysis. These events were recorded by low-gain seismic channels of the I.S.N. 3-component short period seismometers MKT (Machtsh Katan), ZNT (Zur Natan) and ATZ (Mt. Atzmon). The evaluated response spectra and the normalized response spectrum are characteristic of earthquakes in the Gulf of Eilat which may affect structures in the populated areas of Israel.

Scanning Acoustic Microscopy for Petrographic Imaging

Golan G.,¹ Shoval S.,¹ Pitt C.W.²

1. Physics and Geology Groups, The Open University of Israel, Klauzner 16, 61392 Tel Aviv

2. Department of Electronic and Electrical Engineering, University College, London, Torrington Place - London

Scanning Acoustic Microscopy (SAM) may provide the bridge between the traditional Light Microscopy and the Transmission Electron Microscopy (TEM). The potential performance of SAM, operating in the reflection mode, for petrographic imaging, was examined on sedimentary and magmatic rock samples from Israel. A novel technique for achieving high resolution acoustic images by employing thermal effects has been studied and demonstrated. The experiments with the Scanning Acoustic Microscope were carried out in the Wolfson Unit laboratories at University College London. Acoustic images were created by exciting a PZT transducer on top of a sapphire rod which had a lens ground into its tip. A drop of water formed the coupling medium between the cavity of the transmitting lens and the specimen. Effective scanned surface of the rock planes was in the order of $800 \mu\text{m}^2$. The experiment was performed at a resonance frequency of 41 MHz with a lens having a 1.7 mm focal length.

The obtained results indicate that scanning acoustic microscopy provides improved petrographic images of rocks. This capability stems from the ability of SAM to distinguish between various minerals and rock components. SAM measurements can also indicate on the presence of components or rock structures in what would otherwise appear as homogeneous features. In polymineral rocks SAM technique emphasizes the fabric of different crystals and the boundaries between them. Furthermore, it identifies compositional variation in single crystal and the presence of zoning and inclusions. One of the most important advantages of SAM is its ability to penetrate into opaque minerals. This property can be suitable for the investigation of ore deposits. In carbonate rocks the SAM is sensitive to the distribution of accessory materials, namely, clay minerals, iron oxides and silica. SAM technique allows for the detection of fine features of fossil structures or micro-structures like oolite that are marked by oxides. By defocusing the acoustic beam below the rock surface a three-dimensional reconstruction of fossils and micro structures is possible. This fact is suitable for better identification of micro fossils even in reminiscence structures. SAM, as a non-destructive testing method is useful for the examination of ancient pottery as well. It should be emphasized that SAM does not provide direct mineralogical analysis, however, the minerals content can be estimated according to their specific acoustic material signatures.

Subsurface Structure and Composition of the Ramon Region

Goldshmidt, V.,¹ Rybakov, M.,¹ Segev, A.,² Itamar, A.²

1. The Institute for Petroleum Research and Geophysics, P.O.B. 2286, 58122 Holon

2. Geological Survey of Israel, 30 Malkhe Yisrael Street, 95501 Jerusalem

The Makhtesh (crater) Ramon is a "Geological window" where Early Mesozoic rocks are exposed. Compiled petrophysical data show that these rocks (mainly terrigenous) have relatively a lower density than the Upper Cretaceous sequence, mainly carbonate rocks. Thus, a negative gravimetric anomaly may be expected in this area. In fact, a large (up to 20–25 mgal) positive gravimetric anomaly was measured in the Ramon region. The same area is also typified by high frequency magnetic anomalies. The above gravity and magnetic features can be explained only by a deep regional block comprised of basic magmatic rocks, which partially crop out in Makhtesh Ramon.

The deep structure and its composition were studied using 2D gravity and magnetic modelling, together with the relevant information from deep drillholes (Zavoa, Nakha-1,2, Ramon-1 and Hameishar) where magmatic rocks were drilled in Nafkha-1 and Zavoa, north of the Ramon region).

The block boundaries are marked by a steep gravity gradient on linear magnetic anomalies. The southern boundary coincides with the Arif fault and the northern one is situated within the boundaries of Makhtesh Ramon, about 1–2 km south of the Mitzpe Ramon scarps, with no traces on the surface. The Ramon fault, which is a main structure on the surface, is only weakly noticed by the geophysical data and thus it reflects an internal structural element, of minor importance for the deep structure, within the Ramon block.

A local negative gravimetric anomaly (up to 5–7 mgal) is superimposed on the large regional positive anomaly at an area which includes the Shen ramon and the Gavnunim acid intrusions. Its main minima located between these intrusions and south of the Ramon fault suggests the presence of such rocks towards the south. Similar anomalies are also observed towards Mitzpe Ramon (NNW); the calculated model suggests a shallow (<500–700 m) depth for these acid igneous rocks.

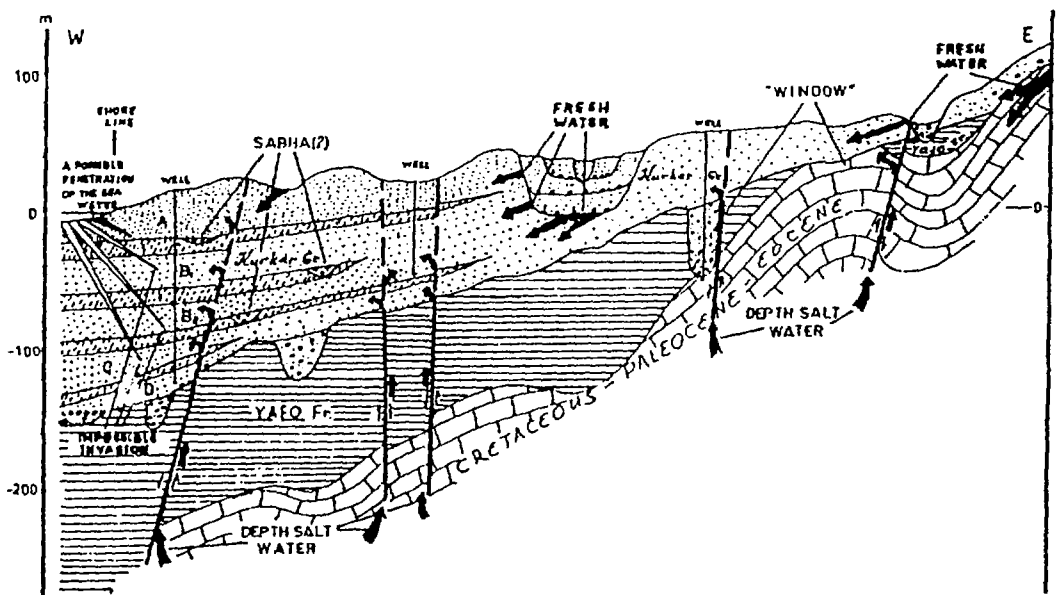
The Influences of Tectonics in Salinization in the Coastal Aquifer

Golts, S., Kolton, Y.

Morphoproject Consulting Group, 41/4 Meir Naqar Street, 93803 Jerusalem

The Plio-Pleistocene coastal aquifer is the major groundwater reserve in Israel. It is composed of clastic sands intercalated with clays. The Yafo Formation is composed of impermeable marine clays and separates the fresh upper Kurkar from a underlying aquiferial unit containing saline (3,000-60,000 ppm cl) water. The Yafo Formation which attains a thickness of several hundred meters at the coast, diminishes eastwards where it eventually disappears at the foothills.

At present the worrisome phenomenon of increasing salinization of the fresh coastal aquifer is attributed to incursion of sea water due to overpumping. Recent seismic and stratigraphic analyses reveal the presence of numerous fault zones that slice up the Cretaceous-Neogene succession. Morphotectonic analysis clearly reveals that vertical displacements are active and affects the Plio-Pleistocene succession as well. This tectonic movement and structural displacement creates conduits along which underlying saline water can rise in response to the new pressure gradients developed by the continued pumping.



Hydrogeological model of the Coastal Plain

Laboratory Simulation of Aquifer Remediation: In-situ Vapor Stripping

Gonen, O., Gvirtzman, H.

Institute of Earth Sciences, The Hebrew University of Jerusalem, 91904 Jerusalem

This study tests the in-situ vapor stripping (IVS) method as a mean of cleaning aquifers contaminated with Volatile Organic Compounds, (VOCs), originating from petroleum products, oil and solvents. The main concept being that injecting air into a well results in air-lift pumping of the contaminated water. During the process, VOCs are stripped from the water phase into the air bubbles. The VOCs are then collected at the top of the well. The partially treated water is forced into the unsaturated zone where it reinfilters. As water continues to circulate, VOC concentration is further reduced.

Our experiment was conducted in a room size model of a phreatic sandy aquifer. Inside the model there is a well. Air is injected into the well and released beneath the water table, creating bubbles that rise. Due to the density difference between the water column outside the well and the water-air bubble mixture column inside the well, a lift is created. The pumped water is diverted away from the well and then recharged back to the aquifer by gravitational seepage through the unsaturated zone. This creates circulation of water around the well such that a larger pore volume will be affected by the well.

During the experiment we used 3 different contaminants: trichloroethylene, toluene and chloroform. In the first stage the remediation efficiency was checked under stagnant conditions. The efficiency is effected by different parameters: the VOC's concentration, temperature, Henry's coefficient, (partitioning of VOCs between water and gas phase), specific surface area of the air bubbles and the rate of air flow. After running the experiment for 48 hours the contaminant's concentrations were reduced drastically. The remediation efficiency was found to depend on three main factors:

1. The flow field within the well-influence zone: along short flow paths between the recharge area and the pumping well, the VOC concentrations reduced rapidly, while elsewhere concentrations reduced slowly.
2. The absorption affinity of the compounds: molecules with a larger tendency to be absorbed to the solid matrix will circulate at a slower rate within the well influence zone; thus, will be removed at a slower rate.
3. The vaporizing affinity of the compounds: the water/air partition coefficients, determine the relative mass of the VOCs that is removed by the air bubbles while lifting within the well.

These experiments show that IVS of VOCs in a contaminated site is feasible for in-situ remediation and prevention of the spreading out of contaminants.

Paleofloods in Nahal Zin

Greenbaum, N., Schick, A.P.

Institute of Earth Sciences, The Hebrew University of Jerusalem, 91904 Jerusalem

Geomorphological relics suggest larger floods occurred in the past (paleofloods), than today. The Paleohydrology deals with the reconstruction of hydrologic regimes using geomorphological and botanical evidence. The object of this research was to reconstruct the peak discharge of paleofloods in Nahal Zin and to determine their ages. Paleohydrological data belong to a high-magnitude, low-frequency, population. Such data is very important in deserts, where the number of flows and of gauging stations are few, and where available flood records are limited. Short records tend not to contain many or any large floods, and the prediction of flood magnitude for the periods needed by engineers is based mainly on statistical extrapolations. Paleohydrological data can extend a flood record period and permit a more reliable flood frequency analysis. Most of drainage basins are not hydrometrically instrumented, and the only flow data available is that of paleoflood data.

Field evidence includes fine-grain slackwater deposits (SWD), sand to clay in size, carried as suspension at the high stage of the flow and deposited in preferable sites in which the velocity decreases drastically. Such sites include tributary mouths, channel expansions, shadows of obstacles in the channel, caves and alcoves in the banks, etc. Other paleostage indicators (PSI) involve both driftwood and silt lines and can be used are also used although they preserve shorter periods. The organic material which floats on the water is deposited at the same sites and forms organic beds which are datable by radiocarbon and provide the age of the flood. The research sites are canyon-like reaches in which the cross section and the trend are stable.

The measured hydraulic and geometric parameters are entered into an hydraulic engineering program, HEC-2, which uses step-backwater procedure and generates various water surface profiles for various water stages and discharges.

Nahal Zin - a 1400 km² watershed, has a 40 year hydrologic record from 5 gauging stations along the main channel. Twenty seven floods, larger than 200m³/s, were reconstructed, for the last 2000 years. Maximal measured peak discharge - 550m³/s in October 1991. The reconstructed peak discharges are 2.5-3 times larger and exceed 1500m³/s. The temporal distribution of the paleofloods show clusters of floods during some periods, while other periods have few or no floods. High flow magnitudes characterizes periods with many floods. These fluctuations between periods of many floods and periods with few floods are evidence of changes in the hydrologic regime, which may suggest climatic fluctuations during the last 2000 years.

Mechanical Behavior of some Dolomites from the Judea Group: Preliminary Results

Hatzor, Y.,¹ Mimran, Y.²

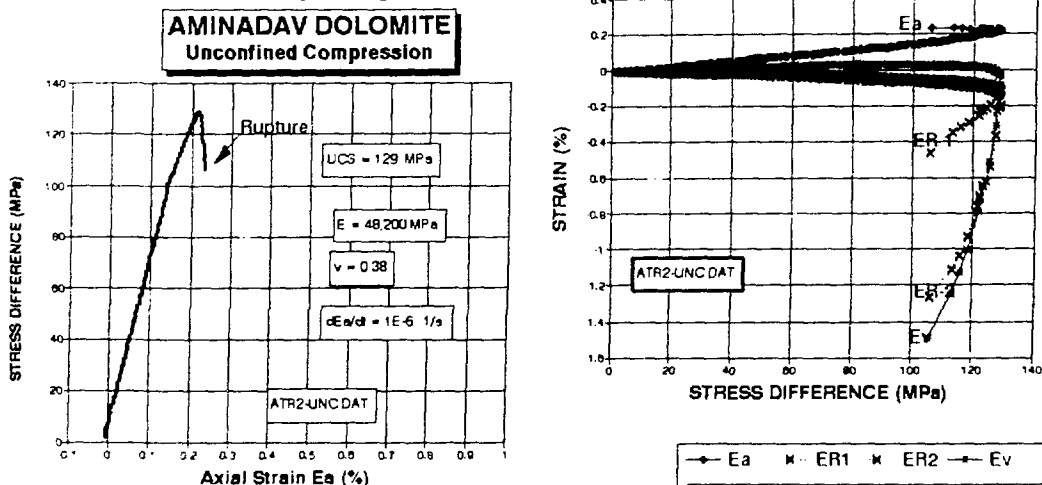
1. Department of Geology and Mineralogy, Ben-Gurion University of the Negev, 84105 Beer Sheva

2. Geological Survey of Israel, 30 Malkhe Yisrael Street, 95501 Jerusalem

A few samples were taken from massive dolomite blocks interbedded in a cohesionless matrix of dolomitic sand at the base of the Aminadav Formation, near the Southern Portal of the Giloh Tunnel, currently excavated in the Judean Mountains near Jerusalem. Geotechnically this unit is problematic due to the extreme range of mechanical characteristics of its constituents. The massive dolomite is very inhomogeneous, characterized by variable grain size and pores of different geometries. The average porosity is estimated at about 10%.

Three samples were loaded uniaxially in a stiff, closed-loop servo-control system with axial load capacity of 1.5 MN and confining pressure of up to 70 MPa. The samples were prepared according to ISRM standards having NX core diameter of 54mm, length to diameter ratio of 2, flatness to 0.02 mm and perpendicularity to 0.005 radian. The samples were loaded at a constant strain rate of 1×10^{-5} and 1×10^{-6} sec⁻¹.

The samples showed a dependance of unconfined compressive strength (UCS) on strain rate, the higher rate resulting in a higher UCS. The samples revealed a very brittle behaviour at strains beyond peak stress. At the 1×10^{-5} 1/sec strain rate the sample failed violently at peak stress. At the slower strain rate of 1×10^{-6} 1/sec a controlled failure process was partially achieved (see figure). Onset of dilatation was detected at about 85% of peak stress, judging from volumetric strain data. At the post peak region volumetric strain rate has increased markedly (see figure) indicating rapid fracture propagation culminating in rupture.



Tectonic Setting and Crustal Structure of the Eastern Mediterranean

Hirsch, F.,¹ Flexer, A.,² Rosenfeld, A.,¹ Yellin-Dror, A.²

1. Geological Survey of Israel, 30 Malkhe Yisrael Street, 95501 Jerusalem

2. Dept. of Geophysics and Planetary Sciences, Tel Aviv University, 69978 Tel Aviv

Palaeozoic and Mesozoic stratigraphy and palaeo-biogeography suggest a fairly continuous unity of epicontinental African, Apulian and Arabian areas during the entire time span of the Phanerozoic era, prior to and after the Early Triassic opening of the Mesozoic Tethys.

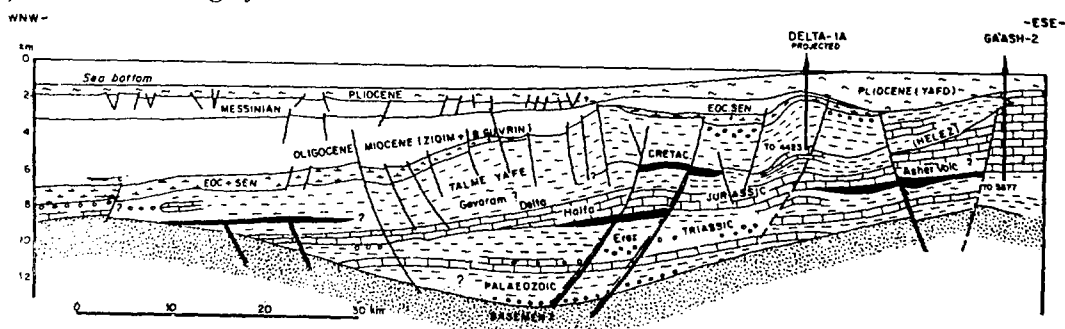
The allochthonous ophiolite-bearing terranes, that cover the edges of the Gondwanian plate, optimally fit within a palinspastic model of a single Tethys ocean, north of the African-Apulian-Arabian palaeo-edge.

Seismic reflection and refraction, magnetic and gravimetric measurements of the present eastern Mediterranean and Levant crust show a thick Phanerozoic succession of 13-14 km overlying a 8 - 12 km thick crust.

The geological and geophysical reevaluation suggests that the Levant Basin is paved mainly by continental crust with embedded Infracambrian ocean-crust relics (Pan African), which explains its enormously thick sedimentary cover. The apparent thinner crust under the Levantine Basin is presumably due to subcrustal thermal erosion.

The possible existence of a western palaeo-high offshore the Levant coast calls for a reassessment of hydrocarbon exploration in the eastern Mediterranean. The previously proposed "hinge belt" along the Levant coast would merely represent the transition from the eastern platform to the graben that separates the eastern (onland) from the western (offshore) highs.

The rather passive extensional regime of the Gondwanian eastern Mediterranean plate during most of the Phanerozoic era ended with the Late Cretaceous - Paleogene Alpidic compression of its margin and the activation of the onland and offshore Levantinid Syrian Arc folding system.



A New Palyno-Zonation Scheme for Campanian-Maastrichtian Organic-Rich Carbonate Sequences in Israel

Hoek, R.,¹ Eshet, Y.,² Almogi-Labin, A.²

1. Laboratory of Palaeobotany and Palynology University of Utrecht, The Netherlands

2. Geological Survey of Israel, 30 Malkhe Yisrael Street, 95501 Jerusalem

A detailed palynological study of Late Campanian-Early Maastrichtian sequences was conducted in core sections from the Be'er Sheva Valley (M-8) and the Shefela Basin (Zor'a B and Hartuv B). Very rich and diverse palynological assemblages were recovered from most samples. Assemblages are dominated by dinoflagellate cysts with minor amounts of colonial algae. Land-derived particulate organic matter (pollen, spore, woody tracheid, cuticles) is extremely rare, indicating a negligible role of the continent as a source of organic matter (<1%).

The proposed palynostratigraphic zonation allows, for the first time, to subdivide the Campanian-Maastrichtian time-interval into five dinoflagellate cyst-based interval zones which are controlled by both calcareous nannoplankton and foraminifera. The proposed zones are:

- * *Odontochitina costata* Interval Zone (Late Campanian)
- * *Xenascus ceratioides* Interval Zone (latest Campanian)
- * *Chordosphaeridium* sp. A Interval Zone (earliest Maastrichtian)
- * *Ceratium diebelii* Interval Zone (Early Maastrichtian to earliest Late Maastrichtian)
- * *Cannosphaeropsis utinensis* Interval Zone (earliest Late Maastrichtian)

The consistent occurrence of these palynozones in the two studied sections demonstrates the potential of a dinocyst-based zonation in correlating Campanian-Maastrichtian successions in Israel. The present zonation scheme was found useful especially in determining the position of the Campanian-Maastrichtian boundary that is not always well-defined by other groups.

Methusaleh — or Lazarus — Effect in the Ostracod Species *Cythereis Mesa*

Honigstein, A.,¹ Hirsch, F.,² Rosenfeld, A.,² Flexer, A.³

1. Ministry of Energy and Infrastructure, Oil and Gas section, 234 Yafu St., 94387 Jerusalem
2. Geological Survey of Israel, 30 Malkhe Yisrael Street, 95501 Jerusalem
3. Dept. of Geophysics and Planetary Sciences, Tel Aviv University, 69978 Tel Aviv

Two subspecies of the ostracod *Cythereis mesa* Honigstein, which were reported from the Late Santonian-Campanian strata in Israel, re-occur surprisingly in Early-Middle Paleocene sediments of the Sede Boqer area.

The Santonian-Campanian rocks in Israel are rich in ostracods (over 50 species), whereas they occur in the Maastrichtian only in low population densities and poor diversity (approximately 10 species, but most of them are non-age diagnostic). Indicative ostracod species re-occur in the Paleocene sediments, in higher numbers and with over 20 species present.

The two subspecies of *C. mesa* (*C. mesa mesa* and *C. mesa ventroreticulata*) were found in the Senonian S-3 to S-5 zones, and again in the lower 30 meters of the Paleocene successions in the Negev. These ostracods do not occur in all investigated sections in Israel throughout the whole Maastrichtian stage (about 10 m.y.).

The possibility of redeposition could be ruled out due to the good preservation of the ostracods and the absence of redeposited Late Cretaceous foraminifera and calcareous nannoplankton in the Paleocene samples. Therefore, the reappearance of these ostracod taxa after a long gap must be related to other factors.

The Lazarus-effect means an iteration of a distinct species, caused by backward evolution due to environmental stress. On the other hand, species may have very long stratigraphic ranges, explained by high adaptive tolerance of these taxa - Methusaleh effect.

The Ghareb Formation was deposited under oxygen deficiency which probably caused the disappearance of this species. The re-establishment of better ecological conditions during the Paleocene (Taqiyeh Formation) may be the cause of the reappearance of those relatively large and ornamented ostracod species. The question of which effect is responsible for the re-occurrence of *C. mesa* remains unsolved for the time being, as long as these taxa are not reported from other sections in our area.

The Neanderthal Site of Amud Cave, Israel

Hovers, E.,¹ Goren, Y.,² Rabinovich, R.,³ Rak, Y.⁴

1. Institute of Archaeology, Hebrew University of Jerusalem, 91905 Jerusalem

2. Israel Antiquities Authority, P.O.B. 586, 90014 Jerusalem

3. Department of Evolution, Systematics and Ecology, Hebrew University, 91904 Jerusalem

4. Department of Anatomy and Anthropology, Sackler Medical School, Tel-Aviv University, Ramat Aviv

The Amud Cave, discovered and excavated in the 1960s' by a Japanese archaeological team, contained the remains of several hominids, including the relatively complete skeleton of a male, argued to be an unclassical Neanderthal. In the lack of adequate absolute dating methods, the site was attributed to the Middle-Upper Palaeolithic transition on the basis of its lithic and faunal assemblages. Recent progress in dating techniques and recent excavations in the Levant resulted in revolutionary implications for the understanding of Upper Pleistocene human cultural and biological evolution. Following those developments, the renewed multidisciplinary project at Amud Cave is designed to obtain new data pertinent to the main questions raised in current research of the Middle Paleolithic.

Major archaeological research questions relate to topics such as the radiometric dating of the site (currently conducted by ESR, TL and AAR techniques) and its temporal relations with other hominid-bearing sites. Special attention is given to studying the detailed stratigraphy of the Palaeolithic deposits at the site, their origins and nature, and the mechanisms and degree of post-depositional disturbances that affect our interpretation of the finds. This is done by painstaking mapping of finds and sedimentological features, micromorphological and chemical analyses. Another set of research problems addresses the structure of the lithic assemblage at the site, its diachronic change (if any) and its affinities with either Middle Palaeolithic or transitional lithic assemblages known today in the Levant. Mobility and subsistence patterns of the group(s) occupying the site are also discussed.

Being the only Middle Palaeolithic site in the Dead Sea Rift, Amud Cave provides the opportunity to study an ecological regime not known from other sites of broadly the same time span, through a detailed archaeozoological (e.g., paleontological and taphonomic) research on both mega -and micro- mammals.

An important aim of the renewed project - subject to the finding of new hominid remains - is the enlargement of the hominid sample from the site, re-assessment of the biological taxonomic status of the site's occupants and clarifying its implications for understanding the evolutionary relationships between the Levantine Middle Palaeolithic populations.

The renewed project, going on since 1991, has come up with rich sets of data relevant to many of the basic questions. In the present contribution we describe the preliminary results of field work and the interdisciplinary methods used to obtain those results.

Late Holocene Palaeogeography of the Bethsaida Area

Inbar, M.,¹ Shroder, J.²

1. Department of Geography, University of Haifa, 31905 Haifa

2. Department of Geography and Geology, University of Nebraska at Omaha, NE 68182 USA

The Bethsaida (Beteiha) plain, situated at the Jordan mouth north of Lake Kinneret, has been subjected to rapid geomorphic changes in historic times. The archaeological site of E-Tell, about 3 km north of the present shoreline, is considered to be the fishing village of Bethsaida. An Early Bronze to first century CE habitat span has been established by recent archaeological excavations to the site.

Thicknesses of sediment in the Bethsaida plain exceed 100 m along the shoreline and boreholes drilled across the Jordan river are about 40 m depth about 1 km north of the river mouth, overlying basaltic layers. Two meters of fine grained floodplain deposits over coarser probably shoreline deposits occur on 7 boreholes one km north of the present shoreline. Analyses of aerial photographs of the plain reveal that the Meshushim river, which now flows southwest, probably flowed west. Paleochannels on the Meshushim fan also show channels to the south, and it is possible that the main south-oriented channel is a remnant of a filled estuary to the Bethsaida site now buried beneath the Meshushim alluvial fan gravels. Recent floodplain coarse sediments cover the area close to the archaeological site, impounding probably previous coastal lagoons which provided harbour facilities for the fishing village of Bethsaida.

The landform processes that can be observed at present have allowed formulation of hypotheses that this former village of Bethsaida was close to the water edge of Lake Kinneret through some combination of: (1) uplift of the site away from the lakeshore by rift faulting (shore-up hypothesis); (2) sediment filling of the plain around the site by flash flooding of the Jordan and other nearby rivers (shore-out hypothesis); and (3) drop in water level of Lake Kinneret away from the site by climate-controlled reduced inflow, or by downcutting of the Upper Jordan channel inlet (water-down hypothesis). The aim of this study is to determine the processes and time of the Kinneret shoreline changes and its relationship with the Bethsaida archaeological site.

Fluorescence Photography of Minerals

Isaac, Y.

Golomb Street 9, 84428 Beer Sheva

Photographing types of minerals which fluorescence under ultraviolet irradiation supplies a new way for studying and demonstration of this phenomenon. One of the common methods in scientific research is analysis of fluorescence from minerals due to ultraviolet irradiation.

I have joined a research group from the Open University, Ramat-Aviv, which among other things works on locating minerals (especially in the Negev) and also on ways to enrich the minerals.

Fluorescence is a property of materials to absorb light of a certain wavelength and emit light of longer wavelengths. In the area of geology on which I report in this work, the term luminescence is used. This includes fluorescence and it is used in research and geology. Luminescence is emission of light in a wide range from ultraviolet (UV) to infrared (IR).

The main reason for UV photography of objects is obtaining new information about them, which could not be obtained using other photographic methods. When two materials look differently in visible or infrared light, usually there is no need to use ultraviolet illumination. If however, the other two methods fail or other information is required, there is a chance that the third one will succeed.

The regions beyond the visible are not recorded by human eyes but making use of appropriate photographic conditions enables the emulsion to record some information from these regions.

There are two ways of using UV light in photography:

- 1) Photography of the reflected UV radiation.
- 2) Fluorescence photography.

There are many sources of light which contain UV radiation. However, not all of them can be used in all kinds of UV photography. The longer wavelengths in the UV region are the most common for fluorescence excitation. Shorter wavelengths are sometimes used in photography of certain minerals.

Two filters must be used in fluorescence photography. The first, between the object and the source of radiation, and the second, on the lense to remove unwanted UV radiation and transmission of fluorescence light only.

Volcanic Phenomena in Quartz-Syenite Bodies in Gavnunim and Shen Ramon

Itamar, A., Segev, A., Peltz, S.

Geological Survey of Israel, 30 Malkhe Yisrael Street, 95501 Jerusalem

Acidic rock bodies in Gavnunim and Shen Ramon in Makhtesh Ramon were previously studied and were interpreted as intrusions. New evidence indicates that at least some of the rocks building these bodies are volcanogenic, formed as a result of explosions or lava flows.

The layered magmatic acidic body overlying part of the Gavnunim intrusion, previously interpreted as sill, has a typical lava-flow structure: a brecciated base (both where it overlies sedimentary rocks and where it overlies the quartz-syenite intrusion), a vesicular top, and columnar structures in between. Its lateral contact with Triassic sedimentary rocks appears as channel infill rather than intrusion. Thus, it seems that this body formed from lava that flowed over a low relief, came up against a wall of sedimentary rocks and was stopped. Petrographic evidence for a volcanic source can be seen in the large, rounded vesicules created by the release of gases, polymictic fragmentation of the quartz-syenite rock and its consolidation in a glass matrix which subsequently was devitrified.

In some places in Shen Ramon, brecciated bodies are found with polymictic fragments different in part from the nearby country rocks. Rocks, in which there are crystals, sometimes broken, that are consolidated in a glassy matrix (part of which was devitrified), are classified as crystal lithic-tuff. Some of the fragmented rocks appear to be layered tuff and agglomerates. In contrast, some fragmented rocks appear as elongated, sub-vertical bodies of tuffisites along a straight or curved eruption fissure. Red, soft friable rock found in drillhole cores from Shen Ramon was determined as fossil soil.

The question whether the Triassic rocks hosting these bodies in Gavnunim were exposed during the Early Cretaceous (124–128 Ma, the time of their emplacement), must be addressed. Previous studies show basalt and the Arod Conglomerate overlying similar Triassic rocks about 500 m east of the Gavnunim outcrop, thus acid volcanic rocks might also be found in the same relationship.

In Shen Ramon clear intrusive contacts between hypabyssal magmatic rocks and the surrounding country rocks were found as well as bodies of tuffisite, tuff and evidently fossil soil.

Shen Ramon is a plutono-volcanic complex in which sills and small intrusions are exposed, as are, likewise, eruption fissures and various volcanoclastic rocks. Thus, in addition to the basic intrusive and extrusive phenomena recognized in Makhtesh Ramon, there is also a wide variety of acidic rocks, extrusive as well as intrusive.

Micromagnetic Study of Archaeological Sites in the North of Israel

Itkis, S., Seligman, J. , Israeli, S.

Israel Antiquities Authority, P.O.B. 586, 90014 Jerusalem

A number of large sites in the north of Israel were investigated during the year 1993 by the micromagnetic methods. The sites surveyed were Baniyas, Beit Shean Citadel and Nahal Hagit. Their geological and geophysical conditions differed widely. Constructions on the first two were mainly of basalt set in a basalt soil matrix and problems involving the detection of walls and others structures could be successfully solved.

At first glance the site of Nahal Hagit was less suited for a magnetic survey. Both building material and the limestone bedrock were practically unmagnetic and the soil fill gave only low values of magnetic susceptibility. The magnetic anomalies obtained with the help of highly precise investigations were insignificant in intensity (between 2 to 5 nanoteslas) but the features that create these weak anomalies can be traced on the map due to their specific shape. Nevertheless magnetic materials, such as basalt vessels and installations, ceramics, fired structures ("tabuns") and pieces of slag were easily detected at the site. The results obtained on each site show the necessity for preliminary investigations of the area prior to excavation.

Fractal Analysis of the Earthquake Catalog of Israel

Kanel, E.

The Institute for Petroleum Research and Geophysics, P.O.B. 2286, 58122 Holon

This study concentrates on analyzing the existing earthquake catalog of Israel in order to determine fractal dimensions and identify fractal characteristics as functions of sub-catalogs extracted from the whole earthquake list according to time, space and magnitude. We demonstrate that the temporal and spatial distribution of earthquakes in the region can be modeled by the one dimensional Cantor Set. Consequently, we may apply this model to define the parameters involved in fractal analysis and self-similarity investigations.

Fractal dimensions were calculated for different periods, various sub-regions and different magnitude ranges. The results show that the fractal dimensions obtained before and after the occurrence of a strong earthquake are different. In general, the fractal dimensions tend to decrease prior to the occurrence of a strong earthquake, yet the rate of decrease and its duration depend on choices related to the selection of the sub-catalogs.

From general observation of the behavior of temporal and spatial fractal dimensions, we can conclude that earthquake hazards are time dependent, even over a relatively short time interval. Problems associated with these estimations and the uncertainties involved will be discussed.

Oil and Gas Bearing Prospects of the Continental Shelf of Israel

Kapulsky, M.

P.O.B. 489, 31000 Haifa

In the 70s our research emphasized the high oil-bearing prospects of the Israel Continental shelf. Additional study of local geological materials enforced that prediction (Kapulsky, 1972, 1993). As it was mentioned by Israeli scientists (Livshits, 1993), the region is characterized as a most preferable one among the other geological regions in the area of Israel.

Factors such as the highly-developed continental shelf (Bradshaw, 1972) and the geological depositions similar to the industrial oil strata of the Sinai peninsula help us to determine the off-shore region as an urgent object for drilling for oil and gas. The prospecting should be carried out in calcareous rock of the Jurassic and the Miocene periods and sandstone in order to find convex-type accumulations of oil and gas and stratigraphic and tectogenetic screened deposits, coincided with asymmetrical block-type anticlines.

As a matter of fact the drilling procedure will be marked by specific difficulties, caused by geological structures and provided by accumulations of sediments, bituminization, formations and reservations of oil and gas. It could be explained by the specific characteristics of the oil and gas basins in inter-mountain depressions, formed on the base of singular synclinal bowls or local grabens, mentioned in the researches (Cohen, 1991). The East Mediterranean oil and gas basin is the typical one (Brod, 1962). The specific characteristics is provided by formation conditions of the oil and gas depositions regions on the basin's synclinal-bowing edges, as much as those regions were formed either during the geosynclinal phase of development or right after that phase.

That phase of development is characterized by the following processes:

- burial and conversion of organic substance are provided by rapid accumulation of thick sedimentary complex, contending terrigenous components.
- deep and powerful immersion causes increase of temperature and pressure, facilitating more rapid disintegration of organic substance, creating bitumen.
- high static pressure of thick sedimentary complex.
- numerous interruptions of all measures of the thick strata continuity facilitating middle migrations through the thick sedimentary complex.
- frequent and remarkable oscillations of erosion base and the bottom of deflection leading to time and space changes of facias and consequently leading to conditions changing of organic substance and reservoir depositions.
- frequent dislocation maximal deflection regions, formation of new structural anticlines and depressions leading to dislocation of oil and gas areas.
- intensive water circulation and migration processes leads to disturbance of the performed oil and gas depositions and causes reintegration of the hydrocarbons.

The undermentioned characteristics proofs the lack of heredity in oil and gas regions of the previous geological ages and vitally makes the process of prospecting more complicated.

Neutron Shielding by H₂O in Clay Minerals - an Explanation for ³⁹Ar Deficit in Irradiated Clay Fractions

Kapusta, Y., Steinitz, G., Kotlarsky, P.

Geological Survey of Israel, 30 Malkhe Yisrael Street, 95501 Jerusalem

The neutron fluence and its variation as utilized in ⁴⁰Ar-³⁹Ar dating is determined by using a mineral-monitor which is irradiated in a nuclear reactor together with the sample. It is assumed that the efficiency of the ³⁹K(n,p)³⁹Ar reaction in the monitor and the sample is the same. Using standard monitors (LP-6, HD-B1, MMhb-1 etc.) for ⁴⁰Ar-³⁹Ar dating of clay minerals yields ages significantly too high. The conventional explanation assumes a ³⁹Ar deficit within the mineral, due to its "recoil" from the fine grains, as the cause for the phenomenon.

Two different aliquats (0.028, 0.351 gr) of the same clay fraction (<0.2μ) irradiated together contained different amounts of ³⁹Ar (1.3*10⁻⁷, 1.96*10⁻⁷ cc/gr). The dependence of the ³⁹Ar concentration on the mass of the sample indicates a varying neutron flux in the sample. In the irradiated samples no loss of ⁴⁰Ar_{rad} was observed nor could implanted ³⁹Ar be detected in the aluminum foil used for packing the samples.

The measured ³⁹Ar content in different clay fractions irradiated together shows a linear correlation between the calculated ³⁹Ar deficit (using their K-Ar age) and their H₂O content (determined by DTA). This implies that the water in the clay minerals moderates and/or absorbs the neutrons and thus is the source of the ³⁹Ar deficit relative to the monitors which are devoid of water.

It is suggested to use clay fractions with calibrated K-Ar ages and known water contents as additional neutron flux monitors for ⁴⁰Ar-³⁹Ar dating of fine clay minerals. A first test using this approach yielded ⁴⁰Ar-³⁹Ar ages of H₂O bearing clay fractions close to their K-Ar ages. The deviations may be due to difference in size and geometry between the clay monitors and the samples. The results open the possibility of extending the approach to step-wise heating experiments.

Criteria for Archeoseismic Events: Evidence from Negev Sites

Karcz, Y., Perath, I

Geological Survey of Israel, 30 Malkhe Yisrael Street, 95501 Jerusalem

All untended buildings are eventually destroyed by man-caused, static and seismic causes. Archeological ruins preserve evidence of all three, and can be used to characterize the historical seismicity of their region. To this purpose, Nabatean to Byzantine sites of the Negev were examined for earthquake evidence.

Seismic damage is hard to identify, since it often is not different from damage due to slower (so-called static) causes - the effects of material fatigue (cleavage or cracking), weathering (rotting, pulverization, flushing and deflation), and sequential collapse resulting from the redistribution of structural stresses.

Nevertheless, some destructional features are more likely to be earthquake-caused than others. These are mostly directional, caused by shock waves and ground roll that radiate from the epicenter outward (although local refractions and reverberations may cause some divergence). Thus, preferential directions of leaning, falling, building or bending may indicate preferential acceleration. Since seismic impact is transmitted through the ground, any strains that appear to be propagating from the substrate upward - splays, transpositions, upbulgings, horizontal rotations, offsettings - are also suspectibly seismic. Enhanced damage on waterlogged or earth-filled localities, as opposed to hard substrate, also conform to what would happen in an earthquake.

According to these criteria (evidence for shaking, horizontal accelerations, and signs of substrate distortion) the following features were distinguished and recorded: Preferential directions of leaning/collapse of walls and piers * Directional collapse of vaults and arches * Unidirectional bulging of walls above the socle * Preferential leanings of wall-engaged piers within the wall plane * Horizontal rotation of arch supports (shearing of the arch plane) * Bending or sigmoid distortion of wall planes * Chaotic deformation of wall masonry; extrusion and rotation of individual stones, disalignment of ashlar * Horizontal offsetting between adjacent wall sections and between tiers (displacement normal to the wall plane) * Radial displacement, mutual rotation and imbricated collapse of arch elements * Downwidening cracks, reaching the foundation tier * Synchronous ancient repair ***

Other types of damage were also duly marked as possibly seismic, even though they could equally well be the result of static decay and accumulated damage. These include biconvex sagging, tier-crossing fissures and inter-stone parting, cracking of masonry, the leaning of jambs toward door- or window openings (i.e. within the plane of the wall), bilateral or centrifugal collapse of free-standing walls and structures. An earthquake's magnitude, i.e. its impact on structures, is greater at a site which has been rendered unstable by accumulated damage and smaller at a site in advanced state of decay. Hence, such features are not reliable as archeoseismic criteria.

The Origin of the Kurkar Ridges in the Sharon (Central Coastal Plain, Israel)

Katsav, E., Gvirtzman, G.

Department of Geography, Bar Ilan University, 52900 Ramat Gan

A map of the three Kurkar Ridges in the Sharon is presented, illustrating both the morphology and the geology of the ridges. The map units were correlated with nearby boreholes. In the Western Ridge, whose inner part is exposed along the coastal cliff, the Ramat Gan Kurkar can be seen at the base, the Nahsholim Sand in the middle and the Dor Kurkar at the top. In boreholes these three subunits together comprise the Giv'at Olga Kurkar, since it is impossible to separate them. The Netanya Hamra and the Tel Aviv Kurkar are exposed in the uppermost part of the cliff. The Ridge is covered by the Ta'arukha Sand. The youngest Hadera Sand is found in the Sharon only at the outlet of Nahal Poleg. The Central Ridge, with its typical topography, is not continuous. Its inner part is not exposed and therefore its lithology is correlated to the Giv'at Olga Kurkar without further subdivision. However, in a new roadcut at the Sira Junction, south of Herzliyya, its inner part was exposed and in this ridge too, the Nahsholim Sand separates between the Ramat Gan and the Dor kurkars. It is therefore concluded that both kurkar ridges are composed of the same lithostratigraphic units. The Eastern Ridge, composed of the Ashdod Kurkar, is found only in the northern Sharon, in segments such as Kefar Haro'eh-Elyashiv, Ma'abarot-Mishmar Hasharon and Tel Yizhaq. In the southern Sharon, in Ra'anana and Herzliyya, this ridge does not exist, not in outcrops nor in the subsurface. There is no kurkar ridge in the Sharon which is composed of the Herzliyya Kurkar.

For more than half a century, researchers of the Quaternary of the coastal plain of Israel apply stratigraphic interpretation to the position of a kurkar ridges. Their geographical order from E to W was interpreted as a chronological order, from older to younger, respectively. Fossil shorelines were hypothetically attributed to every ridge. The ridges were considered as analogues of the fossil Mediterranean shorelines and were correlated with the interglacial high-stand sea-levels. This concept, which was rejected for other reasons too, is further proved to be invalid by the new data on the ridges. There is no correlation between the kurkar ridges and the shoreline fluctuations. A single ridge is not continuous, several segments along a straight kurkar line are not necessarily synchronous. The Eastern Ridge south of the Yarqon River is composed of the Herzliyya Kurkar and the Eastern Ridge north of the Yarqon, is composed of the Ashdod Kurkar. The Central Ridge sometimes splits into two parallel kurkar ridges. The Western and the Central ridges were deposited in the Sharon Plain simultaneously. It is therefore concluded that the ridges are fossil longitudinal sand dunes which accumulated during favorable climatic conditions and were later cemented into eolianites. No shorelines were formed near the ridges. Sometimes several parallel ridges were deposited during one period and sometimes no longitudinal dunes accumulated at all. Additional fossil longitudinal eolianites probably exist in the subsurface of the eastern Sharon plain as well as along the present Mediterranean shelf.

Stratigraphy of the Quaternary Sequence of the Coastal Cliff of the Sharon (Central Israel)

Katsav, E., Gvirtzman, G.

Department of Geography, Bar Ilan University, 52900 Ramat Gan

Seven lithostratigraphic units are exposed along the coastal cliff of the Sharon, between the Country Club and the outlet of Nahal Alexander. It is almost impossible to show the distribution of these units on a conventional geological map due to the small size of the vertical outcrops. However, these units are illustrated in a N-S cross section, viewed from the sea to the east, with a vertical exaggeration of X40 (presented as a poster). The cliff is steep, descending from the Kurkar Ridge hilltops, at 30 to 55m elevation, to sea level. The cliff is breached by the outlets of the Gelilot, Poleg and Alexander streams, forming valleys which are bottomed at sea level. The steepest lower part of the cliff is composed of three units and the other four cover the upper part of the cliff and the top of the Kurkar Ridge.

At the base of the cliff, the Ramat Gan Kurkar, a cross-bedded eolianite, 0-40m thick above the sea level, is exposed. The overlying Nahsholim Sand, composed of sand mixed with minute silt and clay, grayish-brown (the color of "cafe au lait" as coined by Avnimelech), 0.1-3m thick, is distributed continuously along the entire cliff. This unit, which contains abundant land snails, was designated as "hamra" although it differs from hamra by its poor pedogenic development and by its light color. The overlying Dor Kurkar is a cross-bedded eolianite, 0-40m thick.

Thus, the steep lower part of the cliff constitutes two cycles of longitudinal sand dunes, cemented to eolianites and separated by a thin veneer of loose sands. Both upper surfaces of the Ramat Gan and the Dor kurkars, have large-scale undulations which are typical to longitudinal dunes.

At the top of the cliff, the Netanya Hamra overlies this relief and its relative loose texture results in a retreat of the cliff edge. The unit is composed of quartz grains coated by iron oxides, mixed with silt and clay, reddish-brown, 0.5-4m thick, with some pedogenic horizons. The overlying Tel Aviv Kurkar, a cross-bedded hard eolianite, 1-5m thick, forms a flat hard surface at its top, protecting the retreating cliff. This surface is typical to sand sheet dunes, forming wide dune fields. The overlying Ta'arukha Sand, 1-5m thick in a N-S belt 1-2 km wide, covers the top of the Kurkar Ridge. The unit is light brown with typical cross-bedding, and is composed of loose sand with minute silt and clay and abundant land snails. The younger Hadera Sand, 5-6m thick of a light yellow color, covers only the breached cliff of the Nahal Poleg valley and the southern part of Netanya. These sands, dunes which are still active, do not cover the hilltops of the coastal cliff. All the units of the coastal cliff were deposited under terrestrial conditions.

Proposed Method for Revealing Hidden Concentric Structures in Complex Geophysical Fields

Khesin, B.

Department of Geology and Mineralogy, Ben-Gurion University of the Negev, 84105 Beer Sheva

Geological bodies having circular and annular cross section form concentric zonal structures (CS). These bodies have different sizes from gigantic astroblemes of cosmic origin to small volcanos and pipes. CS are often characterized by geophysical (particularly, magnetic and gravitational) and topographic anomalies. But it is difficult to single out objects of CS in complex geophysical fields especially taking into account that surveys commonly employ rectangular network of observations. Besides, the researcher has to discriminate between the anomalies caused by ring (annular) structures and the features of the field stemming from its character around the periphery of stock like bodies. For this purpose the author proposes a method for distinguishing CS based on summing up horizontal gradients of the field using circular graticule (zone chart).

Horizontal gradients are determined by the graticule radii passing through 45° interval. When summing-up the gradients in the various directions, the presence of circular feature should be intensified whereas other signals are levelled up. In doing so, the correlation of the sum of gradients (or the average gradient) for a circle with radius R_n and a ring external to this circle limited by R_n and R_{n+1} radii makes it possible to determine whether the circular feature revealed reflect centric or ring structures. The sum of gradients inside a circle tends to zero in the absence of a centric texture.

This proposal was successfully tested using model magnetic field. The further elaboration of quantitative (informational) criterion and program realization will allow to solve problems involved with the study of deep structures and will contribute to prediction and location of diamond, rare metals, gold, copper and other metals, as well as to oil-and-gas exploration. It is applicable also in Israel where concentric structures are known (Precambrian caldera in southern Israel, Mesozoic diatremes in the Hermon Ridge etc.).

Sedimentation Rates and Particle Dynamics in the Northern and Central Parts of Lake Kinneret

Klein, M.,¹ Koren, N.,² Nishari, A.²

1. Dept. of Geography, University of Haifa, 31905 Haifa

2. Yigal Alon Kinneret Limnological Laboratory, Israel Oceanographic and Limnological Research Ltd., P.O.B. 345, 14201 Tiberias

The aim of this research was to determine the seasonal, spatial and vertical patterns of sedimentation processes in Lake Kinneret. In addition, the physical, chemical and biological mechanisms, responsible for sedimentation, were investigated.

During the research, suspended solids were sampled from the water by the use of sediment traps and were analysed together with sediments from the lake bottom.

The sediment traps and chemical analyses enabled the measurement of sedimentation rates, chemical composition of settling particles, transport tracks of allochthonous particles and secondary sedimentary movements. These were determined at a number of sample locations in the northern and central parts of the lake. The main findings of the research were as follows:

The gross sedimentation rates measured in sediment traps at station A (the deepest central station), were 1300-1400 gr/m²/year, and the net rates were in the order of 950-1100 gr/m²/year. The computed net accumulation rate on the bottom was 3.45 mm/year.

During the lake stratification period, sedimentation rates were higher in the epilimnion, whereas during the mixing period they were greater in the hypolimnion. The main reasons for this pattern are: 1) the water viscosity gradient prevailing across the metalimnion; 2) the preferential dissolution of calcite in the hypolimnion during the stratified period; and 3) the subsequent disappearance of these physico-chemical patterns during the mixing period.

The seasonal sedimentation pattern at the center of the lake revealed 8-9 relatively low flux months (1/4-4 gr/m²/day) and 3-4 peak sedimentation months (up to 11 gr/m²/day). This pattern shows a high correlation with the sedimentation of calcite. Maximum sedimentation of calcite occurs in the lake due to intensive photosynthesis during the boom period of *Peridinium gatunense*.

Gross sedimentation rates at the intake region of the National Water Carrier (station T) were 4060 gr/m²/year, while at the inlet of the Jordan River they were 13030 gr/m²/year (station J). Net accumulation rates for these stations have not been evaluated.

Infrared Study of the Carbonate Ions in Apatites from the Negev Phosphorites

Knubovets R.,¹ Shoval. S.,¹ Gaft, M.,¹ Nathan, Y.,² Rabinowitz, J.,³ Pregerzon, B.³

1. Geology and Physical groups, The Open University of Israel, Tel-Aviv

2. Geological Survey of Israel, 30 Malkhe Yisrael Street, 95501 Jerusalem

3. Rotem-Amfert-Negev, Yeruham

The carbonate substitution in apatite is the most characteristic and important substitution in francolite. The extent of this substitution has been observed (by X-ray diffraction and thermal analysis) to be between 0.5 and 6% in apatites from the Negev. Infrared spectroscopy is a very sensitive method for the study of the environment of carbonate ions in apatite. The (FTIR) absorbance spectra of 100 phosphorite samples were examined. In all samples, a doublet was observed for the nondegenerate ν_2 mode at about 870 and 880 cm^{-1} and at least *three* bands could be distinguished in the doubly degenerate stretching mode ν_3 at 1430, 1460 and 1540 cm^{-1} . The occurrence of a doublet for ν_2 is well known in francolites (the main mineral in marine phosphorites) and dahlites (biological apatites); its explanation remains controversial to this day. Among others the following have been proposed: CO_3^{2-} in two different environments, CO_3^{2-} with two different cationic bondings, CO_3^{2-} with two different orientations.

We found significant differences in the intensities of the bands at ~ 1430 and 1460 cm^{-1} in the Negev samples. In general the intensity of the band at 1430 cm^{-1} is larger than that at 1460 cm^{-1} . Nevertheless some samples, and in particular some apatites from porcelanite beds, were found to have a higher intensity of the $\sim 1460 \text{ cm}^{-1}$ band. This is considered by some authors to be an indication of diagenetic processes. Furthermore the presence of more than two bands ν_3 also needs an explanation.

Detection of Underground Caves and Voids Using Georadar

Kofman, L., Cnaan, D., Gadot, I., Klar, I.

Cnaan-Engineering Services Ltd., 55 Liberia St., 34980 Haifa

Klar Israel Soil Mechanics Consult. Eng., 28 Holland St., 34987 Haifa

A section of Shezaf street in Haifa is planned for construction on a steep slope full of caves which are partly visible and partly concealed. Experimental drilling and testing by means of ground penetrating radar type SIR-10A (GSSI, USA) were conducted along the survey line. The survey has been performed with two antennas 100 and 300 MHZ.

The imaging of the layers structure along the line of movement of the antennas is displayed in real time on the color screen, printed on the graphic printer and recorded on digital tape for complete post-processing. The results registered by means of the 300 MHZ antenna determined with high accuracy the position of the voids and caves on the survey line. Due to the phenomenon of the electromagnetic waves reverberation in void reflections into the karst voids were distinctly seen on the records of printer (on the screen of color display). The 100MHz antenna of approximately 3m wave length was used for mapping surface contact between a very cracked rock (or filling of voids) to the monolithic rock under it. According to the results by georadar, the depth to the stable rock, in the survey section, varies within 2-13 meters. These depths correspond to the results of the experimental of the drilling probs. The georadar method enables a correct determination of positioning of experimental drilling, minimizes the number of drilling, contributes to the slope stability and correct foundation planning.

Peak-Flow Prediction of Perennial and Ephemeral Streams

Krasilshikov, L., Carmi, G.¹

1. Water Resources Research Center, Jacob Blaustein Institute for Desert Research, Ben-Gurion University of the Negev, 84993 Sede Boker Campus

Perennial and ephemeral streamflows are an important aspect of the hydrologic budget in arid regions, particularly in Israel. Here most streams flowing from mountain have irregular flow character. Analysis has showed that 75-90% of the amount of annual runoff from mountain rivers (nahal) occur during 2-3 months and within each month runoff occurs during a 5-6 day period. A significant part of runoff after heavy rainfalls is not taken into consideration even at gaged watersheds as the watersheds are overtopped. Heavy rainfalls cause floods which inflict a large damage.

In addition to comprising a component of surface water budgets, ephemeral and perennial streamflows can be an integral part of the groundwater budget, since it may serve as a source of natural recharge via streamflow infiltration (Keith, 1980, Truschel and Campana, 1983), or may provide water for artificial recharge (Dowden, 1981). Ephemeral and perennial streamflows are often an important factor in the design and construction of public works projects. Since ephemeral and perennial streamflows often occur as floods or flash floods, prediction of the magnitudes and frequencies of these phenomena is critical to the proper location, design and construction of populated areas including roads, bridges, sewers, etc. that may be subject to flooding.

The need for accurate and comprehensive runoff information has brought about many recent developments in hydrologic modeling. Runoff simulation has many advantages over the conventional design and maintenance of a watershed gaging network: economy, convenience and a reasonable degree of accuracy (Truschel and Campana, 1983).

Petrology and $^{40}\text{Ar}/^{39}\text{Ar}$ Dating of the Qarney Ramon Basalt — Makhtesh Ramon

Lang, B.,¹ Kilinc, A.,² Steinitz, G.¹

1. Geological Survey of Israel, 30 Malkhe Yisrael Street, 95501 Jerusalem

2. Dept. of Geology, University of Cincinnati, USA

Qarney Ramon Hill consists of a 60 m succession of lava flows located in the westernmost part of the Makhtesh Ramon erosion cirque. Seven samples, representing different flows were analysed for major, trace and RE elements and $^{87}\text{Sr}/^{86}\text{Sr}$ isotopes. Three samples taken from the bottom, middle and the top of the section were dated using the Ar-Ar stepwise heating technique.

The geochronological data show that there is not a significant age difference between the base and the top of the lava succession. Similar plateau and isochron ages were calculated, with averages between 118 and 120 ma. It can be assumed therefore, that the samples represent a relatively short volcanic event, eventually shorter than 1 ma, within the limits of the analytical error of the measurements. The ages are in accordance with the paleomagnetic data in the area.

All samples from Qarney Ramon are alkali basalts. The alkaline character becomes stronger towards the top of the succession. Projection of the bulk composition of the rocks into olivine-pyroxene-nepheline (+plagioclase) tetrahedron (Sack, 1987) shows that all rocks plot between 8-30 Kb and 1 atm cotectics, closer to the high pressure cotectic. This completely eliminates the possibility of low pressure fractionation of these magmas. The high pressure of the magmas is seen also in their chondrite normalized plots. The very low and almost identical Yb values for all rocks indicate that they are generated from the same source rock containing garnet.

Data from high pressure melting experiments with peridotites show a linear relationship between the calculated (according to Sack et al., 1987 algorithm) olivine/albite+anorthite ratio and temperature. We have used such a plot to obtain temperature estimates for the Qarney Ramon basalts. The estimated temperatures were used together with the calculated nepheline/(nepheline+olivine+diopside) ratios to estimate the pressures from Fig 13 of Sack et al., 1987. The obtained P-T values range from about 28 to 34 Kb and 1438 to 1532°C.

Major and trace element geochemistry of the Qarney Ramon basalts support the conclusion that they resulted from melting of a garnet lherzolite source rock at about 30 Kb. Following a slight high pressure fractionation, they reached the surface without pooling at shallow depths and without fractionating at low temperatures.

Groundwater Pollution at the Hadera Waste Disposal Site, in the Coastal Sandstone Aquifer (Pleshet Formation)

Levitte, D.

Geological Survey of Israel, 30 Malchei Yisrael Street, 95501 Jerusalem

The Hadera Waste disposal site some 2 km southwest of Hadera, is a source of potential groundwater pollution. It is located in a series of abandoned sandstone quarries excavated into the local water table. Surface pools and waters from twenty-two monitoring and production wells from various depths around the site were analysed. Pollutants concentrations diminish markedly with distance from the site. Chlorine diminished from 2130 mg/l to 163 mg/l some 300 m east of the site. Apparently pollutants such as halogens and heavy metals are removed by means of either ion exchange in the clayey layers interbedded with the Peleshet sandstone or adsorption to iron hydrates and carbonates.

The Platform Structure of Israel and Sinai (Main Elements)

Livshits, Y.

Kimron Oil and Minerals, 21 Yona Hanavi Street, 63302 Tel Aviv

The Israel-Sinai region is situated on the boundary of the northwestern Arabian-African platform with Mediterranean marginal trough. Most of the region belongs to the western, very strongly dislocated part of the North Arabian antecline or rather to the Levant uplift (Livshits, 1992). This uplift is cut by the Jordan-Dead Sea rift system on the west, near the Mediterranean part, and the intercontinental part in the east.

On the coastal plain between the platform and marginal trough many authors postulate a paleodepositional hinge-belt (Bein and Weiler, 1976; Bein and Gvirtzman, 1977; Druckman et al., 1975; Klang and Gvirtzman, 1986, and others). Gvirtzman and Klang (1972) also postulated a longitudinal coastal plain fault zone.

All pre-Senonian platform history of Israel and Sinai is the history of block movements. Only in the Late Cretaceous-Early Cenozoic did intraplatform folding and faulting take place and in the Neogene-Quaternary the present geological structure, caused mainly by the Jordan-Dead Sea transform, was formed.

There are three main platform structure zones (from south to north):

1. The Sinai brachisyncline zone is not very intensely dislocated. In this zone rejuvenated basement faults and faults connected with young movement in the Jordan-Dead Sea valley are very important. The zone's northern boundary is the Sinai-Negev Shear-Zone (Bartov, 1990).
2. The northern Negev zone of discontinuous northeast anticlines (steeper eastern flanks) with Triassic and Jurassic outcrops in axial parts (Makhtesh Ramon, Makhtesh HaGadol, Makhtesh HaQatan and others). This zone extends from Sinai to the southern part of the Dead Sea and probably to northern Jordan and southern Syria.
3. The central and northern Israel zone (main part of Israel) is formed by a series of north-northeast linear asymmetrical (steeper western flanks) anticlines and synclines, inverted in the Late Cretaceous (Mesozoic horst and graben system — Cohen et al., 1990).

The structures are cut by a series of normal, reverse and strike-slip faults. A series of west-east and northwest strike-slip faults caused mainly by the Jordan-Dead Sea transform zone are especially important. The largest of all the fault zones are the Yizre'el and Beer Sheva valleys.

Zero Moveout (ZMO) Stacking

Loewenthal, D.,¹ Kagansky, A.,¹ Buchen, P.²

1. Dept. of Geophysics and Planetary Sciences, Tel Aviv University, 69978 Tel Aviv

2. School of Mathematics, The University of Sydney, NSW 2006, Australia

In standard processing of reflection seismograms, stacking is performed after normal moveout (NMO) correction of each trace within a common midpoint (CMP) gather. The principal effect of the NMO and stack is to enhance primary reflection and suppress multiple reflections. The resulting stacked trace attempts to represent a noise reduced zero-offset trace containing primary energy only. This energy appears as both reflection and diffraction energy. The method is subject to error in picking primary events in the preceding velocity analysis stage.

In this paper we describe a simple stacking procedure based on summing the traces of a common shot gather without relative time shifts. We refer to this procedure as zero-moveout or ZMO stacking. The stacking procedure we shall examine may include offset dependent weighting function which is determined by the dimensionality of the data. It will be shown that for the correct choice of weighting functions the resultant stacks are exact zero-offset one dimensional seismograms for horizontally layered media. All primary and multiple energy are retained in this stack, but all diffraction energy (such as head waves) is collapsed. In other words, for horizontally layered medium, these unshifted stacks (unlike NMO stacks) are equivalent to the full normally incident plane wave response of the medium. As such they can be used for both source estimation and inversion.

The procedure discussed is investigated with synthetic data obtained both analytically, using Cagniard method, and by finite difference numerical schemes. Effects of finite aperture width is also considered.

The Origin of the Dead Sea Rift: Results of Computer Simulations

Lyakhovsky, V., Ben-Avraham, Z., Achmon, M.

Dept. of Geophysics and Planetary Sciences, Tel Aviv University, 69978 Tel Aviv

The Dead Sea rift is considered to be a plate boundary of the transform type. Several key questions regarding its structure and evolution are: Does sea floor spreading activity propagate from the Red Sea into the Dead Sea rift? Did rifting activity start simultaneously along the entire length of the Dead Sea rift, or did it propagate from several centers? Why did initial propagation of the Red Sea into the Gulf of Suez stop and an opening of the Gulf of Elat started?

A mathematical model of the evolution of the Dead Sea rift suggests that the rift was created as a result of the propagation of two fracture zones at its northern and southern ends toward each other. Due to the collision of Arabia with Eurasia and the strike-slip motion along the east Anatolian fault a new fracture zone was created and formed the northern part of the Dead Sea rift. It propagated from the north to the south. Active tectonics in the northern part of the Arabian plate also causes a dramatic change of the stress field around the northern Red Sea. As a result, rifting activity changes its direction of propagation from the Gulf of Suez into the Gulf of Elat and a new plate boundary of the transform type was created.

In particular, the Yammuneh fault, the restraining bend of the Dead Sea transform, probably could not have been formed if the propagation of the Dead Sea rift had occurred only northward from the south. It is possible, then, that restraining bends in general, which are common features along continental transform faults, are formed when two segments of a transform propagate toward each other.

Latest Results of the Experimental Seismic Antenna on Mt. Tur'an, Israel

Malitsky, A., Shapira, A.

The Institute for Petroleum Research and Geophysics, P.O.B. 2286, 58122 Holon

After the first study on experimental monitoring and computer experiments (August 1992 to July 1993), a suitable seismic antenna geometry was selected and one three component and eight vertical seismometers were installed on Mt. Tur'an in August 1993.

In order to process the seismic records from the Tur'an antenna, we applied frequency-wave number analysis, various methods of correlation analysis and polarization analysis (for the three-component seismograms). The results obtained show a stable determination of the seismic wave parameters (azimuth and apparent velocities). Further beamforming significantly improved the signal-to-noise ratio and, consequently, improved detection capability.

Software Package "Seismological Bulletin of Israel"

Malitsky, A., Shapira, A.

The Institute for Petroleum Research and Geophysics, P.O.B. 2286, 58122 Holon

The software package "Seismological Bulletin of Israel (from 1900)" was developed by the Earthquake Seismology Division of the Institute for Petroleum Research and Geophysics to display the earthquake catalog on the screen. The area, time period and magnitude range of events to be plotted can be selected according to the user's request. The software provides the user with several options for arranging the graphic outputs, such as the size, shape and color of the symbols. Also displayed, at the user's request, the main cities of the region, the seismic stations in Israel and the geographical locations of the sub-regions in the investigated area. The user can also plot histograms of the events by year for different magnitude ranges. The program also prepares a separate earthquake list according to user-selected parameters and provides some basic statistics. The bulletin is updated annually and distributed free of charge on an individual basis to earth scientists.

The Flow Field Between the Mediterranean Sea and the Jordan Rift Valley

Matmon, D., Gvirtzman, H.

Institute of Earth Sciences, The Hebrew University of Jerusalem, 91904 Jerusalem

The Dead sea rift valley is the deepest region on earth. The difference between the levels of the Mediterranean Sea and the Rift Valley creates a regional drainage basin for both runoff and groundwater, and it causes a large hydrological gradient that influences the potential and the flow fields in deep layers. In this research we examine the possibility that the salinization phenomena in the rift valley are mainly due to this gradient. The hydraulic head gradient pushes the water in the deep part of the stratigraphic cross section to the east, brines in deep layers are pushed eastward and up toward the surface. In this research we develop a quantitative hydrogeological model that sketch the flow field in the complete cross section between the sea and the rift valley. The research uses geological and hydrological information that was collected over the years and it includes computer numerical models of flow and transport.

SUTRA is the numerical model we use to solve the potential and flow fields in the cross section . The program SUTRA (Saturated-Unsaturated TRANsport) of the U.S.G.S is a computer program simulating flow and transport of energy or solute mass in a one or two dimensional medium.

The first stage is discretization of the cross section, namely dividing the cross section into a mesh of square elements. The input file includes porosity and permeability values for each element, as well as initial conditions (pressure and salinity). Other geohydrological parameters of the solid phase (compressibility and density) and the fluid phase (compressibility, density, viscosity and salinity) are included as well. The model computes fluxes and mass balance of the fluid in each element according to mass conservation law, Darcy law and the given boundary conditions.

In the first stage, simulations were implemented on a simple cross section of a dam, in which the water levels on each side are different. In each simulation, different geometry and different values of the layers' permeability were taken, and the resulting flow net was analyzed. In the next stage, increasing complexity was introduced, in the form of a layered geometry similar to field data. The last stage will simulate the geometry and permeability of a real cross section from the Mediterranean Sea to the rift valley.

Analysis and Estimate of Interrelation between Ecologic and Geodynamic Processes

Mavashev, B.

Jerusalem College of Technology

The objective of the present investigation is to estimate the interrelation between geodynamic and eco-meteorological processes under the prevailing conditions in Israel. On the basis of the investigation results it is suggested to create the automated control system management of eco-geodynamic situation in the region, the development of a model and computer program for ecologic and seismic processes prediction.

The methodology of the research on the given subject, involves developing theoretical foundations of interrelation between ecological and geodynamic processes, as well as the carrying out of a complex of experimental studies of the variations of radon emanations in ground waters and sources, in relationship between meteorological parameters.

The scientific novelty of the development lies in the fact that for the first time seismic and eco-meteorological processes are considered as interrelated. The main application of the proposed method is the short-term prediction of earthquakes.

Horizontal Drilling

May, P. R.

P.O. Box 1853, 91015 Jerusalem

Horizontal drilling has come into use for oil and gas production since the 1980's. In 1992 in the U.S. nearly 10% of all rigs were employed in horizontal drilling and more than 500 horizontal wells were planned for 1993. Greatest activity is in the Senonian Austin Chalk, where over 2500 wells have been completed. Most recover 3-4 times more oil than vertical wells, and average initial production is 4.8 times greater. In Canada more than 700 horizontal wells were completed by 1992 and it is estimated that 10,000 will be drilled in the next 15 years. In Saudi Arabia 29 horizontal wells were producing in 1993 at rates 2 to 6 times that of vertical wells. During the next 10 years 50% of the Saudi drilling budget will be for horizontal wells.

Drilling and completion cost is 1.2 to 2 times that of a vertical well to the same depth. Usually a vertical hole is drilled to below the target and the horizontal hole is deviated from above the objective. Length of horizontal holes ranges from a few hundred meters to more than 5000 m. They are best used in reservoirs with high vertical permeability: fractured shale, chalk and limestone; and beds with discontinuous porosity such as karst limestone. Water or gas can be reduced or eliminated. Due to long contact of the reservoir with the well, beds with low permeability, thin oil columns, or heavy oil can be exploited. Success depends on understanding reservoir anisotropy and fluid flow. Horizontal drilling is not suitable for all reservoirs. Well-bedded sediments with good horizontal permeability or with dense, interconnected fractures, are drained efficiently by vertical wells.

In Israel there are possibilities of production by horizontal drilling where vertical wells failed. Among these are: 1. Senonian in the Rift and the Mediterranean coast. 2. Heavy oil. 3. Oil shows that failed to produce due to water entry. 4. Restoring production that has declined due to water influx.

Groundwater Composition in Lithostratigraphic Units, Israel — Scientific and Management Implications

Mazor, E.

Dept. of Environmental Sciences and Energy Research, Weizmann Institute of Science, 76100 Rehovot

Aquifer definition. The basic definition of an aquifer is "a rock body that contains water in all its voids and can sustain economical wells". This leaves room for active aquifers (with recharge, through-flow and discharge) and passive aquifers (trapped). In each case are all parts of an aquifer hydraulically interconnected, resulting in homogenization of water properties (pressure, temperature, concentration and relative abundance of dissolved ions, isotopic composition and age). Hence, adjacent wells with water of similar properties are likely to tap the same aquifer, whereas wells tapping water with significantly different properties belong to distinct aquifers (overlying, or laterally separated by a geological barrier).

In practice, lithostratigraphic units are often applied to define aquifers, e.g. the Kurnub Group aquifer, the Judea Group aquifer etc. However, these units occur in topographically separated regions so they can not constitute a single aquifer, and they encompass alternations of permeable and impermeable rock beds constituting many aquifers.

The chemical composition of groundwaters in the lithostratigraphic units in Israel reveals: (a) concentration ranges of two to three orders within each unit, (b) significant diversity of the ionic ratios within every unit, (c) complete overlapping between the properties of the different units. These observations are demonstrated on 370 wells that have been analyzed in two systematic surveys (Arad, Kafri, Halicz and Brener, 1984; Halicz, Kafri and Bein, 1991).

Scientific and management implications: (a) there is no ground to define aquifers by lithological or stratigraphical units, (b) we have to get rid of water quality tags assigned to lithological or stratigraphic units (there is no specific composition of water in Nubian Sandstones, Judea Group or Senonian!), (c) flow velocity and water age can be calculated only for specifically defined aquifers and not for lithostratigraphic units, (d) the lithostratigraphic units in all the regions of Israel contain groundwater that has to be protected against pollution.

The Influence of a Year Abundant in Precipitation on the Groundwater Quality: The Case of the Israeli Coastal Aquifer in 1991/92

Melloul, A.,¹ Goldenberg, L.C.²

1. The Hydrological Service, P.O.B. 6381, 91063 Jerusalem

2. A.M.C, 70600 Yavne

The 1991/92 winter was characterized by an amount of precipitation higher by 150 to 200% relative to the representative (1930-1960) multi-year average. This caused an increase of the groundwater levels by up to 2 - 3 m in the Israeli Coastal aquifer which is higher by about 10 times than in a normal year. Thus a relative dilution of the groundwater T.D.S. (total dissolved solids) was expected. Surprisingly, a general trend of increase in Chlorides concentration up to 500% was also observed in the groundwater.

The model suggested to explain the phenomenon is based on the findings of laboratories experiments which simulated conditions characteristic to the unsaturated zone of granular aquifers. The results reveal that the development of the internal network of drainage is enhanced by cycles of drying and moisturing (hydration and dehydration) of the aquifer matrix: In real aquifers:

- (a) during seasons of low precipitations, most recharge water passes through large pathways of the drainage networks which form "hydrological shortcuts", while the other parts of the matrix use as "accumulators" for pollutants.
- (b) during abundant rain seasons, a larger part of the network becomes active, and pollutants are flushed from these "accumulators" and reach groundwater.

The large increase in chlorides in the groundwater of the Israeli coastal aquifer during the precipitation-abundant 1991/92 season is in accord with the model presented above.

Thermal and Formation Pressures Study: Implication for the Further Development of Nearly Depleted Petroleum Areas

Modelevsky, M.

Dept. of Geophysics and Planetary Sciences, Tel Aviv University, 69978 Tel Aviv

Two examples of nearly depleted areas exist both in Israel (the Helez oil field) and in ex-USSR (the reservoirs of the Pricaspian Depression). The Helez field was discovered in 1955 and it has produced since about 2.5 MMT of oil which accounts for about 42% of the original oil-in-place (Gilboa and Fligelman, 1991). Therefore, the field is considered to be nearly depleted. Complex geology of the field, numerous reservoirs, and the water flooding should all be considered in the design of the development of the remaining reserves. Small oil fields of the Pricaspian Basin have similar characteristics. They have been producing since 1930s and the cumulative production has reached 50-60% of recoverable oil.

Formation pressure and temperature (FPT) studies contributed much to the discovery of several new small reservoirs within the depleted fields. They are predominantly confined to stratigraphic traps with a fault seal component or with permeability traps. The FPT investigations allow the study of oil migration paths and conditions of oil accumulation and conservation in potential reservoirs and traps. Similar methods can also be applied to the Helez field. Abnormally high or low pressure may be indicative of stratigraphic traps. Stratigraphic traps made up of sandstone is usually noted for low formation pressure. In deep wells formation pressures remain normal hydrostatic down to the seal and become abnormally high beneath (Dickey and Cox, 1977) which makes it possible to reveal permeability barriers as well as traps.

The FPT method includes the following assignments: the construction of paleogeological sections and maps, the definition of regional bubble-point pressure/formation pressure relationship, of the tectonic movements stress trends, etc.

Geodynamic evolution of Andros island (Greece) Based on Structural Analysis

Mukhin, P., Garfunkel, Z.

Institute of Earth Sciences, The Hebrew University of Jerusalem, 91904 Jerusalem

Metamorphic rocks of Andros island are typical representatives of the NW part of the metamorphic belt of the Cyclades. The stratigraphic succession consists of polymetamorphic sedimentary and volcanic rocks of submarine origin, which were multideformed during the Late Paleogene - Early Neogene. According to previous investigations these rocks usually preserve only secondary metamorphic and deformational structures.

During our field works on Andros island we found numerous outcrops with preserved relicts of primary bedding of rocks. Often preserved is graded bedding which allows to determine the original top and bottom of the layers. Our study of the structure of the island (about 40 km) giving us new information about its features led us to reconstruct four post depositional major geological events in the geodynamic evolution of this area:

1. The blueschist facies metamorphism with normal stress position to bedding plane.
2. The greenschist facies metamorphism (overprint) and shaping of rocks into recumbent isoclinal folds (NE-SW direction of hinges) with WNW direction of synmetamorphic transportation. The initial folding may have formed at stage (1), but was overgrown by the greenschist assemblages.
3. The deformation of twice metamorphosed rocks into big open anticlinal structures with the same orientation of hinges like the 2nd one.
4. The deformation of the area into big asymmetric anticlinal with NW-SE direction of hinge.

The first two events reflected the dipping of primary sediments into subduction zone and successive uplift to the upper part of the crust. The next two events probably reflected exhumation of metamorphic rocks and their progressive deformation in new conditions.

Water Levels of Lake Kinneret: New Archaeological Evidence

Nadel, D., Nir, Y.

M. Stekelis Museum of Prehistory, 124 Hatishbi St., Haifa
Geological Survey of Israel, 30 Malkhe Yisrael Street, 95501 Jerusalem

One of the methods of dating past shorelines is based on the location of archaeological sites. In the Jordan Valley, this method was used to date the retreat of the Lisan.

The Kinneret lake was formed only after the retreat of the Lisan lake to the south. Estimations of the age of the lake range between ca. 25,000 and 15,000 B.P. New archaeological data collected from the shores during the low water levels of 1989-91 enable a better evaluation of the age and past fluctuations of the lake.

In a complete survey of the lakes' shores (1990) at elevations between -211 - 213 m, 42 prehistoric and later archaeological sites were found.

Sites with the oldest remains were found along the northern half of the lake. The rolled and heavily patinated flint implements are dated by their characteristics to the Middle Palaeolithic period: 160,000 - 45,000 B.P. They were probably transported by wadis to their current location.

The oldest in-situ archaeological site on the shore of the lake is Ohalo II, at -212.5 m. 26 charcoal samples from the site were studied by three C-14 labs, and all but one (15,550 B.P.) concentrated around 19,000 B.P.

Floors of huts and hearths were preserved, with food remnants and many tools still intact. The most common animal bones are of fish, indicating the importance of fish in the local diet. They also point to a nearby body of fresh water. The identification of seeds and fruits of more than 30 species of plants and trees shows a range of species very similar to the current range at the region.

The Ohalo II features - huts, hearths and a grave - were dug into the local Lisan bedrock. It is thus clear that by 19,000 B.P. the Lisan lake had retreated to the south. It is also reasonable to assume, based on the quantities of fish and fresh-water flora, that the Kinneret was already there.

In-situ remains from the Neolithic period (ca. 6,000 B.P.) and the Early Bronze Age (ca. 5,000 B.P.) were discovered at elevations of -213 m. It is concluded that the water-levels during these periods was not higher than -213 m.

The distribution of sites shows that some shores are devoid of finds, while the largest concentration (including Ohalo II) was observed near the former outlet of the Jordan river.

The Geochemistry of Cadmium in the Negev Phosphorites

Nathan, Y.,¹ Soudry, D.,¹ Dorfman, E.,¹ Levy, Y.,² Shitrit, D.²

1. Geological Survey of Israel, 30 Malkhe Yisrael Street, 95501 Jerusalem

2. Rotem-Amfert-Negev, Yeruham

The concentration of cadmium, in the Negev phosphorites, appears to be a function of the lithotypes and the stratigraphy. The highest concentrations are found in laminated rocks. Furthermore, as a rule, the interbeds have a higher Cd content than the economic phosphorite beds. This is the cause of the lack of a positive correlation between P_2O_5 and Cd, at times even a negative correlation has been observed. Lower Cd concentrations are found in the uppermost part of the phosphorite unit; while the above mentioned trends are general, there are differences in Cd concentrations in the various phosphate fields and each field has a different signature. In the fields studied, the Zin fields have the highest Cd concentrations followed by the Oron field. The Zefa'-Zohar and Hazeva fields have the lowest Cd content.

The Cd-rich horizons appear to have been originally extremely rich in organic matter (reaching up to 20% Org. Mat.). It is interesting to notice that later oxidation of the organic matter in these rocks does not, in general, alter their laminar organisation. However it causes a redistribution of the cadmium in the rock but does not change its overall content.

The distribution of Cd between the different components of the phosphorites was studied by selective dissolutions, statistical treatment of analyses and electron-probe direct analysis of single mineral grains. Three types of phosphorites can be distinguished: Organic-rich, "Normal" and Altered. In the organic-rich phosphorites, Cd appears to be concentrated in the sulphide phase (sphalerite). In some "normal" and altered phosphorites Cd seems to be concentrated in tiny grains of iron oxides, these are in general oxidised pyrite grains. It should be emphasized that the chemistry of trace elements in the iron oxides is varied. In both the organic-rich and "normal" phosphorites no zinc was found in apatite grains. Therefore, in view of the very good correlation between Cd and Zn, it is inferred that Cd is also absent in the apatite crystals (the Cd concentration is too low to be directly observed with an electron-probe). Statistical analyses and selective dissolution tests confirm the above assumptions. In the altered phosphorites, Zn is found in some apatites and it is probable that in these cases some Cd is also part of the apatite structure.

Finally, it should be emphasized that although there is a certain correlation in unweathered phosphorites, between organic matter and Cd, the Cd concentration drops dramatically in the Ghareb Formation even though the base of the Ghareb is very often extremely rich in organic matter.

Geological Map of the Quaternary of Gush Dan (Central Coastal Plain, Israel)

Netser, M., Gvirtzman, G.

Dept. of Geography, Bar-Ilan University, 52100 Ramat-Gan

A geological map, based on the lithostratigraphic nomenclature of the Kurkar Group, is presented. Only one quarter of the Quaternary sequence is exposed in the coastal plain of Israel. The outcrops are scattered along the coastal cliff and in small patches in the region. The stratigraphic identification of the outcrops is based on correlation with boreholes. The Hadera Sand has covered a large area since 1500 years BP. Settlements ranging in age from the Middle Bronze to the Byzantine period were found below the Hadera Sand. The Ta'arukha Sand, an older generation of dunes, is found north of the Yarqon River underlying the Hadera Sand. The Tel Aviv Kurkar and the Netanya Hamra, known from the Sharon, were identified in Gush Dan. The Giv'at Olga Kurkar, considered one unit in boreholes, is divided in the outcrops into three different units, the Ramat Gan Kurkar, Nahsholim Hamra and Dor Kurkar, a nomenclature used previously for the coastal cliff only. Several lithostratigraphic units, which have been known previously from boreholes only, namely, the Caesarea Hamra, Ashdod Kurkar, Poleg Hamra, Herzliyya Kurkar and the Kefar Vitkin Hamra, were recognized in outcrops. The Caesarea, Ashdod and Poleg units were included previously in the Rehovot Formation. A new unit, composed of dark clay and named En Haqore Clay, 1 m thick, was discovered in an area of 4-5 sq. km below the Hadera Sand during road construction in Holon and Rishon LeZiyyon. The map is illustrated in two versions: one shows the natural landscape of Gush Dan as of 100 years ago, before the modern urbanization; the other shows the region as of 1500 years ago, before it was covered by the Hadera Sand.

Three kurkar ridges are found in Gush Dan. In the Ramat Aviv area the central ridge splits into two parallel subridges. The western and the central ridges are composed of the Ramat Gan Kurkar overlain by the Nahsholim Hamra and the Dor Kurkar. The eastern ridge is composed of the Herzliyya Kurkar. The Ashdod Kurkar constitutes a ridge in Rishon LeZiyyon and southwards. North of Rishon LeZiyyon the ridge is obscured by hills of hamra. There is no connection between the geographical position of the ridges and their chronological order. The map was used by the authors for a further study of the relationships between man and the environment during 6000 years of human habitation in Gush Dan.

Lake Lisan and Dead Sea levels from Seismic Reflection Profiles in the North Dead Sea Basin

Niemi, T. M., Ben-Avraham, Z.

Dept. of Geophysics and Planetary Sciences, Tel Aviv University, 69978 Tel Aviv

Over 1900 km of 3.5 kHz and Sparker seismic reflection data provide a record for the interpretation of climatic changes and neotectonic activity in the north Dead Sea basin. We identify four prominent subsurface seismic reflectors on the 3.5 kHz seismic profiles. Based on short sediment cores, the seismic reflectors probably represent the contact between rock salt and marl layers. Using an actualistic model provided by a recent change in the Dead Sea sedimentation from marl to halite, we interpret strong seismic reflections as halite deposited during warm climatic phases when unstratified conditions in the Dead Sea prevailed because the upper-most water mass was subject to excessive evaporation.

The seismically-transparent layers on the 3.5 kHz profiles represent marls precipitated from a stratified Dead Sea water during wet climatic phases when the runoff-to-evaporation ratio was high and brines were more diluted. We correlate the seismic reflectors with four lowstands since 5 ka that were previously identified in the south basin of the Dead Sea based on the deposition of rock salt and elevation of drainage outlets on the Mt. Sedom diapir. The magnitude of Holocene Dead Sea lowering could not be resolved in the south basin because of the presence of a sill that disconnects the basin from the main water body of the Dead Sea when the level drops below -400 m. Our seismic reflection data of the north basin of the Dead Sea reveal several relict canyons and buried channels of the Jordan River that show the Dead Sea level fell below -400 m in the Holocene. The deeper seismic stratigraphy seen on Sparker profiles indicate that the Holocene Dead Sea levels are part of large-scale, late Quaternary lake level fluctuations.

Sequence stratigraphic boundaries in the submerged Jordan River delta define cycles of major high- and lowstands that began approximately 25-30 ka during the late stages of the Dead Sea precursor, Lake Lisan.

Geological Sites in Danger of Destruction

Orion, N.

Dept. of Science Teaching, Weizmann Institute, 76100 Rehovot

An international conference on geological and landscape conservation took place in July 1993, in Malvern, England. Following this conference an international association for geological conservation was established.

England itself is characterized by intensive efforts to conserve valuable geological sites. These activities are supported by the government organization, English Nature, and are conducted by regional groups of professional and amateur geologists who voluntarily document important geological sites.

In Israel, unfortunately, there is minimal awareness of the need for conservation of important geological sites. In the last few decades many unique geological sites have been destroyed or damaged without any appropriate response from the public or the scientific community. The extensive construction projects of buildings and roads which have been ongoing the last few years have put many other important geological sites in danger.

Action for the protection of valuable and unique geological sites in Israel should be led by the geological community. In order to protect our geological heritage, the following is suggested:

1. A survey be made of important geological sites in Israel that should be protected. This survey could be executed voluntarily by the members of the Geological Society who live and work in different parts of the country. Geological sites that should be protected will be determined according to three criteria: scientific importance, educational importance and landscape importance. Reports on suitable sites will be made in special forms prepared for this purpose. A special form has already been prepared for the reporting of such sites.
2. A committee of the Geological Society should sort out the accumulated reports and the sites selected as suitable be published. The published list should then be distributed to the bodies involved in the protection of nature and to the relevant government offices.
3. People should lobby for execution of actions needed for protection of the selected sites.

Sedimentation of Iron in Lake Kinneret

Parparova, R.

Yigal Alon Kinneret Limnological Laboratory, Israel Oceanographic and Limnological Research Ltd., P.O.B. 345, 14201 Tiberias

The iron (Fe) cycle in freshwaters is an object of increasing interest as a result of understanding of its significance in bioproductive and physicochemical processes (coprecipitation, redox conditions and so on). Sedimentation is predominant component of the iron cycle in waterbodies. The objectives of present study are as follows:

- a) to estimate the settling flux of Fe and to examine the factors determining this in Lake Kinneret;
- b) to investigate the possibility of using Fe as a potential tracer of resuspension processes in the lake;

The results of this study are based on determinations of Fe concentrations in suspended matter from the Jordan River and in the water column of Lake Kinneret (seston) and, in addition, material collected in vertically and horizontally oriented sediment traps (tripton) and from the surface layers of bottom sediments from the deepest (ca 40 m) part of the lake. Exposure time of sediment traps varied from 2 weeks (in 1991-1992) to 1 day (in 1993).

The following conclusions were deduced from analysis of the results:

1. Settling fluxes of Fe, evaluated from vertical traps only (more than 1000 t/y) significantly exceeded storage of this element (ca 250 t) in the lake (as estimated from different time exposures). To explain this we suggest that significant resuspension occurs even in the deepest parts of the lake.
2. In the vertical traps we suggest, that settling the flux of Fe was overestimated by a factor of two because of entrapping of horizontally transported suspended matter.
3. When the sedimentation values of Fe were corrected for the horizontally advected Fe, and the lake's morphometry, they appeared to be close to the value of the iron retention in the lake (Input - Output = 200 ton/year). This, together with relatively content of Fe in particulate organic matter (C:Fe=4400), indicates that the downward flux of Fe is mainly associated with the mineral fraction of suspended matter.
4. The resuspension value obtained from differences of Fe content in seston, tripton, and bottom sediments, was considerably lower, than the values, defined from organic matter content of sedimentary content alone.

Red Valley and Other Concentric Morphostructures in the Eastern Makhtesh Ramon

Patyk-Kara, N.,¹ Plakht, J.²

1. Russian Academy of Sciences, Moscow, Russia

2. Ramon Science Center, Mitzpe Ramon, P.O.B. 194

The Red Valley Structure (RVS) is manifested in the Makhtesh Ramon relief as a small oval depression surrounded by ring scarps. The western and central parts of the RVS are covered by Late Pleistocene river terraces overlying Pliocene (?) lake deposits, whereas the uplifted eastern part is built by the Jurassic Inmar Formation. In the northern part of the RVS, rocks by the Lower Cretaceous Hatira Formation, including the Red Member, are exposed.

The inner part of the RVS has a clear division, which is typical to all domal or caldera-like morphostructures. The most subsided part occupies the center of this structure; the more moderately subsided parts are located along the western and southern boundaries of the central structure. This indicates that the subsidence of an area above a shallow-intrusive body, as revealed by TDEM (Baer, et al., 1989), is accompanied by differentiated block movements. The eastern part of the morphostructure is manifested in the relief as the most uplifted block.

Besides the RVS, a number of different-scale concentric morphostructures are also discerned in this area. They are embodied in radial and concentric structures that stand out in the drainage network, in ancient terrace fragments, and in ring-like scarps. One of the largest concentric morphostructures covers about 2.6 km² and includes the RVS within it.

Concentric morphostructures are the reflection of deep-seated structures — mainly major magmatic bodies; their size is related to the depth and time of endogenic activity. Since the depth of the basaltic body as estimated by TDEM is 100 m, the largest concentric morphostructure must have deeper endogenic roots. The entire area in eastern Makhtesh Ramon, which has an exceptional abundance and density of ring morphostructures, can be interpreted as a center of endogenic activity.

Effective Noise Suppression for the Detection and Discrimination of Seismic Array Signals

Pinsky, V.

The Institute for Petroleum Research and Geophysics, P.O.B. 2286, 58122 Holon

From seismological practice it is known that the noise wavelets recorded by short period, closely spaced (up to 1-2 km apart) sensors are highly correlated at frequencies around 1 Hz. Furthermore, the main noise source is concentrated in this frequency band. Based on these facts, it is possible to enhance greatly the seismic array signal-to-noise ratio using the linear transform of the multidimensional observational space.

At the NORSAR Institute in Norway, a prominent leader in seismic array data processing, compensation for noise due to spatial correlation is performed for different frequency bands by beamforming the various subarrays of NORESS, ARCESS, etc., data.

A more general approach is the application of the Capon-like multichannel Wiener filter. This filter produces minimum noise at the output without distorting the signal waveform for known a spectral matrix of noise and slowness vector of the signal. The spectral matrix is deduced from the array noise records preceding the signal onset using a multidimensional autoregressive model. This facilitates adaptation of the filter to the time varying noise field.

The filter appears to be effective in picking up seismic phases missed by the conventional procedures used by NORESS, ARCESS, FINISS and in discriminating the Eurasian earthquakes and nuclear explosions recorded by NORESS. An analysis applied to the P and P-coda spectral parameters of nuclear explosions and earthquakes from east Kazakhstan showed no misclassifications for filtered data.

Pedimentation as the Leading Geomorphic Process in the Evolution of Makhtesh Ramon

Plakht, J.

Ramon Science Center, Mitzpe Ramon, P.O.B. 194

Pediments occupy more than 40% of the western part of Makhtesh Ramon, approximately three times the area of the fluvial relief. They form a "geomorphological staircase" along the perimeter of the makhtesh with relative heights of 5–6 m, 8–10 m, 13–15 m and approx. 20 m (two higher pediment surfaces) above the river bed. All pediments grade towards river terraces at their base and both should be regarded as synchronous elements. Thus, the number and relative height of the pediment levels in the makhtesh is in keeping with the number of river terraces and both reflect the changes in the erosion base-level.

The process of pediment surface formation requires a sufficient period of stabilization. Each pediment as well as river terrace connected with it indicates the certain period of stability. The sequences of pediments testify to several stable periods, alternating with periods of base-level changes.

The rate of pedimentation (the process of pedimentary erosion) is very high. It depends on the thickness, the lithology and the degree of weathering of the eroded rock. Approximate calculations show average rate as 3.1–5.7 cm/yr during the formation of the medium and lower pediments, and 0.25–1.0 cm/yr during the higher pediment formation.

The role of pedimentation in the development of Makhtesh Ramon is probably higher than the role of stream erosion. In the earlier stage, during the Pliocene, pedimentation (together with the river erosion) caused both the widening and the deepening of Makhtesh Ramon. The Recent relief, as seen today, was mainly formed already in this stage. Since the Pleistocene this process led mainly to deepening of the bottom.

Features of the Late Pleistocene Development of Western Makhtesh Ramon

Plakht, J., Zaslavsky, N.

Ramon Science Center, Mitzpe Ramon, P.O.B. 194

Some differences between the development of the western and central parts of Makhtesh Ramon are observed:

- (a) In the western part, there are only lower terraces (3–4, 5–6 and 8–10 m) and pediments, whereas in the central part, the whole spectrum of terraces and pediments is present;
- (b) thick layers of deposited loess are a significant component of alluvium in the western Ramon;
- (c) river terraces in the western Ramon are completely accumulative, whereas the thickness of alluvium in the central ramon does not exceed 3–5 m.

A strip of sharp change in the Nahal Ramon longitudinal profile, caused by the presence of partly cut-off basanite stock (Becker, Samoilov, pers. comm.), separates the western and central parts of Makhtesh Ramon. In the lower part of the 8–10 m terrace shallow-water lake remains of gastropods *Valvata (Cincinna) saulcyi* with very delicate shells, *Botryococcus* algae and fish teeth of *Chiclidae* were found. The latter were also found in the Pliocene lake sediment in the Nahal Zihor basin.

The 5–6 m terrace alluvium in western Makhtesh Ramon includes calcium carbonate nodules and well-developed buried soils.

The data allow concluding that the very intensive Late Pleistocene sedimentation in western Makhtesh Ramon took place in an almost isolated basin with the local base of erosion near Har Arod.

The presence of redeposited loess in the terrace sections, calcium carbonate nodules and shallow-water lake organic matter indicates relative humid semi-arid climatic conditions. The annual precipitation exceeded 200–250 mm during the formation of the 5–6 m terrace and of at least the lower part of the 8–10 m terrace.

Stress Measurement on Eocene Chalk Rock Mass by the Hydrofracture Test

Polishook, B.,¹ Flexer, A.²

1. Petroleum Services Ltd.

2. Dept. of Geophysics and Planetary Sciences, Tel Aviv University, 69978 Tel Aviv

The measurement of the stress condition in the rock mass is extremely important for purpose of determining the stability of the tunnel in the rock mass.

The stress field at every point in the rock mass can be represented by one vertical and two horizontal stresses perpendicular to each other (minimal and maximal). While the vertical stress can be easily calculated and is the product of the depth and the specific weight, the horizontal stress has to be measured on site.

The hydrofracture test is a method developed for the purpose of determining the in situ stress condition. The test is based on pressing the unfractured rock mass by means of water in a specific interval of the borehole. The water pressure causes the formation of fracture in the rock mass. The plane of the fracture opening is perpendicular to the minimal horizontal stress.

Petroleum Services Ltd., has performed a hydrofracture test in a chalk rock mass in two areas:

1. In the rock mass of the Zora Formation (Hashephela synclinalorium) in the Eshtaol area.
2. In the rock mass of the Adulam and Maresha Member (Hovav syncline) at Ramat Hovav area.

These tests were carried out in depths of between 50 to 75 meters, in a dry rock mass and the first time such tests under these conditions are reported in the literature.

The test results show that the average magnitude of the minimal horizontal stress in the Hashephela synclinalorium is 24 kg/cm² and it is higher than the stress found in Hovav syncline which has an average magnitude of 12 kg/cm². Presently in both areas the principal horizontal stress is in the northwest-southeast direction.

IRSL Dating of Fault-Related Sediments at the Nahal Shehoret Alluvial Fan, Southern Arava, Israel

Porat, N.,¹ Amit, R.,² Wintle, A.G.³

1. Geological Survey of Israel, 30 Malkhe Yisrael Street, 95501 Jerusalem

2. Dept. of Physical Geography, Hebrew University, 91904 Jerusalem

3. Institute of Earth Studies, University of Wales, Aberystwyth, UK SY23 3DB

Ages determined by Luminescence methods define the last event of full exposure to sunlight, which zeros the luminescence signal and resets the clock. For Thermoluminescence (TL) several hours of exposure are necessary for full resetting. This dating method is readily applied to wind-blown sediments, since transportation time is long and the grains are sufficiently exposed to light. For Optically Stimulated Luminescence (OSL) an exposure of a few minutes is sufficient for zeroing the signal. Therefore the method is particularly useful for colluvial sediments, which are transported over short distances and may not be exposed long enough to sunlight to zero the TL signal.

One such dating method was applied to a section exposed during a study on the Recent tectonics and landscape development in the arid Southern Arava. Trenches dug in the alluvial fan of Nahal Shehoret exposed fault-related sediments. The trench walls were logged and sedimentary units were defined using pedologic and sedimentological criteria. The units define a sequence of faulting events, represented by a series of colluvial wedges which accumulated on the down-faulted block. Each wedge can be attributed to a tectonic event, while periods of quiescence between events are represented by soil formation at the top of the wedge.

The stratigraphic data show that the total displacement on the fault is 7-8 m, when most of the displacement was caused by 4-5 events, each causing ~1.5 m throw. Age estimates, based on pedogenic and geomorphic criteria, assigned an Upper Pleistocene age to the older terrace; the time gap between each faulting event to several thousand years; and a Holocene age to the young terrace, which post-dates most of the displacement.

Samples from the fault related sediments were collected. Fine-sand size K-Feldspar grains were separated and used for age determinations. Infrared wavelengths were used for stimulation. The resulting Infrared Stimulated Luminescence (IRSL) was used to determine the Equivalent Dose by the Single Aliquot Additive Dose method. The environmental dose rate was measured separately for the α , β and γ components.

The IRSL ages define the following events: The older terrace was deposited ~60 ka. The first faulting event occurred at ~38 ka and the third event at ~20 ka. The large displacements ended between 19 and 15 ka, when the younger terrace was deposited. The recurrence time for the large faulting events is ~5000 years. The results show that the IRSL method is highly suitable for dating colluvial sediments from an arid environment.

IRSL Dating of Kurkar and Hamra from the Givat Olga Member in the Sharon Coastal Cliff, Israel

Porat, N.,¹ Wintle, A.G.²

1. Geological Survey of Israel, 30 Malkhe Yisrael Street, 95501 Jerusalem

2. Institute of Earth Studies, University of Wales, Aberystwyth, UK SY23 3DB

The Givat Olga Member forms the most western ridge of the coastal plain sequence of Kurkar ridges. It comprises alternating beds of Kurkar and Hamra and is exposed along the coast between Netanya and Ga'ash, forming the coastal cliff. The Netanya Hamra bed was assigned an Epipaleolithic age (20-10 ka) on the basis of prehistoric finds and the Tel Aviv bed was dated by ¹⁴C on whole-rock carbonates to 10 ka. The age of the lower beds was estimated as Upper Pleistocene by employing the concept of Pleistocene sedimentary cycles which correlate with global climatic and sea-level changes.

Ages determined by methods based on Optically Stimulated Luminescence (OSL) give the last event of full exposure to sunlight and the method is particularly useful for dating eolian sediments. For Kurkar the age will be the timing of stabilization of the dunes while for Hamra the age will give the end of pedogenic-biological processes, i.e. age of burial. Absolute age determinations were applied to the entire Givat Olga member as part of assessing the potential of OSL dating of Late Quaternary sediments in Israel.

Fine-sand size K-Feldspars grains were separated and used for age determinations. Infrared wavelengths were used for stimulation. The resulting Infrared Stimulated Luminescence (IRSL) was used to determine the Equivalent Dose by the Single Aliquot Additive Dose method. The environmental dose was measured separately for the α , β and γ components.

The Givat Olga Member includes 2 events of dune mobilization and stabilization, dated to ~60 and ~50 ka. The Netanya Hamra was an active soil until 4-5 ka, when it was covered by the Tel Aviv unit. Events of dune stabilization occurred within isotopic Stage 3, but cannot yet be correlated with particular climatic changes.

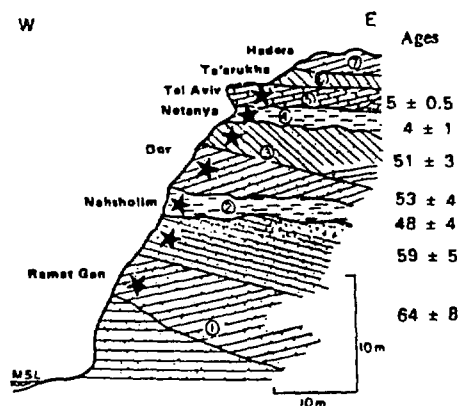


Fig. 1. Type section of the lithostratigraphic units exposed along the coastal cliff in the Sharon area (From Gvirtzman et al., Current Research 1984). * - location of samples. Ages in ka.

Is it Possible to Reach a Consensus in Seismic Hazard Evaluation in Israel?

Rabinowitz, N.

The Institute for Petroleum Research and Geophysics, P.O.B. 2286, 58122 Holon

A common approach in the practice of seismic hazard assessment is to ask, in the first stage, several experts to evaluate independently the hazard assessment and, in the second stage, to form a uniform evaluation which weights each independent evaluation optimally in an attempt to reach a consensus.

In areas where the seismicity level is relatively low, as in Israel, there is a high uncertainty level regarding the value of the seismotectonic parameters affecting hazard assessment. Thus, it is to be expected that this uncertainty will be reflected in the diversity of expert opinions.

In this work we investigate several avenues of research as well as partial results of work planned to enable experts in Israel to reach a consensus with regard to creating a seismic hazard map of Israel.

Tracing of Water Movement in Unsaturated Sandy Dunes Using Stable Isotopes of Hydrogen and Oxygen

Raz, I., Adar, E., Issar, A.

Water Resources Research Center, Jacob Blaustein Institute for Desert Research, Ben-Gurion University of the Negev,, 84993 Sede Boker Campus

The purpose of this study was to trace and estimate the rate of water evaporation and water movement in a sandy, semi-arid, unsaturated zone (Retamim Sand Dunes) using stable isotopes of hydrogen and oxygen. In order to understand the water movement mechanism in the sand, the isotopic composition in rainfall and soil moisture was measured. This was related to soil moisture content and profiles of soluble salts in the soil matrix in both forested and bare sand dunes.

A quantitative model was used in order to estimate the evaporation rate from the soil. The results showed that effective evaporation in the bare sand dune area during the 1990-91 rainy season was 58.2 mm, about 70 to 90% of the potential evaporation. In addition to the evaporation rate, deep percolation beyond 2.2 m was about 2 mm only.

Due to gravity, right after a rainstorm, water percolates as a piston flow. This water mixes with the residual soil water while blurring the isotopic profile found in the rain water. At the end of the main advective stage, the water moves mainly in a very slow diffusive flux from the wetting front downward and upward from the wet soil due to evaporation.

Analysis of the grain size distribution indicates the existence of many silty layers which form unisotropic and non homogeneous stratigraphy. Taking in consideration that the silty and loess layers can produce preferential flow surfaces, those preferential courses have a much higher rate of penetration than the vertical course. The morphologic structure of the dune creates a situation in which two or more of the silty layers cross each other and produce an impenetrable conic casing (funnel). The infiltrated water brakes out toward the shallow aquifer.

The minimal flux calculated by the quantitative model is compatible with the assumption that in arid and semi-arid areas intensive evaporation eliminates the possibility of recharge to groundwater. The source of the main recharge arrives from floods in the surrounding wadis. Nevertheless, the fact that the isotopic composition of $\delta^{18}\text{O}$ in the dunes groundwater is similar to the isotopic composition of $\delta^{18}\text{O}$ in the soil water beneath the evaporation front (-4 to -5 ‰), and different from the isotopic composition of $\delta^{18}\text{O}$ in the water from near-by floods (-7 to -9 ‰) suggests a recharge from the dune itself. Based on the above mentioned hydrological and morphological model, and on the isotopic composition distribution in the soil water, recharge to groundwater in the dune may take place at the silty cone from accumulated soil water. The calculated vertical flux of 2 mm per year does not represent the entire system, but represents the vertical course through the silty layer.

Structure of Lake Kinneret Region from Gravity Analyses

Reznikov, M., Ben-Avraham, Z.

Dept. of Geophysics and Planetary Sciences, Tel Aviv University, 69978 Tel Aviv

Analyses of new gravity data from Lake Kinneret resulted in a free-air anomaly map, a variable density Bouguer anomaly map, a horizontal first derivative map of the Bouguer anomaly and a second vertical derivative map of the Bouguer anomaly.

These maps, together with gravity models of profiles across the lake and the areas north and south of it, were used to infer the geometry of the basin in this region and the main faults of the transform system. Lake Kinneret can be divided into two units. The southern half forms the northern edge of the Kinarot Valley, which is located south of the Lake, while the northern half was formed by two sets of faults, the north-south trending Dead Sea rift and the east-west to northwest-southeast trending eastern Galilee branching faults. As a result, three sub-basins were formed within the area covered by the lake.

2-D gravity models across the lake show the geometry of the three sub basins. Two of the basins were formed as pull-apart which are bordered on their longitudinal sides by segments of the Dead Sea transform. The third basin was formed by branching faults. The southern sub-basin is the deepest with about 5 km of sediments. The northeastern sub-basin is bathymetrically the deepest. It is probably the most actively subsiding area in Lake Kinneret.

Initial Results of a Seismic Reflection Survey in the Yizreel Valley

Rotstein, Y.,¹ Shaliv, G..²

- 1. The Institute for Petroleum Research and Geophysics, P.O.B. 2286, 58122 Holon**
- 2. Israel Defence Forces**

Previous seismic reflection surveys in the Yizreel Valley were aimed at obtaining deep information and met with only limited success. Seismic lines over much of the Valley gave no indication of the subsurface structure and, in some locations, only information on the shallow subsurface was derived. In view of the inability to collect usable deep information from the Valley, we carried out a reconnaissance survey using field parameters designed for shallow, high resolution study. The lines were located throughout the Valley, perpendicular, where possible, to known faults and trends. The initial results show that the Yizreel Valley is considerably more faulted than previously thought and parts of it are intensely sheared. Among the new faults mapped are one along the northern boundary of the valley in its western part and one further south which passes near the Shani and Saifan springs, south of Nahalal. The faults observed in the Valley can be divided into strike slip faults and faults which are associated with tilted blocks and, thus, are likely to have a normal component.

The Complex Deformation North of the Carmel-Fari'a Line and its Structural Significance

Salamon, A.,¹ Ron, H.,² Garfunkel, Z.,¹ Hofstetter, A.²

1. Institute of Earth Sciences, The Hebrew University of Jerusalem, 91904 Jerusalem

2. The Institute for Petroleum Research and Geophysics, P.O.B. 2286, 58122 Holon

Three distinctions which emerged in the present research emphasize the complexity of the processes accompanying the northern Dead Sea Transform (DST): (a) seismic moment release in the western side of the DST is larger than on the Arabian side. (b) the mechanisms of some earthquakes reflect a complex relationship with the motion of the transform. (c) the stress fields around and north of the Carmel and Fari'a line have been heterogeneous in time and space since the Middle Miocene.

Furthermore, structural features indicate that the deformation along the plate margins near the DST decreases the relative offset northward. Also, the Syrian segment of the DST lacks the transpressional component that might have been expected from the southern DST pole of rotation.

The inevitable conclusions of the present research and the work of Freund et al. (1970) is that the nature of the DST north of the Carmel-Fari'a fracture line is changing, and that deformation in the Sinai subplate margins is more intensive. These phenomena show that the Sinai subplate is losing its coherency and that it deforms in the region north of the Carmel-Fari'a fault line. As a result, this line forms an intraplate border between the stable and the disintegrating parts of the subplate.

Har Arod — an Early Cretaceous Basanitic Volcano with a Fossil Lava Lake

Samoylov, V.,¹ Bekker, A.,² Eyal, M.¹

1. Department of Geology and Mineralogy, Ben-Gurion University of the Negev,
84105 Beer Sheva

2. Ramon Science Center, Mitzpe Ramon, P.O.B. 194

The Har Arod volcano (diameter 900 m, height 180 m) is situated in the western part of Makhtesh Ramon and represents an eroded eruption center. The remains of three basanitic lava flows are preserved around the southern and western slopes of Har Arod. Their thickness is 3–10 m, and they dip outward from the volcanic center 10–30°. The lava flows are interbedded with tuffs and paleosols, 1.5–8 m thick.

A fossil lava lake with diameters of 220 m x 330 m and a thickness >80 m, is situated at the top of the volcanic structure. The basanites of the lava lake have vertical contacts with the surrounding lava flows and tuffs. Three zones are observed in the lava lake: 1) *The lower columnar prism zone* is >40 m thick, with columns 0.5–1.5 m in diameter. At the lower part, the columns turn toward horizontality, reflecting the concave shape of the lava lake bottom. 2) *The intermediate zone* is 5–10 m thick, and is characterized by chaotically oriented columnar prisms. 3) *The upper columnar prism zone* is >30 m thick, with vertical columns 5–20 cm in diameter, reflecting the upper horizontal cooling surface.

Basanitic dikes and stocks (diameter 60–150 m) form a half-arc at the northern slope of Har Arod. Their uppermost level of intrusions is not the lower part of the Hatira Fm. Subhorizontal columnar prisms, perpendicular to dike walls and radial in stocks, are common. At the eastern slope of Har Arod, a diatreme (diameter 100 m) penetrates the upper part of the Mahmal Fm. It is composed of tuffs, basanitic bombs and fragments of shales, apparently of the Ardon Fm. The diatreme represents a gaseous explosion that happened in a parasitic volcanic crater, probably at the level of the Ardon Fm.

The Har Arod basanites are rich (>50%) in olivine and pyroxene, contain plagioclase as low as 30%, and nepheline, more than 10%. The lower parts of the flows are enriched in olivine phenocrysts, whereas the upper parts have higher content of plagioclase. The intrusive basanites are enriched in large pyroxene crystals.

KNO₃ Stalactites in a Cave at Har Nitai

Sandler, A.,¹ Dolev, M.²

1. Geological Survey of Israel, 30 Malkhe Yisrael Street, 95501 Jerusalem

2. North District, Nature Reserves Authority, Beit Hasochnut, Zefat

Active stalactites made of KNO₃ (potassium nitrate) were found recently in a cave at the center of the south cliff of Har Nitai, near Arbel. The biggest are about 1cm in diameter and about 70cm in length. This is apparently the only phenomenon of its kind in Israel and it is unique on a worldwide scale. The cave, approximately 10x10x15m in size, is one of many holes of differing sizes, opened in the Bar Kokhba limestone (Eocene) cliff. The salt precipitation is concentrated in the inner part of the cave when stalactites even meet the underlying stalagmites. It seems that activity is related to wide fissures above, but not to the karstic action that formed the cave. No calcite or other deposits could be observed in addition to the KNO₃. It is believed that the salt precipitation is recent and followed the extremely rainy winter of 1991/1992.

The mineralogical composition (determined by XRD) and the chemical composition of the stalactites, the stalagmites and the wall crusts is of the mineral niter (KNO₃). It is accompanied by traces of KCl and Na (as NaNO₃?). Precipitation of the salt from seeping groundwater indicates high concentrations of K and NO₃ in this water. Outstanding concentrations of nitrate have been found occasionally in groundwaters in Israel, even in Soreq Cave waters, but similar high concentrations of potassium are not known since potassium tends to be fixed in soils, both by plants and soil clays.

Chemical analyses results of nearby springs and of water extractions of a series of soils, rocks and other cave sediments exclude the possibility of rock or soil as the source of K and NO₃. A possible source for the salt is the irrigation water of a mango orchard, which is fertilized by K and NO₃ through drip irrigation. However the orchard (about 1.5km away) is planted on a dip slope in another direction. It seems, therefore, that an hydraulic connection cannot exist between the draining water and the cave. The most reasonable source for the salt is manure of animals, both domestic herds and wild animals, prevalent as bottom sediments in the cliff openings above the cave. The water extractions of two such sediments had a relatively high content of potassium and nitrate with an extremely high K:NO₃ ratio.

It seems that this cave salt formation is a rare and marginal phenomenon because of the circumstantial combination of chemical and physiographic conditions. Yet it illuminates a hidden segment of the complex hydrogeochemical cycles of potassium and nitrogen in vadose regimes.

Chemical Seasonal Variations in the Water Column of Lake Kinneret

Sandler, A.,¹ Hambright, K.D.,² Brenner, I.,¹ Halicz, L.¹

1. Geological Survey of Israel, 30 Malkhe Yisrael Street, 95501 Jerusalem

2. Yigal Alon Kinneret Limnological Laboratory, Israel Oceanographic and Limnological Research Ltd., P.O.B. 345, 14201 Tiberias

The vertical distribution of trace and major components in the water column of Lake Kinneret at its deepest point (station A), was recorded from November 1986 to January 1988. Sixteen monthly sampling sets of five depths each, were analysed for the filterable (<0.45 μ m) and acid extractable components. Conclusions from the four profiles of a single annual limnological cycle (1987) for selected constituents (filterable concentrations) are given below:

- a. Seasonal biological activity superimposed on the physical stratification of the lake affects the distribution of Ca, HCO₃, pH and the associated trace elements Sr and Ba through algal activity and calcite precipitation and dissolution. SiO₂ consumption by diatoms is a major sink that keeps SiO₂ concentrations lower in the lake compared with streams and saline springs. We suggest that this process is also accompanied by biogenic barite precipitation in a manner similar to that in the marine systems.
- b. Redox conditions that are developed in the hypolimnion during stratification affect mainly the vertical distribution of Fe and Mn. It seems that both have two maxima, at the metalimnion and near the bottom, and denser sampling could establish this pattern explicitly. Aside from the seasonal distribution, Fe concentrations are controlled by sinking mechanisms which are assumed to be precipitation of FeS₂ and algal uptake and sedimentation.
- c. Release from bottom sediments besides Mn, Fe and SiO₂, was also detected for Al and Cu. This was observed at 39 m during a period of low lake water level. Future investigations should consider a sampling regime relative to the lake bottom in order to eliminate confounding effects of variable lake water level.
- d. Evaporation (summer and autumn) versus dilution from stream floods and direct rainfall could be clearly detected in the profiles of Na, K and Cl, despite the masking by the large contribution of these constituents by sublucustrine saline springs. The increase of the Na/Cl ratio in summer and autumn suggests a surficial Na input probably as halite in aerosols.
- e. It seems that seasonal changes in Mg and B concentrations are associated with enhanced saline spring discharge in response to high head pressure in freshwater aquifers. Monitoring these two elements might contribute to the understanding of salinization mechanisms in the lake.
- f. A dominant factor in the distribution of Zn and also of Cu is surficial enrichment, which is attributed to motor boat activities or to polluted fallout.

Copper Sulfides in the Cambrian Timna Formation

Scholomovich, N.,^{1,2} Bar-Matthews, M.,¹ Segev, A.,¹ Matthews, A.²

1. Geological Survey of Israel, 30 Malkhe Yisrael Street, 95501 Jerusalem

2. Institute of Earth Sciences, The Hebrew University of Jerusalem, 91904 Jerusalem

Spheroids, 0.1 to 5 mm in diameter, composed of copper sulfides are distributed randomly throughout the dolomitic lithofacies of the Sasgon member of the Timna formation. The copper sulfide minerals identified within the spheroids are: chalcocite ($\text{Cu}_2\text{-1.96S}$), djurleite ($\text{Cu}_{1.93\text{S}}$), digenite ($\text{Cu}_{1.80\text{S}}$), anilite ($\text{Cu}_{1.75\text{S}}$), and covelite (CuS). Texturally they are observed to show intimate intergrowth with each other. Silver occurs within the sulfides as notable trace element (0.3-3%), and also occurs as an independent mineral acanthite (Ag_2S).

Inclusions of gypsum, quartz, calcite and native sulfur are found within the sulfide minerals and serve as indicators of the original sedimentary assemblages. The sulfides are replaced by secondary copper minerals in the form of green alteration rims. The sequence of the secondary alteration follows the following paragenetic order: 1) malachite ($\text{Cu}_2(\text{OH})_2\text{CO}_3$); 2) paratacamite ($\text{Cu}_2(\text{OH})_3\text{Cl}$); 3) mottramite ($\text{Pb}(\text{Cu}, \text{Zn})(\text{VO}_4)(\text{OH})$). Chrysocolla ($\text{Cu}_{2-x}\text{SiO}_5(\text{OH})_3 \cdot x\text{H}_2\text{O}$) replaces quartz relics within the spheroids. The size and the textural form of the alteration depends on the character of the host dolomite. Where dolomites are massive and with low detrital content, the green alteration rim is narrow and has a sharp contact with the host rock. In contrast, at the base of the main dolomite unit detrital minerals (mainly clays and micas) occur together with copper mineralization in the form of green laminae mainly composed of paratacamite. Microanalysis indicates that these laminae consist of networks of dense paratacamite veins originating from altered spheroids containing relics of primary copper sulfides and secondary malachite, paratacamite, chrysocolla, and mottramite.

The occurrence within the dolomite of spheroids of copper sulfide minerals containing relics of gypsum, quartz, calcite and native sulfur indicate that they were formed in a shallow lagoonal (reducing) environment. Oxidation and hydration reactions during and post dolomitization resulted in the development of secondary minerals. Malachite may have formed during dolomitization, but paratacamite formed later. Further copper mobilization occurred in the presence of chloride bearing solutions which deposited paratacamite veins and laminae. However, the timing of the chrysocolla alteration with respect to the alteration of sulfides cannot be determined. Thermodynamic analysis suggests that chrysocolla replaces quartz with the increase of the pH and possible activity of dissolved silica. The study shows that primary copper mineralization occurred in the form of copper sulfides and that alteration processes were function of changes in geochemical conditions, i.e., Eh-pH, solution chemistry, and permeability of the host rock.

Isotopic Differences Between Bones of Different Periods: Climatic or Diagenetic Changes?

Shahack-Gross, R.,^{1,2} Tchernov, E.,² Kolodny, Y.,¹ Luz, B.¹

1. Institute of Earth Sciences, The Hebrew University of Jerusalem, 91904 Jerusalem

2. Dept. of Evolution, Systematics and Ecology, Institute of Life Sciences, The Hebrew University of Jerusalem, 91904 Jerusalem

The isotopic composition of oxygen in bone phosphate (δ_p) in mammals is related to the isotopic composition of the carbon in bone carbonate ($\delta^{13}C$) in herbivorous mammals yields information about the kind of vegetation in the mammal's diet. Both δ_p and $\delta^{13}C$ depend on the climate in the mammal's habitat.

δ_p and $\delta^{13}C$ were measured in two mammal species from Israel: vole (a rodent) and gazelle. The analyses were carried out on recent populations from different areas of the country and on fossil populations from Ha'yonim cave (western Galilee). The cave material we selected derives from two prehistoric periods: the Kebaran (19–14500 years B.P.) and the Natufian (12500–10300 years B.P.).

In order to make sure that the isotopic results reflect the original δ_p we measured the state of preservation of the material (bones and teeth) by X-ray diffraction, IR spectroscopy and the isotopic composition of oxygen in bone carbonate (δ_c). In the first two methods crystallinity indices were calculated.

The spectral methods show change in the crystallinity indices between recent and fossil material, due to diagenesis, but among fossil samples there are no clear criteria to distinguish samples with original δ_p from samples with diagenetic δ_p . According to the IR data, the fossil vole bones and the fossil tooth enamel of the gazelles did not change their mineralogical structure. Thus we assume that they preserve their original isotopic signature. δ_c results do not show any clear connection to diagenesis.

δ_p results of the recent vole populations show good correlation with the relative humidity of the collection sites. The results of the fossil voles are qualitative. It shows that relative to present levels, humidity in the Ha'yonim cave area was lower during the Kebaran and slightly higher during the Natufian. The gazelle populations shows the same pattern. These results agree with palaeontological and palynological studies on the same periods.

$\delta^{13}C$ results shows similarity in the diet of Natufian and recent gazelles, which implies no severe change of temperature. These results do not agree with palaeontological and palynological studies.

The Case for Early Miocene Deposition of the Hatseva Formation in the Dead Sea Rift

Shahar, J.

Jerusalem

The Hatseva Formation was deposited through the Early and Middle Miocene in an inland basin - the early Dead Sea Rift - that had no drainage toward the Mediterranean (as has been postulated by Zak and Freund, 1981). The evidence includes:

1. The greatest thickness of Hatseva sediments coincides with axial part of the Rift (700m in 'Ami'az 1 borehole, Horowitz 1987), suggesting syn-sedimentary subsidence.
2. The Be'er Sheva' channel, thought by some to have drained the early Rift toward the Mediterranean (Neev, 1960), flowed initially eastward toward the Rift. It is at its widest near Kurnub, narrowing westward. Its western segment between Be'er Sheva' Valley and the Mediterranean was not incised before the end of the Miocene. The Soreq River on the other hand, thought by some to have drained the Rift westward, never crossed the Judean arch.
3. Deposits of allochthonous flint are found *in situ* as far westward as the western foothills of the Hebron arch (La'hav-Goral area), indicating that the present-day water divide had not yet been formed by the Middle Miocene.
4. Similar thicknesses and compositions of the Hatseva sediments in the Negev synclines indicates that uplift of the northern Negev structures began only after the Middle Miocene. There are no east-west gradients in facies, but rather a north-south gradient. This is exemplified by the earlier arrival of allochthonous flint pebbles in the north ('Arad) than in the south (upper flanks of Ramon). Allochthonous flint at 'Ein Boqeq and in the Rotem syncline occurs in entirely comparable sections (Agnon, 1983), indicating similar and synchronous levels of deposition. At both localities they were deposited on a near-horizontal outwash plain.
5. The Hatseva sediments have remained horizontal and unfaulted, despite differential subsidence and uplift. A morphological analysis pre-deformational of this, the youngest pre-deformational rock unit, holds the clue to the style and mechanism of these movements.

Reconstruction of Fault Patterns Underlying Folds - Mechanical Constraints

Shamir, G.,¹ Eyal, Y.²

1. The Institute for Petroleum Research and Geophysics, P.O.B. 2286, 58122 Holon
2. Department of Geology and Mineralogy, Ben-Gurion University of the Negev, 84105 Beer Sheva

Monoclines are typically associated with buried reverse faults and have attracted interest due to oil reservoirs found in many. Mechanical constraints are suggested for reconstruction of such fault patterns, particularly when derived from field mapping and interpolation between seismic profiles. The uplift pattern produced by prescribed slip on a set of buried reverse faults is calculated, assuming that the deformation *pattern* is determined by the elastic strain induced by fault displacement at depth, while fold *amplitudes* and local geometrical variations are a consequence of accumulating plastic strain.

The configuration of the northern Negev monocline belt is simulated as a test case, with fault trends compatible in plan view with monoclinical axes. Faults are modeled as dislocation planes embedded in an elastic half-space, which is otherwise continuous, and uniform.

Our preliminary model strictly follows the compiled structural map of the northern Negev, based on field mapping in the east and on interpretation of geophysical surveys in the west. It is characterized by long, continuous faults which follow axis variations and often extend beyond the limits of specific folds. Uniform slip is assumed along faults. The resulting uplift pattern fails to simulate the configuration and trend variations of the folds, as well as the relative position of synclines, while producing unrealistic flexures where model faults dip eastward.

The second model includes fault discontinuities and decreasing slip gradients towards fault terminations, proportional to the decreasing structural elevation. This model produces a far better simulation of the overall observed structural configuration as well as of specific structures. A major role is played by slip gradients at structure terminations and by superimposed uplift contributions from neighboring structures.

It is concluded that (1) The elastic deformation in the layers overlying reverse faults produces monoclinical configurations; (2) Faults underlying monoclines generally do not extend beyond structure limits and do not simply follow fold axis trend changes; (3) Fault discontinuities are a major cause for fold strike changes and en echelon arrangement; (4) Structural gradients along the monoclines are roughly proportional to the displacement gradients along the underlying faults; (5) The degree of asymmetry of monoclines is a function of fault dip and depth of burial; (6) The Revivim syncline is probably not a down-faulted graben but a structure similar to, and broader than the eastern Negev synclines.

Spatial and Temporal Distribution of Earthquake Sequences in the Gulf of Elat

Shamir, G., Shapira, A.

The Institute for Petroleum Research and Geophysics, P.O.B. 2286, 58122 Holon

The pattern of seismic activity in the Gulf of Elat, at least since the early 1980's, has been dominated by earthquake sequences with a distinct spatial distribution. The January 1983 sequence lasted about two months and was associated with a maximum magnitude of $M_L=5.2$. The spatial distribution of epicenters, 20-70km south of Elat, indicates that these events represented the activity of the northern fault step zone of the Gulf (Elat Deep). Two following earthquake sequences, in April 1990 and in May 1991, had peak magnitudes of 4.3, with epicenters concentrated between 45 and 70km (the Nueba latitude) south of Elat. This indicates a spatial overlap with the southern part of the 1983 earthquake distribution, suggesting that the 1983, 1990 and 1991 sequences represent one tectonic event, with the latter two releasing excess strain energy remaining after the former. The latest earthquake sequence in the Gulf, in August 1993, began with a moderate increase in the frequency of background (i.e. low magnitude) seismic activity over the month of July. An alarm was issued on August 1st by the automatic detection system, based on an algorithm for detecting increased probability of occurrence of a felt earthquake in a short time interval. This was followed by over 400 events with magnitudes $M_L \geq 3.0$ within the three months since, including peak magnitudes of $M_L=5.8$ and 5.6 on August 3rd which were strongly felt in Israel, Egypt, Saudi Arabia and Jordan. The epicenter distribution is clearly bounded from north at the Nueba latitude and concentrated primarily over the central part of the Gulf, i.e. at the Aragonese Deep.

The following preliminary conclusions may be drawn: (a) Seismic activity along the Gulf of Elat occurs in the form of sequences, each lasting one to three months, reaching peak magnitudes of up to about 6.0 and covering a specific tectonic segment of the Gulf; (b) Each tectonic segment goes through a seismic cycle which ends with an earthquake sequence rather than with one major event and whose length should be influenced by activity along neighbouring segments; (c) A sequence may burst in several pulses, separated by several years, if energy release has been incomplete initially; (d) The temporal distribution of events within each sequence is characterized by an initial few days to few weeks of gradually increasing magnitudes, suggesting that the detection of the beginning of a sequence is feasible and can lead to the TIP and to relatively successful short-term earthquake predictions in the Gulf region.

Automatic Identification of the Time of Increased Probability for a Felt Earthquake

Shapira, A.

The Institute for Petroleum Research and Geophysics, P.O.B. 2286, 58122 Holon

Earthquake sequences are known to occur in different seismic areas in and around Israel. The most known are: the Hula-Kinneret area, the Yagur fault area, the Faria fault system, the Arava valley near Zofar and Parran, the Dead Sea and the Gulf of Eilat. Following Shapira (1990) and many others, the occurrence of an earthquake sequence may be an indication for the increased probability of the occurrence of a felt earthquake in the same area within a short time interval (hereafter termed TIP).

Based on earthquake catalogs for the period 1965-1989 for the Yagur-Faria region and for the Gulf of Elat, parameters were set in 1989 to detect automatically the occurrence of an earthquake sequence and indication of a TIP. The automatic detector was activated twice during the only two sequences which occurred since 1989 (both of them in the Gulf of Elat). The first detection was made on 21.4.1990 and, apparently, is characterized as a mainshock ($M=4.3$) followed by a series of aftershocks. The second was made on 1.8.1993 and was followed two and four days later by strong earthquakes of magnitudes 5.8 and 5.6, respectively. These findings are as expected from the 1989 evaluations, i.e. the probability for a follow-up felt earthquake within 3 months increases from a level of maximum 10% (the Dead Sea area) to about 50%.

The Seismicity of the Dead Sea Transform with Application to the Estimation of Tectonic Movement

Shapira, A.

The Institute for Petroleum Research and Geophysics, P.O.B. 2286, 58122 Holon

The tectonic movement along the Dead Sea transform, according to geologically based estimations, is much higher than that inferred from seismic information. According to A. Nur and others we miss earthquakes of the order of $M > 8.0$ to compensate for this discrepancy. Taking the transform as an active boundary between plates, we live in a seismically quiet period and should expect strong earthquakes along the Dead Sea transform.

We find it hard to accept the argument of a-seismic slip without the occurrence of small micro-earthquakes. Apparently, since detailed and accurate seismic monitoring began in 1982, the transform between the southern Arava and the Ayun valley is virtually inactive, with the exception of the Dead Sea basin and the junction areas with branching faults. These observations may raise the hypothesis that the current movement, if at all, along the transform is much lower than the average values provided by geological field observations. This idea is supported by the preliminary geodetic observations made by the geodetic network near Mahanaim and those of the laser ranging station at the Geophysical Observatory near Bar Giora.

It should be noted that the locations of historical earthquakes are only rough estimates and the only instrumentally located strong earthquake (1927, $M=6.2$) occurred in the Dead Sea basin and not as estimated previously (along the Dead Sea transform near Damiya). The accumulated tectonic stresses in our region are currently released by earthquakes along the faults branching off the Dead Sea transform. The implications of this hypothesis for seismic hazard assessment, usually made for time intervals of 50 and 100 years only, are most significant and the issue may be resolved in a relatively short time with the operation of a regional geodetic network.

Semi-Empirical Attenuation Functions for Seismic Ground Motions in Israel

Shapira, A., Gitterman, Y., Zaslavsky, Y.

The Institute for Petroleum Research and Geophysics, P.O.B. 2286, 58122 Holon

Assessment of earthquake hazard is primarily an attempt to predict seismic ground motions at a given site. A crucial parameter in the process of earthquake hazard assessment is the attenuation of ground motions with distance from earthquakes of various magnitudes.

Attenuation functions are usually determined empirically from accelerometer measurements. Despite the dense array of accelerometers in Israel, we do not have sufficient acceleration data to perform direct empirical analysis owing to the low seismicity of the region and, currently, earthquake hazard assessment in Israel is based on equations "borrowed" from California.

Using stochastic source models it is possible to synthesize ground accelerations from an earthquake of known magnitude and distance. Various authors have already demonstrated the good fit between observed and synthesized accelerograms from earthquakes of magnitudes 4.0 to 7.7. However, in order to synthesize ground motions we need empirical information about the correlation between magnitudes and seismic moment, estimations of the stress drop, f_{max} and the empirical attenuation of the zero frequency ground displacement. These parameters were estimated for Israel by Shapira and Hofstetter (1992). Based on synthetic ground motion records for various distances and earthquake magnitudes, we developed attenuation functions for Israel. The few acceleration data available agree with the predicted values given by the semi-empirical attenuation functions developed.

Electrotelluric Field Anomalies Associated with Earthquakes

Shirman, B.

The Institute for Petroleum Research and Geophysics, P.O.B. 2286, 58122 Holon

A fluid motion through a porous geological medium can generate an electrical current of observable magnitude. Assuming that changes in the regional tectonic stress field produce fluid motion, we may be able to detect electrical field changes prior to the occurrence of a significant slip along a fault (i.e. a strong earthquake). This concept has been modeled (the electro-kinetic model) and analyzed for local conditions. It has thus been estimated that a dislocation of 1 meter (corresponding to an earthquake of $ML \approx 5$) can generate, in the fluid-saturated elastic porous medium, an electrical field of about 1 mV/m at distances of several kilometers from the fault.

In parallel to these theoretical investigations, in September 1993 we installed an electrotelluric monitoring system at the Bar Giora observatory. The telluric dipoles, constructed from non-polarizable electrodes, are 200m long in both N-S and E-W directions. The data are sampled at one second intervals and averaged over one minute. In order to minimize the effects of external sources on the electrotelluric field, we reduced the electric field (calculated from the magnetic field observations) from the observed data using the impedance relations in the low frequency approximation. The possibilities of inner source identification using data from several electrotelluric stations will be discussed.

A Regional Lower Cretaceous Hydrothermal Circulation in Makhtesh Ramon Area

Shoval, S.

Geology Group, The Open University of Israel, Klauzner 16, 61392 Tel Aviv

The lower cretaceous (140-125 Ma) basaltic and trachytic dykes and sills in Makhtesh Ramon area are characterized in many places by extreme alteration. Some authors reported that this alteration was caused by meteoric water which were heated by each sill and dyke intrusion. In this work it is suggested that the intensive main alteration of sills, dykes and laccolith was a result of a regional hydrothermal circulation which was activated by ground water heated by the large intrusions, like the exposed quartz syenite stoks. This alteration occurred in the hydrothermal water passages connected with the large intrusions and not with each sill and dyke intrusion separately. The main alteration happened some millions years after the sills and dykes emplacement, since the quartz syenite stoks being the youngest intrusions (125 Ma).

Hydrothermal systems have two basic characteristics: they occur in regions of high geothermal gradient where hot rocks lie near the surface and they have a "pluming system" of fractures so that cold water can percolate downward into the rocks and then flow upward to the surface as hot water. The movement of water through these fractures is such that downward percolation occurs over a wide area, whereas the upward flow is concentrated in a limited number of channels.

The suggested paragenesis allows to connect the previous investigations to one uncontradicted model. It could explain why the Ardon dykes were totally altered in the penetrative sand stone of Inmar formation, but the parts of the dykes across clay rocks were relatively isolated and the original magmatic rock is also preserved, like in the Mish'hor and Ardon formations. The temperature of the hydrothermal circulation was differed in various locations due to the distance from the intrusion or the water passages. It seems that this is the reason why in some places the alteration process took place at a relatively low temperature, like in the Ardon dykes. The intensive alteration to alunite probably occurred in water passages and is connected with high sulfates content of the hot solutions which probably derived from the thick underlying gypsum sequence of the Triassic Mohilla Formation.

The hydrothermal circulation effects also the sedimentary rocks in the area. The influence on the country rocks near the magmatic stoks was reported. It seems that the quartzite prisms were formed only in hot reactive water passages. The inner white color of the quartzite prisms indicates intensive leaching. In the famous "Nagaria" area the sill was extremely altered to alunite which is an evidence of the reactivity of the water along this passage. This activity probably influences on additional rocks: the relations between the flint clay and laterite in Mish'hor formation which is also connected with late underground leaching; the relations between anhydride and gypsum in the Mohila formation; the local presence of alunite in Mish'hor formation and also lenses in the Inmar Formation; and the presence of chlorite in Triassic rocks.

Crystallochemical Heterogeneity of Apatites in the Negev Phosphorites

Shoval, S.,¹ Knubovets, R.,¹ Gaft, M.,¹ Nathan, Y.,² Rabinowitz, J.,³ Pregerzon, B.³

1. Physics and Geology Groups, The Open University of Israel, Klauzner 16, 61392 Tel Aviv

2. Geological Survey of Israel, 30 Malkhe Yisrael Street, 95501 Jerusalem

3. Rotem-Amfert-Negev, Yeruham

The crystallochemistry of apatites in the Negev phosphorites was investigated using FT-IR spectroscopy. 100 phosphorite samples were examined. IR spectroscopy is particularly suitable for this study because: 1) Sedimentary apatite crystallites have a very small grain size and are heterogeneous. 2) IR spectroscopy requires very small quantities of sample for analysis. 3) IR spectra are highly sensitive to crystallographic site symmetries and to dynamics of lattice.

The most intense bands of the orthophosphate groups in the spectrum of apatites are the antisymmetrical stretch ν_3 and the antisymmetrical bending ν_4 vibrations. In fluorapatite, the symmetry of the site occupied by the phosphate ion is C_{3v} ; this causes a lowering of the T_d symmetry of the free tetrahedral PO_4 anion. Consequently some modes, inactive in the free tetraheder, become infrared active. In particular the symmetrical stretch ν_1 (965 cm^{-1}) appears in the spectra.

The spectra of all investigated phosphorite samples showed three absorption bands of ν_4 : $605, 580, 570\text{ cm}^{-1}$. This testifies to the complete lifting of the degeneracy of the triply degenerate ν_4 vibration. Thus, two P - O bonds in the orthophosphate groups are non-equivalent to the two others in all the investigated apatites (the symmetry of the site occupied by the phosphate is in this case C_{2v} at most). The relative intensities of the three bands of ν_4 vary and it is possible to classify the apatites into four groups:

- 1) $I_1 > I_3 > I_2$;
- 2) $I_1 = I_3 > I_2$;
- 3) $I_1 > I_3 = I_2$;
- 4) $I_1 < I_2 < I_3$.

(I_1 - intensity of band at 605 cm^{-1} , I_2 - intensity of band at 580 cm^{-1} , I_3 - intensity of band at 570 cm^{-1}).

The existence of four types of IR spectra for the ν_4 vibration implies the existence of four crystallochemical types of apatites. Most of the investigated samples belong to group I (about 65%). These crystallochemical types may be connected to isomorphous substitutions in the PO_4 site in the apatite structure.

The Potential of Resuspension in Lake Kinneret Estimated from Current Velocity Measurements

Shteinman, B., Parparov, A.

Yigal Alon Kinneret Limnological Laboratory, Israel Oceanographic and Limnological Research Ltd., P.O.B. 345, 14201 Tiberias

Changes in the ratio between sedimentation and resuspension of suspended matter is one of the most important consequences of changes in lake morphometry. Changes in this ratio caused by water level fluctuations might significantly effect the ecosystem of Lake Kinneret. Resuspension values derived from budget calculations and sediment trap data may be overestimates. Because of entrapping of horizontally transported particles, effects of turbulent currents and so on.

In the work reported here the potential of resuspension (PR) was evaluated at the surface area of the bottom sediments, from which particles can be resuspended to the water column, under hydrodynamic conditions which exist in the lake littoral. The possible impact of the lake water level lowering on this process was considered. The study is based on field observations of the turbulent structure of water masses in the littoral zone (3-22 m) near the west shore of Lake Kinneret. Derived dependencies of the horizontal and vertical current velocities on depth were analytically approximated. This enabled us to estimate current velocities at the interface and to compare them with critical shear velocities.

As a result, PR of the littoral zone of Lake Kinneret was evaluated for different current velocities and sediment type and under different lake water levels as well. A reasonable correspondence between results and estimates of PR made using morphometric indices only enable us to use our approach for predicting consequences of lower Lake Kinneret water level.

The Yasaf Member: A *Strombus* Bearing Unit on the Coast of Galilee Representing Tyrrhenian Event in the Mediterranean

Sivan, D.,¹ Gvirtzman, G.,¹ Kaufman, A.,² Sass, E.³

1. Geological Survey of Israel, 30 Malkhe Yisrael Street, 95501 Jerusalem

2. Isotope Department, Weizmann Institute of Science, 76100 Rehovot

3. Institute of Earth Sciences, The Hebrew University of Jerusalem, 91904 Jerusalem

The late Pleistocene Tyrrhenian stage is interpreted as a paleo-oceanic event in the Mediterranean during which warm-water Senegalian fauna entered the basin. This fauna includes the gastropod *Strombus bubonius* and the colonial coral *Cladocora caespitosa*. In 1971 Kaufman asserted that the dating of corals by means of uranium series can be considered reliable, since their isotopic system was found to be closed, while the dating of mollusks is generally not reliable. Indeed, *Strombus* and *Glycimeris* samples from Spain were dated by means of uranium series, showing a wide age range, which covers also the time intervals of isotope stages 7 and 5, but the isotopic ratio of $^{234}\text{U}/^{238}\text{U}$ in the examined material indicated the system had been open at one point in time.

Fossil Tyrrhenian beaches which contain *Strombus bubonius*, usually at two different levels, at 0-120 m, are scattered all over the Mediterranean basin. In some of these coasts the *Strombus* fossils are associated with the coral *Cladocora*. Surveys in Majorca, southern Italy, Tunisia and Cyprus, only from locations of well documented stratigraphic relationships, indicate that ages of corals which aragonitic composition was preserved, cluster around the ages of the isotopic substages 7.1 (peak at 194 thousand years BP) and 5.5 (peak at 122 thousand years BP). Along the Lebanese and Israel coasts only one *Strombus*-bearing unit was found, known as the Yasaf member, on the Galilee coast. It occurs at levels of 0-3 m and contains abundant *Strombus* specimens. Some of the specimens are complete and morphologically well preserved.

Nine samples of pure aragonite composition, which were dated by means of uranium series at the Weizman Institute in Israel and at the University of Quebec, Canada, gave unreliable ages: two pieces of the same snail gave different dates (143 and 166 thousand years), two snails from the same unit gave ages of stages 7 and 5, and in all the cases the uranium 234/238 ratio indicates that the isotopic system had been open. The results of the Galilee coast again show that dating of mollusks by means of uranium series is not reliable, and that one should rely on age clusters obtained from corals. According to stratigraphic considerations it was determined that the Yasaf member belongs to isotopic substage 5.5, while the marine ingression of isotopic substage 7.1 is in the subsurface of the Galilee coast.

Geological Map of Israel 1:200000 Scale, North Sheet

Sneh, A., Bartov, Y., Rosensaft, M.

Geological Survey of Israel, 30 Malkhe Yisrael Street, 95501 Jerusalem

A new 1:200000 geological map of Israel is being prepared in three sheets: North, Central and South. The work on the North sheet has been completed and the poster displays the map before submission for publication. The geological map is based on a computerized edition of existing maps and on mapping being carried out at present; and it can easily be combined with other, computerized, information layers.

The list of sources on which the map is based comprises a large number of maps which have been prepared following the 1:250000 geological map, North sheet, by Picard and Golani, published thirty years ago, a map which by and large serves as a basis for the new map. The sources for the North sheet are:

Arad 1965; Bein 1974; Belitzky 1987; Bender 1968; Benjamini 1973; Bentor 1946; Braun 1992; Cook 1971-72; Dan and Raz 1970; Dekel 1988; Dicker 1969; Dubertret 1955; 1957; 1961; Eliezri 1965; Flexer 1959; Freund 1959; Glikson 1966a, 1966b; Golani 1962; Grader 1950, 1958; Greenberg 1964; Hatzor 1988; Heimann 1985, 1990; Hildebrand-Mittlefehldt 1993; Ilani 1985; Kafri 1972; Kafri 1991; Karcz 1959; Kashai 1966, Levitte 1993; Levy 1983; Michelson 1970; Michelson 1974; Michelson and Mor 1985; Mimran 1969; Mor 1987a, 1987b, 1991; Nevo 1956; Picard and Golani 1965; Ponikarov et al 1983-4; Rabinovitch 1953; Rofe and Raffety 1965; Rosenberg 1960; Saltzman 1964; Saltzman and Dekel 1981; Sass 1966; Schlein 1961; Schulman 1962; Shaliv 1979, 1991; Shifan, 1955; Shimron 1988; Sneh 1994; Sneh, Druckman and Mimran 1985; Sneh and Rosensaft 1994; Sneh, Sass, Bein, Arad, Levitte and Rosensaft 1993; Sneh and Siman-Tov 1994; Vroman 1958; Weiler 1968.

What is the "Age" of the Sedom Formation?

Stein, M.,¹ Agnon, A.,¹ Starinsky, A.,¹ Raab, M.,² Katz, A.,¹ Zak, I.¹

1. Institute of Earth Sciences, The Hebrew University of Jerusalem, 91904 Jerusalem

2. Geological Survey of Israel, 30 Malkhe Yisrael Street, 95501 Jerusalem

An effort was made to determine the age of deposition of the Sedom Formation by using strontium isotopic composition of evaporite samples from Mt. Sedom and from several boreholes in Mt. Sedom, Amiaz plain and Dead Sea shore. The idea was to achieve high precision strontium isotope data and to compare the results with the curve of secular variations of strontium in the oceans (assuming that the Sedom Formation evaporites were deposited from normal seawater and that the strontium isotope system remained closed since the time of deposition). The samples show $^{87}\text{Sr}/^{86}\text{Sr}$ in the range of 0.70820 to 0.71931. No systematic differences were found between surface and subsurface samples, or between different stratigraphic units of the Sedom Fm. The lowest values are shown by dolomites from Mt. Sedom (0.7082) and the highest values were yielded by two samples of almost pure carnallite and sylvite ($^{87}\text{Sr}/^{86}\text{Sr}$ of 0.71153 and 0.71931 ratios respectively). Provided that the original Sedom lagoon was connected with the open sea, the lowest $^{87}\text{Sr}/^{86}\text{Sr}$ values of the dolomites would correspond to an age of 22 ± 4 Ma on the secular variation curve. Yet, it was found that $^{87}\text{Sr}/^{86}\text{Sr}$ ratios of several evaporites are positively correlated with potassium concentrations. This correlation may indicate that the Rb-Sr isotopic system was disturbed and that there was a regional homogenization and resetting of the strontium isotope values around $^{87}\text{Sr}/^{86}\text{Sr} = 0.7082$. This process could have been caused by metamorphism of the evaporites at depth.

Sr Isotopes in a Red Sea Core — Inferences for the Red Sea History During the Last 400 kyr.

Stein, M.,¹ Almogi-Labin, A.,² Goldstein, S.L.,³ Hemleben, C.,⁴ Starinsky, A.¹

1. Institute of Earth Sciences, The Hebrew University of Jerusalem, 91904 Jerusalem

2. Geological Survey of Israel, 30 Malkhe Yisrael Street, 95501 Jerusalem

3. Max-Planck Institute für Chemie, Postfach 3060, Mainz

4. Tübingen University, Tübingen

We report on $^{87}\text{Sr}/^{86}\text{Sr}$ ratios in seventeen carbonate samples (foraminifers, pteropods and secondary carbonate) from the Red Sea core KL11 (located at $18^{\circ}46.3'\text{N}/39^{\circ}19.9'\text{E}$). The core, 20.93 m in length covers the last 400 kyr. Strontium isotopes were measured in dynamic mode on a Finnigan MAT261 at MPI-Mainz. Twenty five measurements of NBS-987 standard yielded $^{87}\text{Sr}/^{86}\text{Sr} = 0.710259 \pm 9$ (2s). The samples were measured in duplicates. The foraminifers are mainly *Globigerinoides sacculifer* made of low magnesium calcite, and the pteropods are made of aragonite. The average $^{87}\text{Sr}/^{86}\text{Sr}$ ratios of samples from glacial and interglacial periods are 0.70917 ± 1 (1s) and 0.70921 ± 4 (1s) respectively. In comparison, a core from the Arabian Sea (Clemens et al. 1993) which represents open ocean conditions shows similar, but less amplified patterns of $^{87}\text{Sr}/^{86}\text{Sr}$ ratios. While most samples from glacial periods yielded the same $^{87}\text{Sr}/^{86}\text{Sr}$ ratios in both localities, two samples from maximum glacial conditions in the Red Sea have slightly lower ratios than contemporaneous episodes in the Arabian Sea. On the other hand, samples from several episodes of high sea-level stand in the Red Sea show higher $^{87}\text{Sr}/^{86}\text{Sr}$ ratios than those from the Arabian Sea with differences up to 0.0001. These observations suggest that: (1) at maximum glacial conditions the Red Sea became an almost closed basin, circulation with the open ocean was limited and the composition of strontium in the water was affected by magmatic-hydrothermal input; (2) during interglacial high sea level stands the Red Sea surface water was affected by local input of more radiogenic strontium which was derived from the surrounding shield.

^{40}Ar - ^{39}Ar Age of Authigenic Feldspar from the Cenomanian Hazera Formation

Steinitz, G., Kapusta, Y., Sandler, A., Kotlarsky, P.

Geological Survey of Israel, 30 Malkhe Yisrael Street, 95501 Jerusalem

K-feldspar was separated from a dolomite from the Hevyon Member of the Hazera Formation (Cenomanian-96-91 ma). The rock contains 3-4% K-feldspar. SEM observations show that the crystals are idiomorphic and predominantly in the size range of 4-10 μ , indicating its authigenic origin. K-Ar analysis yields an age of 97.7 ± 1.9 ma (%K=12.22).

^{40}Ar - ^{39}Ar age spectra were determined for two size fractions: >4 μ and 4-10 μ . The high temperature (>400°C) steps of the step-wise extraction yield a plateau with an age of 97-99 ma. The low temperature steps of the age spectrum yield ages which are circa 5% lower. It is assumed, at this stage, that this represents a somewhat later closing of the K-Ar system in this mineral phase, due to diagenetic processes.

Kinetics of the argon release shows a peak (more than 50%) in the temperature interval 300-400°C and a small peak at around 700°C.

The Radon Flux Along the Western Rift Fault at Enot Zuqim — Evidence for Geophysical Control

Steinitz, G.,¹ Vulkan, U.,² Assael, Y.,² Yaffe, Y.²

1. Geological Survey of Israel, 30 Malkhe Yisrael Street, 95501 Jerusalem

2. Soreq Nuclear Research Center, Yavne

Monitoring of the radon flux along the western boundary fault of the Rift is being carried out at Enot Zuqim, northwestern corner of the Dead Sea, over a 3 km long sector along the Rift main fault. Three monitoring sites are located on Rift alluvium adjacent to the fault scarp. Two additional sites are located within the Rift, 100 and 500 m east of the main fault. The measurements are integral over 3-4 days.

Data collected for 1992 (and partially 1993) show that the high radon flux is controlled by relatively deep features and events in the subsurface. Thus the temporal variation of the radon flux is considered to be a geophysical phenomenon. Among the indicative features are:

1. Large (order of magnitude) temporal variations in the radon flux are recorded within site and between sites.
2. The three on-fault sites show a similar long term variation (circa 1 year cycle).
3. The two off-fault sites also show a concordant long term variation, which differs from that of the on-fault sites (circa 1/2 year cycle).
4. Statistical analysis indicates a significant correlation of the (temporal) flux between the three on-fault sites.
5. Short term fluctuations (7-20 days) are superimposed in all sites on the long term variation. These fluctuations are radon flux "events". Out of the 18 events defined in the time interval of days 80-366 in 1992, 5 were recorded at all five sites, 2 at four sites and 3 events at three sites.

Fluid Inclusion and Fracture Study of the Elat Granite

Vapnik, Y., Frid, V.

Department of Geology and Mineralogy, Ben-Gurion University of the Negev, 84105 Beer Sheva

In the previous study of the Campus Area metamorphic complex (Vapnik, 1992) it was assumed that the appearance of brine fluid inclusions was connected with both superimposed greenschist facies metamorphism and meteoric water flow. The present research attempts to clarify this assumption. Elat granite intruded after a greenschist facies metamorphism event (Shimron, 1972) and before a hypothesized meteoric water flow. Thus, several samples of the Elat granite, characterized by certain orientation and divided by fractures into nearly isometric blocks (Nahal Shlomo Area), were investigated in detail.

Sample and in situ observations distinguished two fracture systems. The first creates the blocks and the second intersects the blocks. Orientation and density of fluid inclusion trails observed in quartz under the microscope coincide with the second fracture system. The composition of these fluid inclusions is similar to one of bulk distributed (primary) inclusions and moreover to the brine inclusions in adjacent rocks of the Campus Area. Thus it was concluded that: a) the Elat granite was a possible source of fluids that led to brine fluid inclusion formation in the rocks of the Campus Area; b) the primary fluid of the Elat granite was redistributed during the earlier fracturing, and there was no other infiltration into the system. Data indicate that this fracturing is connected with burial and deformation during a nape structure development that manifested itself in the formation of tectonic schist in the Nahal Shelomo. Based on fluid inclusion data the conditions of the early fracturing and fluid reequilibration were determined as $T \geq 300^\circ\text{C}$ and $P \geq 1.0$ kbar, respectively.

The second fracture system dividing granite and adjacent rocks into blocks developed under the stress field caused by a meridian fault in the Nahal Shelomo area.

Tracing the Sources of Contaminated Groundwater by Boron Isotope Composition

Vengosh, A.,¹ Heumann, K.G.,² Juraske, S.,² Barth, S.³

1. The Hydrological Service, P.O.B. 6381, 91063 Jerusalem

2. Institute of Inorganic Chemistry, University of Regensburg, Universitätsstrabe 31, Regensburg D-93053, Germany

3. Centre de Recherches Petrographiques et Geochimiques (CRPG-ENSG), 15 rue Norte Dame des Pauvres, BP 20, F-54501 Vandoeuvre-les Nancy Cedex, France

The boron isotope variations were examined in both sewage effluents and contaminated groundwater (by municipal treated sewage) in order to evaluate the potential of boron isotope composition as a tracer for sources of groundwater contamination. We show that the boron isotope composition of raw and treated sewage effluents from the Dan Region Project, Israel ($\delta^{11}\text{B}=5\text{‰}$ to 14‰ ; $\delta^{11}\text{B}$ is defined as $[\frac{^{11}\text{B}/^{10}\text{B}}{\text{sample}} / \frac{^{11}\text{B}/^{10}\text{B}}{\text{NBS 951}} - 1] \times 1000$) overlap with those of natural borate minerals (-0.9‰ to 10.2‰), slightly higher than sodium perborate which is added to detergents (3 ± 1 ; a single sample), and is significantly different from those of regional, uncontaminated groundwater in Israel ($\delta^{11}\text{B}\sim 30\text{‰}$) and sea water ($\delta^{11}\text{B}=39\text{‰}$). The application of sodium perborate as a bleaching agent in detergents and some household cleaners and its discharged to the environment during production and end use lead to a significant enrichment of boron in sewage effluents (0.5 to 1 mg/l in Dan Region Project) relative to natural groundwater ($\text{B}=0.05$ mg/l).

The combination of high boron content coupled with a distinguished isotopic signature is reflected by the compositions of contaminated groundwater associated with artificial recharge of treated sewage effluents ($\delta^{11}\text{B} = 7\text{‰}$ to 25‰). The elemental B and $\delta^{11}\text{B}$ variations reflect both mixing with regional groundwater and boron adsorption onto clay minerals. Nevertheless, the distinctive isotopic signature of anthropogenic boron can still be recognized in most of samples and is different from those of other (natural) sources of salinization in the Coastal Plain Aquifer of Israel, such as marine-derived saline groundwater ($\delta^{11}\text{B}=35\text{‰}$ to 60‰). This enables using the boron isotope composition of groundwater as a tracer for elucidating the sources of contamination of groundwater, particularly for distribution of detergents compounds in aquatic systems.

Multi-Criterion Estimation of Geological Prospecting Effectiveness

Vilen, M., Eppelbaum, L.

Department of Geology and Mineralogy, Ben-Gurion University of the Negev, 84105 Beer Sheva

All geological investigations are made in definite succession in time and space. For this different geological means (mining works, drilling, geophysical and geochemical investigation, etc) are employed.

The problem of means rational integration can be solved using following criteria:

- (1) Necessary expenditures for realization of the integration (cost criterion C);
- (2) Necessary time for realization of the integration (time criterion T);
- (3) Informativeness of the integration (informational criterion Γ).

The assumed criteria are universal and the suggested approach can be used for estimation of any informational system. Criteria C and T can be easily determined by direct calculation, but estimation of criterion Γ is a complex investigation problem.

Available geological information can be represented in the classic three-level variant: (a) syntactical - amount of information; (b) semantic - substance of information; (c) pragmatic - value of information. An elaborated logical-heuristic model of the geological information has the following form:

$$\Gamma = QURUV,$$

where Q is the quantitative estimation of information, R is the estimation of informational reliability corresponding to the syntactical criterion, V is the estimation of informational value by degree of aim achievement according to the pragmatic criterion, U is the symbol of unification.

This model is a humanistic model, where the essential roles are experience, knowledge and the capacity of man for solving problems. For control of this model the most suitable apparatus is a diffusion set and a dialogue man-computer system.

This approach was used in particular for optimization of mining works in pyrite deposits on the southern slope of the Greater Caucasus.

Large-Scale Asymmetries Across the Dead Sea Rift: a Half Graben Model for the Formation of the Arava Valley and Dead Sea Basin

Wdowinski, S., Zilberman, E.

Geological Survey of Israel, 30 Malkhe Yisrael Street, 95501 Jerusalem

Large scale asymmetries with respect to topography and structure are characteristic of continental rift systems. Along the Dead Sea Rift (DSR), these asymmetries are best observed in the Northern Arava Valley segment (30-31° N). The eastern side is topographically and structurally higher and is flexed upward toward the rift margin. The western side is flexed downward toward the rift axis and its overall structure resembles an asymmetric anticline ("arching"). The Dead Sea Basin lies to the north (31-32° N) and shows similar asymmetries; however, it is bounded by two major faults parallel to the rift axis.

We propose that the asymmetry of the DSR reflects a first order half-graben structure, in which the border fault lies east of the rift and is westwardly dipping. Smaller scale structures within the rift, such as pull-apart basins, are superimposed on the larger scale half graben.

The formation of the rift's morphology in the studied area is explained by a four stage kinematic model: (a) initial regional low relief topography with a slight westward gradient; (b) formation of a half-graben structure by normal faulting in response to E-W extension; (c) isostatic rebound due to the rift's negative mass anomaly, and (d) erosion and deposition. The model predicts: the large scale topography on both sides of the rift, the uplifted footwall structure east of the rift, and the "arching" structure west of the rift. According to our model, the Dead Sea Basin is part of a half-graben structure that is bounded by an eastern border fault and a western antithetic fault. The deep basins within the Dead Sea, which are a product of a horizontal motion along the Dead Sea transform fault, are sited within the larger scale half-graben structure.

A New Approach to Determine Tensile Strength of Rocks Under Confining Pressure

Weinberger, R.,^{1,2,3} Reches, Z.,^{1,2} Scott, T. E.,² Eidelman, A.^{1,2}

1. Institute of Earth Sciences, The Hebrew University of Jerusalem, 91904 Jerusalem

2. School of Geology & Geophysics, University of Oklahoma, Norman

3. Geological Survey of Israel, 30 Malkhe Yisrael Street, 95501 Jerusalem

Knowing the rock strength in the tensile stress regime is of considerable significance for the analysis of fractures, hydrofractures and reservoir conditions. The tensile strength is usually determined under room pressure and dry conditions, because it is experimentally difficult to determine the tensile properties under more realistic conditions of confining pressure. Although the tensile part of a yielding envelope on a Mohr diagram is significant to the analysis of hydrofractures, only a few polyaxial tests have provided the needed data.

We present here a new approach to determine the strength and elastic properties of rocks under confining pressure. We placed a four-point beam device inside a pressure vessel (MTS-315). The rock samples were machined into beams (2 cm.*2 cm.*15 cm.), and were deformed by superposition of bending load and confining pressure. The tensile and compressive strains of the beam were continuously monitored by two or four strain gages cemented on the top and bottom surfaces. The tensile and compressive stresses within the beams were determined from the measured bending load and the top and bottom strains using the formulation of Yokoyama (1986). In some tests acoustic emission activity within the samples was monitored with two piezoelectric transducers. This configuration enables the determination of tensile strength, and tensile and compressive Young moduli of the rocks under polyaxial state of stress and confining pressures ranging up to 50 MPa.

Twenty two experiments were conducted with Tennessee Sandstone (8 tests), Berea Sandstone (4 tests), Indiana Limestone (8 tests), and composites of sandstone layer embedded in epoxy (2 tests). The beams were loaded to yielding under strain rates as low as 10^{-6}sec^{-1} .

The experimental results show that samples yielded by tensile fracturing under strain of 0.0013 or less. The tensile strength depends only slightly on the confining pressure and it is 7.2 ± 2.0 MPa for Tennessee Sandstone, 6.4 ± 2.3 MPa for Berea Sandstone, and 4.5 ± 3 MPa for Indian Limestone (tensile stress is positive). Using these results we traced the yielding envelope within the tensile stress regime, and it appears in good agreement with Griffith's envelope.

In all experiments the compressive stress-strain curves are linear and the tensile stress-strain curves are non-linear. We found that the stress-strain relationship is best represented by $\sigma_t = A\epsilon_t^B$, where σ_t and ϵ_t are the tensile stress and tensile strain respectively, and A and B are constants.

Application of the Spectral Time Analysis Technique (STAN) in the Central Coastal Plain Area

Weinstein, A.

Dept. of Geophysics and Planetary Sciences, Tel Aviv University, 69978 Tel Aviv

The Central Coastal Plain Area (CCPA) is Israel's most significant oil producing area. Most of the structural-stratigraphic traps in the CCPA are connected with Neocomian sand beds, Jurassic reef and calcarenite and are characterized by complex subsurface seismogeological conditions.

Analysis of different seismic lines in the CCPA shows:

1. Nonconfident correlation of the main seismic horizons for the mapping of traps;
2. Difficulties in recognizing faults, especially of small-scale, which may control traps.

Small-scale faults are determined by minimum vertical resolution and they may easily be missed in the presence of wave noise and other reflection.

In order to investigate the possibility of increasing the reliability of mapping of stratigraphic traps and small-scale faults, the STAN technique was applied. This technique consists of frequency sounding of migrated time sections at the different filters and is highly efficient in seismic survey for solving different geological problems. In stratigraphy these problems include classification, correlation, stratification and identification of geological objects of different size and range according to frequency composition (reef facies, etc.). In tectonics the problems are as follows: delineation of structures of different size and range; determination of relations of movements; identification of small scale faults by suppressing frequency components (wave noise), which prevent their identification.

The STAN technique has been tested in three seismic lines in the CCPA. Comparison of conventional and STAN time sections showed significant advantage of the STAN sections for mapping faults, especially small-scale and declination anomalies of wave-field-type "reefs" and objects of complex configuration. The STAN technique is a good key to constructing a new seismogeological model for prospecting.

SR Isotopic Calibration of N. African-Arabian Neogen Vertebrates

Whybrow, P.J.,¹ Savage, J.R.G.,² Rothman, S.,³ Elderfield, H.,⁴ Goldsmith, N.F.⁵

1. Department of Paleontology, British Museum (Natural History), London SW7 5BD, UK

2. Department of Geology, University of Bristol, Bristol BS8 1RJ, UK

3. Department of Geology, The Hebrew University of Jerusalem, 91904 Jerusalem

4. Department of Earth Sciences, University of Cambridge, CB2 3EQ, UK

5. Water Resources Research Center, Jacob Blaustein Institute for Desert Research, Ben-Gurion University of the Negev, 84993 Sede Boker Campus

In an ongoing study of vertebrate migrations and Tethys closure we examine continental vertebrates at Gebel Zelten, Libya, the Hazeva Formation at Yeroham and Rotem Basins, Israel, and the Hadrukh Formation in Saudi Arabia. The fossils are Burdigalian, in the early Miocene (standard datation after Berggren et al. 1985) and their relatedness is typified by the early giraffes and gazelles at Gebel Zelten and their evolved models in the Negev. Saudi and Negev sites share rodents and rhinoceros, taxa that are immigrant from Eurasia. Additional sites in Libya are biostratigraphically dated to the middle Miocene, Al Khums, and Eocene, Dor el Talha; Gharandal formation in Sinai is Oligocene.

To compute numeric values for these sites we use $^{87}\text{Sr}/^{86}\text{Sr}$ isotopic analysis of marine bivalves, either adjacent to the vertebrates or from well-characterized loci. As reported elsewhere the Sr isotopic method in bivalves deviates from biostratigraphic age estimates by 1 m.y.; tiepoints with K-Ar dating are within 0.8 my and with Ar/Ar dating, 0.6-0.5 m.y.

Sr isotopic ages of the Gharandal Formation of Egypt and *Borelis melo* of Libya supply important numerics to Israeli paleogeographic stratigraphy and to Tethys-Mediterranean reconstruction.

Some New Views on the Structure of Central Israel, Based on a Synthesis of Geological and Geophysical Data

Wolfson, N.

Geological Survey of Israel, 30 Malkhe Yisrael Street, 95501 Jerusalem

My concept presented herein differs from the generally accepted views of the structure of central Israel, and was not developed within the framework of the author's Geological Survey projects. A synthesis of combined geological and geophysical data in central Israel reveals two main groups of structures of NE-SW and NW-SE orientations. The NE-SW structures coincide with the anticlines of the Syrian Arc and they are depicted by positive gravimetric highs. The NW-SE structures are transverse faults which divide the NE-SW anticlines into tectonic blocks, with sinistral strike-slip displacements observed along some of them. On gravity and geological maps these faults are manifested by narrow gravity lows or by horizontal dislocations of the NE trending gravity and geological patterns. Some of these faults can be traced as far as the Mediterranean Sea, coinciding with the NW trending canyons on the continental slope and some canyons in central Israel (Gevaram, Beer Sheva). To the SE, they cross into Jordan, dividing the Dead Sea Rift into a series of tectonic blocks with left-lateral displacement. These faults can be considered as transforms, resembling the classical features of such structures. In association with the transform zones, widespread barite, gypsum and calcite veins can be found, along with magnetite, native sulphur and dolomitization. Outcrops of the metamorphic Hatrurim Formation are located within these zones.

^{36}Cl and ^{14}C Measurements of Brines and Fresh Water in the Dead Sea Area, Israel

Yechieli, Y.,^{1,2} Ronen, D.,¹ Kaufman, A.,¹ Carmi, I.¹

1. Dept. of Environmental Sciences, Weizmann Institute of Science, 76000 Rehovot
2. Geological Survey of Israel, 30 Malkhe Yisrael Street, 95501 Jerusalem

The radioactive isotope concentration in salt and water samples of the Dead Sea area were measured in order to determine their age and source. The brines were found to have low ^{14}C concentration (3.8 to 26 PMC) compared to the concentration found in the Dead Sea water (about 80 PMC) and thus a relatively old age (>10,000 years). On the other hand, fresh water was found to be younger, with ^{14}C concentrations being between 55 to 58 PMC.

The $^{36}\text{Cl}/\text{Cl}$ ratio in salt of the Sedom Formation ($1.3 \pm 1.3 \cdot 10^{-15}$; found in Amiaz borehole) and in En Ashlag ($6.2 \pm 1.8 \cdot 10^{-15}$) suggest that the source of the brine chloride is not the salt of the Sedom Formation from which the spring emanates. Moreover, the relatively high $^{36}\text{Cl}/\text{Cl}$ ratio of En Ashlag demonstrates that this brine was not the parent solution from which the salt of Sedom Formation precipitated.

The radioactive isotope content of the studied water samples suggests that the source of the fresh groundwater is relatively recent recharge in the mountain area, while the brines are remnants of very saline water bodies which existed in the area after the deposition of the Sedom Formation (in the last 500,000 years) and probably before the formation of the present Dead Sea (hence, Lake Lisan, Lake Samra or even an older lake).

Freshwater Fauna in a Clastic Lens within the Ghareb Formation: Implications for a "Ramon Island"

Zaslavsky, N.,¹ Avni, Y.^{1,2,3}

1. Ramon Science Center, Mitzpe Ramon, P.O.B. 194

2. Institute of Earth Sciences, The Hebrew University of Jerusalem, 91904 Jerusalem

3. Geological Survey of Israel, 30 Malkhe Yisrael Street, 95501 Jerusalem

Conglomerate and quartzitic sandstone were found within the upper part of the Ghareb Formation in the Loz Escarpment, 4 km. southwest of the Ramon structure. The conglomerate forms a lens within a normal section of chalky clay of Late Maastrichtian age. Among the clastics, a mixture of shallow marine and freshwater fauna was recognized and identified.

The fossil assemblage includes teeth of fish and reptiles, foraminifers, gastropods, spines of echinoids and serpulids, all indicating a marine environment. Association of *Myliobatids* and *Holostean* group *Pycnodontiformes* indicates tropical shallow sea. These species are extremely common in shallow bays and estuaries.

In addition to the marine assemblage, fossils of two freshwater fish families - *Esocidae* and *Chiclididae* were identified. These families are well known from rivers and freshwater environments. The *Esocidea* family is widespread in the North American fauna at the end of the Late Cretaceous. The assemblage described here is the first finding of this family reported from the Cretaceous section in Eurasia.

The freshwater fauna and the clastics were both brought together by a river that flowed into the shallow sea. The quartzitic sandstone derived from the Hatira Formation exposed at the top of the Ramon structure through a long erosive process that began in the Early Santonian. The clastic particles and the freshwater fauna that were carried by the river indicate that the Ramon structure formed an uplifted island. The Ramon island was a part of an island landscape that developed during the end of the Cretaceous at the top of the Syrian Arc structures in the Negev.

Spectral Analysis of Vibrations of Steel Constructions and its Applications for Estimating Dynamic Characteristics

Zaslavsky, Y., Shapira, A.

The Institute for Petroleum Research and Geophysics, P.O.B. 2286, 58122 Holon

Inasmuch as a structure's analytical model represents a significant part of the overall design, it is imperative, particularly in a seismic area, that the model accurately represent the full-scale structure. One means of validating analytical procedures is to perform experimental studies of full-scale structures and compare these results with those of the analytical model.

The main objective of the study was to analyze presumably random vibrations of an electric power station (a steel structure supporting the boiler) and determine the dynamic characteristics of this complex. Background noise measurements were taken at several different positions on the structure and basement on different days and at various times. The dynamic parameters were obtained by separating transient non-periodic data from periodic, complex periodic and almost periodic data. Each period of measurements included simultaneous installation of 3-5 measuring locations, each of them in two perpendicular directions. Measurements were taken at heights varying from 18m to 75m (roof). High fidelity and stability of spectra estimates were achieved through optimal record length selection, optimal smoothing of spectra and seismogram ensemble averaging. By comparing spectral vibrations at various points, we determined the natural frequencies of the first three modes of motion: longitudinal, 0.94 Hz; transverse, 1.00 Hz and torsional, 1.12 Hz. Mode shapes and damping ratios for these frequencies were also experimented with. Apparently the boiler structure interaction has a strong effect on the transverse, longitudinal and torsional responses. The natural frequencies of the boiler were $f=0.70$ Hz (transverse) and $f=0.85$ Hz (longitudinal).

This work demonstrates our ability to determine important dynamic parameters of an existing structure. This type of analysis can, and should, be implemented in further computations to better assess the capability of a structure to withstand seismic ground motions.

Salt Precipitation in Root Zone as Affecting Groundwater Chemical Composition

Zilberbrand, M.

Institute of Earth Sciences, The Hebrew University of Jerusalem, 91904 Jerusalem

Based on field sampling of pore fluids in the deep loessial unsaturated zone (Southern Ukraine) it was demonstrated that in the upper 0.5-2.5 m layer the infiltrating rain water composition may be totally altered. From $\text{HCO}_3\text{-SO}_4\text{-Ca}$ it became $\text{SO}_4\text{-Na}$, corresponding to groundwater composition. Root zone played a role of a geochemical barrier which detained the calcium, predominating in rain and irrigation water, due to calcite and gypsum precipitation. It was accompanied by HCO_3 and SO_4 extraction from the pore fluids and their TDS increases as a result of evapotranspiration. It was shown that observed Ca concentration profiles, alkalization and calcite accumulations' manifestation are explained by specific precipitating action of root zone.

The similar role of root zone was found in the Northern Negev based on the reported data about the composition of rain water, saturated soil extracts and freatic groundwater in sediments of Avdat group. The simple steady state model of rain water composition transforming to groundwater composition was developed and applied. It is based on exclusion of CaCO_3 , MgCO_3 and CaSO_4 from the rain water. Annual precipitation rates (6-13 g/m²/year) and the composition of precipitated salts calculated for the Northern Negev are in agreement with those reported in the literature.

It was shown that the calcite, magnesite and gypsum precipitation in root zone of dry regions explains well the observed change of the $\text{HCO}_3\text{-Ca}$ type of rain water to the $\text{SO}_4\text{-Na}$ or Cl-Na type of groundwater which is fed by it.

Post Arava Conglomerate Tectonic Activity Along the Arif-Batur Fault

Zilberman, E.,¹ Baer, G.,¹ Avni, Y.,¹ Feigin, D.,² Goldman, M.,³ Eyal, A.⁴

1. Geological Survey of Israel, 30 Malkhe Yisrael Street, 95501 Jerusalem

2. Dept. of Geophysics and Planetary Sciences, Tel Aviv University, 69978 Tel Aviv

3. The Institute for Petroleum Research and Geophysics, P.O.B. 2286, 58122 Holon

4. Rotem Fertilizers Ltd., P.O.B 187, Yeroham 8050

Tectonic activity younger than the Arava Conglomerate is evident along the Arif-Batur fault in the Nahal (ephemeral stream) Meshar area. The Arif-Batur fault is one of the E-W trending strike slip faults of the Negev-Sinai Shear Zone. Nahal Meshar is a remnant of a major Pliocene stream, which drained most of the southern Negev, toward the Dead Sea Valley. The present canyon of Nahal Neqarot was part of this ancient drainage system. Fluvial lacustrine sediments, which were deposited in the drainage area of the paleo-Nahal Meshar, forms the Arava Conglomerate.

The thickness of the alluvial fill in the Nahal Meshar valley was measured on both sides of the Arif-Batur fault by shallow seismic reflection, TDEM (Time Domain Electromagnetic Method) and a borehole. A sequence of the Arava Conglomerate more than 60 m thick, fills the southern part of the Nahal Meshar valley, thinning gradually northward toward the Arif-Batur fault. In Nahal Hadav near the fault, the bottom of the Pliocene channel is exposed at the level of the present stream-channel of Nahal Meshar. Further to the north, the ancient channel, and a 40 m thick sequence of the Arava Conglomerate, are elevated 20 m above the present channel. In this area, the alluvial fill in the present stream-channel is thin (6-10 m). Further northward, along the canyon of Nahal Neqarot, rock-cut terraces (strath) capped by relics of the Arava Conglomerate are found 30 m above the present stream-channel.

It is therefore suggested that the northern side of the Pliocene Nahal Meshar with the Arava Conglomerate was uplifted at least 80 m along the Arif-Batur fault zone. The uplift occurred mainly along secondary faults and folds adjacent to the main fault. The elevated position of the Arava Conglomerate further to the north, along Nahal Neqarot, suggests that the entire Neqarot Block was uplifted.



החברה הגיאולוגית הישראלית
Israel Geological Society

אזן שידים הגדול ותחום כל שכט ושכט חלק קלחוי כאשר ענינם תחזנה במשרום וחמשכלים ינינם

תכנס השנתי 1994



אתם ריחים אשר עשיתי למערים
וזשא אתכם על כנפי
נשרים וזכא אתכם אלי

רפסדוח מעער הלבונן של הים
מחירם מלך צור עלים לינו
ושלמה העלה אותם לירושלם

נוף גנוסר

